Methacrylate-based amphiphilic block copolymers in solution and at surfaces: synthesis, characterization and self-assembly

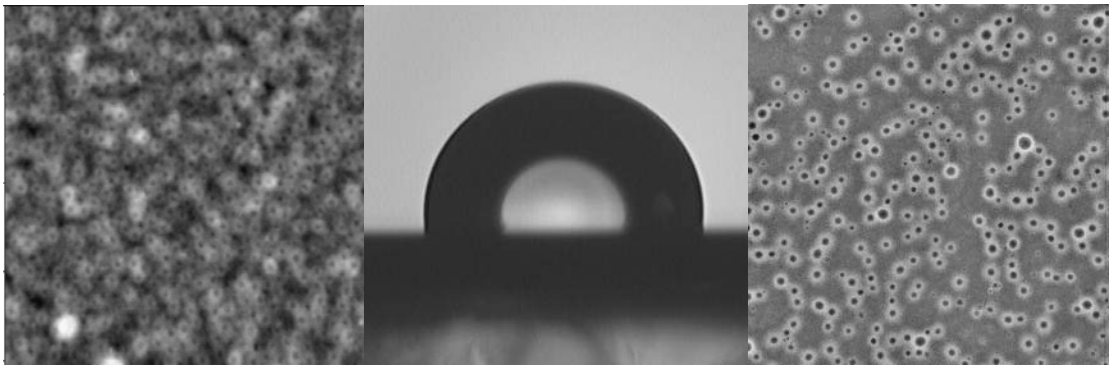

Inauguraldissertation

Zur

Erlangung der Würde eines Doktors der Philosophie

Vorgelegt der

Philosophisch-Naturwissenschaftlichen Fakultät

Der Universität Basel

Von

Ekaterina Rakhmatullina

Aus Sankt-Peterburg, Russland

Basel 2008

UNI
BASEL

Genehmigt von der Philosophisch-Naturwissenschaftlichen Fakultät
Auf Antrag von

Prof. Dr. Wolfgang Meier
Prof. Dr. Marcus Textor

Basel, den 20. Mai 2008

Prof. Dr. Hans-Peter Hauri

Dekan

Declaration of Originality

I declare that I wrote this thesis

Methacrylate-based amphiphilic block copolymers in solution and at surfaces: synthesis, characterization and self-assembly

with the help indicated and only handed it in to the Faculty of Science of the University of Basel and to no other faculty and no other university.

Ekaterina Rakhmatullina

Basel, 05.05.2008

Content

Impact of the work

- ***Articles***

Grafting and characterization of the amphiphilic triblock copolymer membranes from gold supports
Rakhmatullina E., Mantion A., Bürgi T., Malinova V., Meier W., in preparation

Solid supported block copolymer membranes through interfacial adsorption of charged block copolymer vesicles
Rakhmatullina E. and Meier W., accepted to *Langmuir* **2008**, accepted for publication

Self-organization behavior of methacrylate-based amphiphilic di- and triblock copolymers
Rakhmatullina E., Braun T., Chami M., Malinova V., Meier W., *Langmuir* **2007**, 23, 12371-12379

Functionalization of gold and silicon surfaces by copolymer brushes using surface-initiated ATRP
Rakhmatullina E., Braun T., Kaufmann T., Spillmann H., Malinova V., Meier W., *Macromol. Chem. Phys.* **2007**, 208 (12), 1283-1293

- ***Oral presentations***

Amphiphilic block copolymers: from solution to the surface
E. Rakhmatullina, W. Meier,
The global challenges and nanotechnology, Venice, Italy 2008

Temperature sensitive copolymer nanocontainers
E. Rakhmatullina, T. Braun, W. Meier
EMPA PhD symposium, Dübendorf, Switzerland 2007

Small temperature sensitive vesicles from an amphiphilic block copolymer
E. Rakhmatullina, T. Braun, W. Meier
Frontiers Annual Meeting, Leuven, Belgium 2007

Grafting of amphiphilic brushes from gold and silicon substrates
E. Rakhmatullina, T. Braun, T. Kaufmann, H. Spillmann, W. Meier
Exploring New Frontiers in Bio/Nano, Zermatt, Switzerland 2007

- ***Poster presentations***

Methacrylate-based amphiphilic copolymer vesicles: synthesis and characterization
E. Rakhmatullina, T. Braun, W. Meier
The global challenges and nanotechnology, Venice, Italy 2008

Grafting of amphiphilic copolymer brushes from gold and silicon substrates
E. Rakhmatullina, T. Braun, T. Kaufmann, H. Spillmann, W. Meier
NCCR meeting 2008, Basel, Switzerland

Synthesis and self-assembly of amphiphilic methacrylate triblock copolymers
E. Rakhmatullina, T. Braun, W. Meier
Frontiers Research Meeting 2007, Toulouse, France

Growth of amphiphilic copolymer membranes from gold substrates
E. Rakhmatullina, T. Braun, T. Kaufmann, H. Spillmann, W. Meier
NanoBio Europe congress 2007, Münster, Germany

Functionalization of the silicon surfaces by amphiphilic diblock copolymer brushes
E. Rakhmatullina, W. Meier
Frontiers Annual Meeting 2006, Sicily, Italy

Growth and characterization of the amphiphilic copolymer brushes on silicon and gold surfaces

E. Rakhmatullina, W. Meier

Swiss Chemical Society - Fall Meeting 2006, Zurich, Switzerland

Application of surface-initiated ATRP for the synthesis of amphiphilic diblock copolymer brushes from silicon surfaces

E. Rakhmatullina, W. Meier

International Conference on Nanoscience and Technology (ICN+T) 2006, Basel, Switzerland

Synthesis and self-assembly of amphiphilic methacrylate diblock copolymers

E. Rakhmatullina, S.M. Flores, W. Meier

Frontiers Research Meeting 2006, Sicily, Italy

Synthesis of amphiphilic polymer brushes from inorganic substrates using surface-initiated atom transfer radical polymerization

E. Rakhmatullina, W. Meier

Europolymer Conference of the European Polymer Federation (EUPOC) 2005, Gargnano, Lake Garda, Italy

Synthesis and Aqueous Solution behavior of Amphiphilic diblock copolymers based on n-Buthyl Methacrylate and 2-Dimethylaminoethyl Methacrylate

E. Rakhmatullina, W. Meier

7th young scientists' conference on chemistry – Frühjahrssymposium 2005, Berlin, Germany

Summary of the thesis

Part 1. Introduction

General concept of polymer self-assembly, synthesis of amphiphilic block copolymers and their application in biotechnology are briefly presented. Special attention is given to the principles of atom transfer radical polymerization (ATRP) and preparation of solid-supported amphiphilic copolymer membranes. Scope of the thesis and the contribution to the current knowledge in the field are presented.

Part 2. Self-organization behavior of methacrylate-based amphiphilic di- and triblock copolymers

ATRP synthesis of amphiphilic di- and triblock copolymers having different hydrophilic-to-hydrophobic block length ratio is described. The investigation of self-assembly of these AB and ABA block copolymers consisting of poly n-butyl methacrylate (B) and poly 2,2-dimethylaminoethyl methacrylate (A) using combination of DLS, NS-TEM, cryo-EM, and AFM is presented and discussed.

Two populations of self-organized structures in aqueous solution, micelles and compound micelles, were detected for diblock copolymers. Triblock copolymers assembled into vesicular structures of uniform sizes. Furthermore it was found that these vesicles tended to compensate the high curvature by additional organization of the polymer chains outside of the membrane. The chain hydrophilicity of the polymers appeared to have a critical impact on the self-assembly response towards temperature change. The self-reorganization of the polymers at different temperatures and its mechanism are revealed.

Part 3. Solid supported block copolymer membranes through interfacial adsorption of charged block copolymer vesicles

The properties of amphiphilic block copolymer membranes make them promising candidates for the development of new (bio-) sensors based on solid-supported biomimetic structures. Here we investigated the interfacial adsorption of polyelectrolyte vesicles on three different model substrates to find the optimum conditions for the formation of planar membranes. The polymer vesicles were obtained and characterized as described in part 2. We observed reorganization of the amphiphilic copolymer chains from vesicular structures into a 1.5±0.04

nm thick layer on the hydrophobic HOPG surface. However, this film starts disrupting and 'dewetting' upon drying. In contrast, adsorption of the vesicles on the negatively charged SiO_2 and mica substrates induced vesicle fusion and the formation of planar, supported block copolymer films. This process seems to be controlled by the surface charge density of the substrate and the concentration of the block copolymers in solution. The thickness of the copolymer membrane on mica was comparable to the thickness of phospholipids bilayers.

Part 4. Functionalization of gold and silicon surfaces by copolymer brushes using surface-initiated ATRP

To further develop the solid-supported polymer membranes with improved stability and control over the membrane formation, we applied surface-initiated ATRP to grow step-by-step the poly (n-butyl methacrylate)-co-poly(2-dimethylaminoethyl methacrylate) (PBMA-co-PDMAEMA) brushes from gold and silicon substrates. Two different approaches for the initiator immobilization on surfaces were tested to find optimal conditions for the reaction. The polymer brushes were characterized in situ by contact angle measurements, ellipsometry, and XPS. Detachment of the polymer brushes from both substrates allowed an exact determination of molecular weight and polydispersity indexes given by GPC. ^{1}H NMR confirmed the chemical structure of the detached brushes. We used microcontact printing for the structuring of the surface by copolymer brushes.

Part 5. Grafting and characterization of the amphiphilic triblock copolymer membranes from gold supports

Based on the previous experience with the growth of diblock copolymer chains from surfaces and optimized conditions for initiator immobilization (part 4), we continued the developing of the solid-supported copolymer membranes maximally mimicking the structure of biological membrane. Hence, amphiphilic triblock copolymer brushes composed of hydrophilic poly(2-hydroxyethyl methacrylate) (PHEMA) blocks and a hydrophobic poly(n-butyl methacrylate) (PBMA) middle part were synthesized using a surface-initiated ATRP. ATR-FTIR, PM-IRRAS, ellipsometry, contact angle measurements and AFM were used for the characterization of PHEMA-co-PBMA-co-PHEMA brushes. Additionally, a detachment of the polymer membranes from the solid support and subsequent GPC analyses allowed us to establish their compositions. Treatment of the amphiphilic brushes with block selective solvents led to reversible changes in the polymer surface topography. The PM-IRRAS analysis revealed an increase of the chain tilt towards the gold surface during its growth. It was suggested that the orientation of the

amphiphilic polymer brushes is influenced mainly by the chain lengths and interchain interactions. The presented results could serve as a good starting point for the fabrication of functional solid-supported membranes for biosensing application.

Part 6. Conclusions and Outlook

In this section the achievements of the research work are discussed. Further improvements and applications are proposed.

1. Introduction

„The more one knows already,
the more one still has to learn."

Friedrich von Schlegel

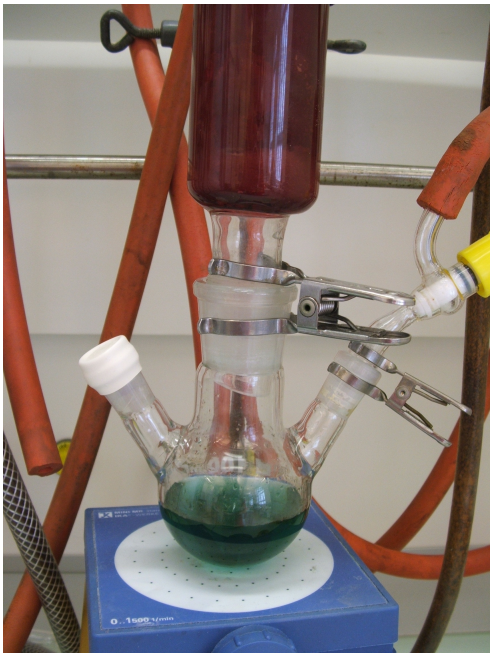

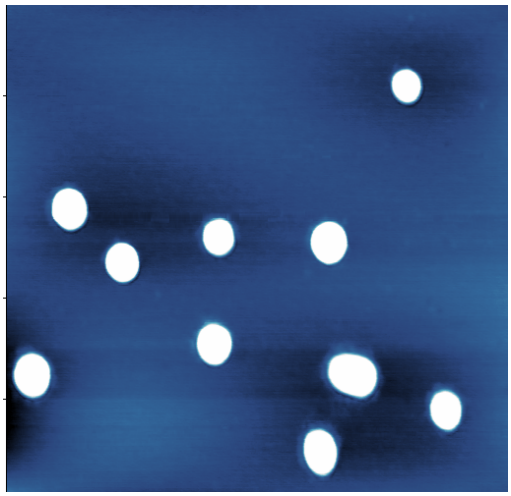

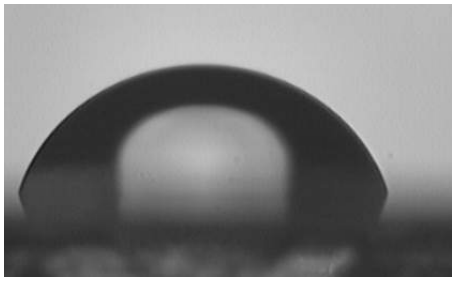

1.1. Self-assembly of amphiphilic block copolymers and its potential for application in biotechnology

Block copolymers are macromolecules consisting of two or more homopolymer subunits linked by covalent bonds or through an intermediate non-repeating unit known as a junction block.[1] Block copolymers can be classified based on the arrangement and order of the homopolymer subunits which are normally marked as A, B, C etc. Figure 1 depicts some examples of block copolymer architectures.

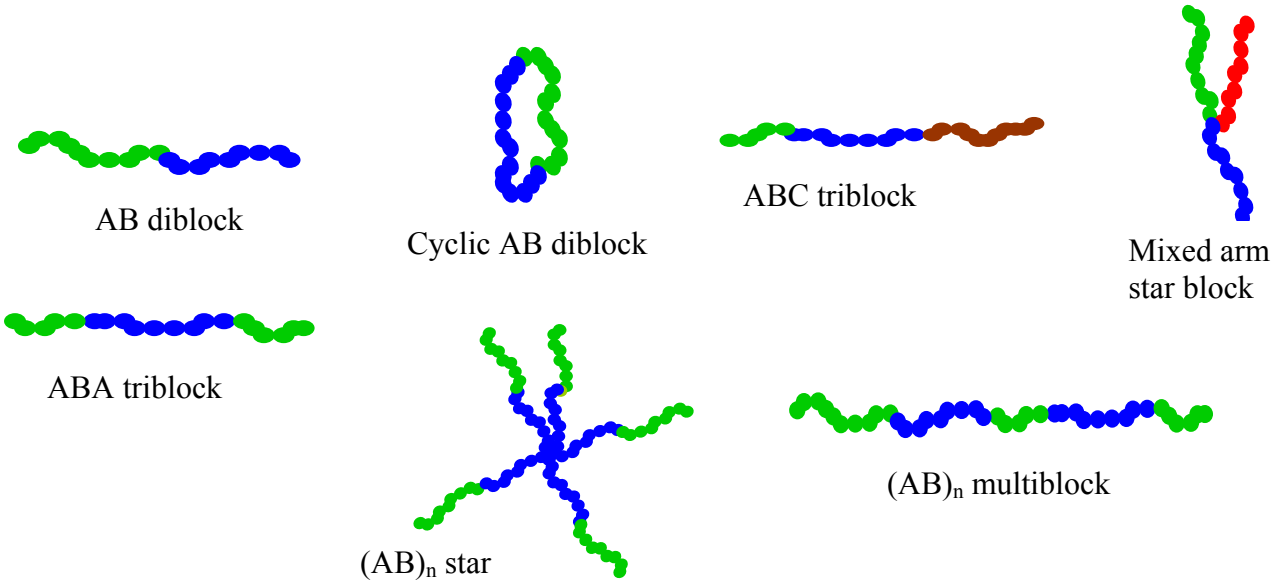

Scheme 1. Block copolymer architectures

Amphiphilic (*amphi*: of both kinds; *philic*: having an affinity for) block copolymers consist of at least two subunits, one of them possessing hydrophilic properties while the other has a hydrophobic character. Similar to low molecular weight amphiphiles (lipids, surfactants), amphiphilic block copolymers self-assemble in block-selective solvents into a variety of structures such as micelles, compound micelles, vesicles, tubes, lyotropic liquid-crystal phases.[2] Scheme 2 shows some examples of copolymer self-assemblies. The type of morphologies can be controlled through variations in the copolymer composition, the initial copolymer concentration in the solution, the nature of the common solvent, the amount of water present in the medium, the temperature, the presence of additives such as ions, homopolymers, or surfactants and the polydispersity of the copolymer chains.[3] The copolymer composition is mostly defined by the molecular weight and size of the homopolymer blocks which, in turn, determine the degree of block stretching.[4] The latter is

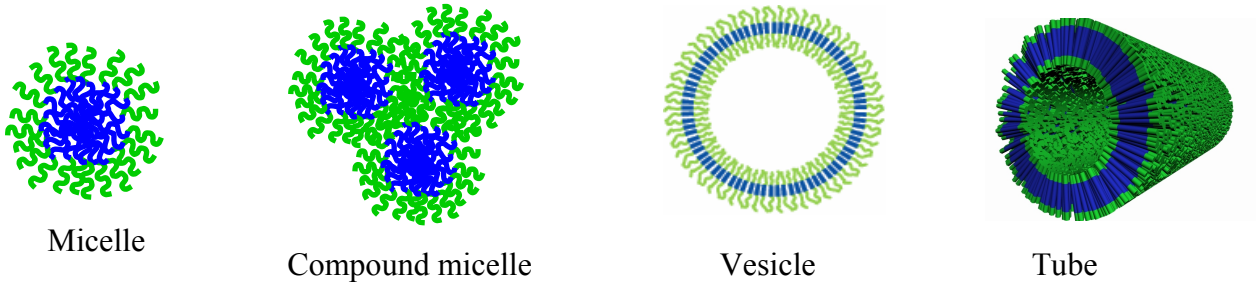

Scheme 2. Examples of amphiphilic block copolymer self-assemblies

an important parameter and its value depends on the type of self-assemblies.[5] For example, Zhang and Eisenberg[6] showed that spheres, rods, and vesicles were formed from polystyrene-co-poly(acrylic acid) PS_{200}-*co*-PAA_{21}, PS_{200}-*co*-PAA_{15}, PS_{200}-*co*-PAA_{8} copolymers, respectively, in dimethylformamide (DMF)/water solutions. The degree of PS stretching in these three types of aggregates was 1.41, 1.26, and 0.99 respectively.[7] This example illustrates that the morphology changes from spheres to rods and to vesicles as the degree of stretching reduces. The dependence of the morphology on the concentration can be clearly seen in the phase diagram of particular copolymer systems. Shen and Eisenberg investigated the formation of PS-*co*-PAA vesicles as a function of the polymer concentration.[8, 9] At fixed water content, vesicles only formed at concentrations greater than approximately 0.6 wt. % of PS_{310}-*co*-PAA_{52} copolymer. They also reported that as the polymer concentration increased from 0.6 to 5.0 wt. %, the mean diameter of the vesicles increased from 90 to 124 nm. Generally, with increasing copolymer concentration, the aggregate morphology tends to change similarly accordingly to what is observed with increasing water content.[9]

In order to induce the copolymer self-assembly a common solvent is often needed to dissolve both the hydrophobic and hydrophilic blocks to form a copolymer solution before the precipitant is added. The choice of common solvent also influences the morphologies of the resulting self-assemblies.[10] Thus, Yu et al. showed formation of spherical aggregates from PS_{500}-*co*-PAA_{58} in DMF, but vesicles were obtained when the initial solvent was tetrahydrofuran (THF) or dioxane.[11] The control of the morphology of block copolymer aggregates can be achieved not only with single but also with mixed solvents.[11] The addition of water serves to modify the polymer-solvent interactions and to induce self-assembly and morphological changes.[12-14] The same can be accomplished in a single solvent through

variation of the applied temperature. However temperature induced changes of the block copolymer self-assembly were reported for polymer systems mostly consisting of thermoresponsive poly(ethylene glycol)[15, 16] or polyelectrolytes[17-19] blocks. The experimental aspects of the influence of ionic strength[11], pH[17, 20], added salt[20-25] and homopolymers[18, 26] were mainly investigated with polyelectrolyte-based amphiphilic block copolymer systems.

The effect of the chain polydispersity on the aggregate morphology was reported by Terreau and coauthors with series of PS-*co*-PAA copolymers[27]. They showed that the size of vesicles decreased as the PAA polydispersity index increased. The decrease of size was ascribed to the segregation of long chains preferentially to the outside and the short chains segregated towards the inside of the vesicle. No segregation into different assemblies but rather segregation within the same type of aggregates occurred.

Generally, the self-assembling behavior of amphiphilic block copolymers can be affected by a variety of different factors. However, there are theories which provide guidelines for rationalizing the observed morphologies and might be used to predict the type of self-assembled structures.[28, 29] From another point of view, the influence of the macromolecular composition or common solvent on the polymer self-assembly can be exploited to tailor the type and properties of the aggregates. Additionally, the macromolecular self-assembly is rather tolerant towards introduction of different functional groups which also allows tuning properties of the assemblies for specific applications.[30] This is one of the main advantages of the polymer self-assembly compared to the one of low molecular weight compounds such as lipids and surfactants. Other advantages include the possibility of introducing additional mechanisms for colloidal stabilization, control over the polymer critical micelle concentration (cmc),[31] lower permeability and improved stability of the amphiphilic polymer membranes[32, 33] which might be used for some technological applications. It is worth mentioning that biological systems employ polymer-like amphiphiles (proteins, polysaccharides) to solve problems of heterophase stabilization. This is a clear hint to all material scientists: it is the macromolecular architecture of the amphiphilic copolymers and their assembly at different length scales, time scales and levels of interaction which make the use of these compounds very attractive. The most interesting examples of their potential applications are delivery of various substances,[34] medical diagnostics,[35] and reconstitution of biological molecules.[36-38] Among different polymer self-assemblies, micelles and vesicles were mostly used in biotechnology so far. For instance, they serve as carriers of hydrophobic molecules (in the hydrophobic shell) as well as hydrophilic compounds (in the aqueous

interior).[39] The use of polymer micelles as drug delivery systems was pioneered by the group of Ringsdorf in 1984.[40] Nowadays polymeric micelles are extensively studied as a promising nanoscopic drug carrier because of their attractive features to fulfill the requirements for selective drug delivery.[41-45] Most notably, the hydrophobic micellar core has a large capacity to accommodate hydrophobic drugs. Recently, polymeric micelles were also investigated as an oral drug delivery system,[46, 47] but originally they were considered to be most suitable for intravenous administration.[39] Extensive variety of drugs such as doxorubicin,[48, 49] paclitaxel,[50, 51] cisplatin,[52, 53] indomethacin[54, 55] and others were incorporated into polymer micelles and tested for drug delivery application. The drug loading and release by polymer micelles, the approaches to further improve the effectiveness of such polymer delivery systems are well described in the excellent reviews of Rijcken et al.[39] and Rösler and coauthors.[56] The polymer vesicular self-assemblies were also used as drug carriers,[57] although more complex systems were achieved by insertion of natural proteins into vesicular membranes.[32]

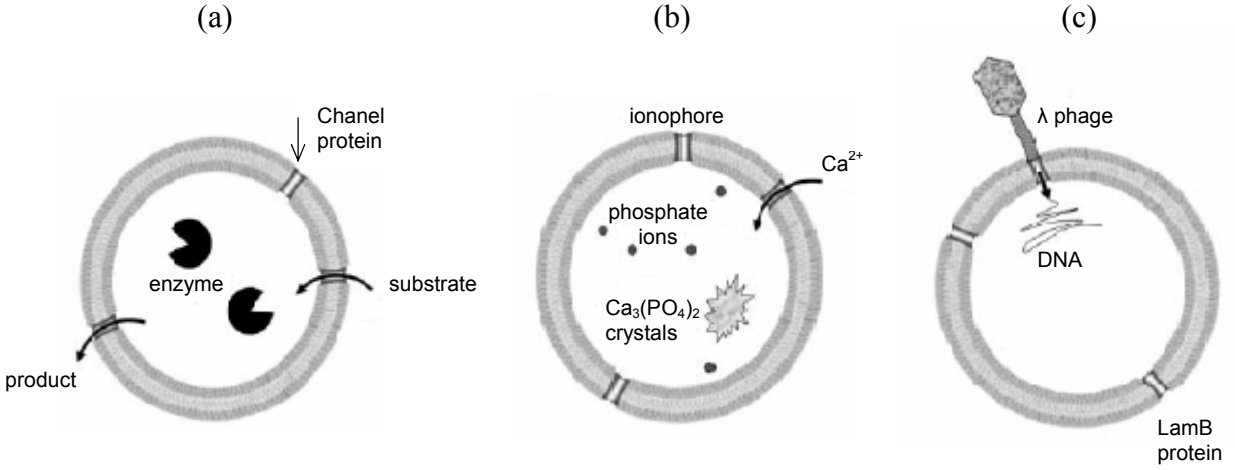

Scheme 3. Schematic representation of polymer nanoreactors. (a) Polymer vesicle with encapsulated enzyme and membrane-embedded channel protein. The substrate entering the vesicle is ampicillin, and the product of the hydrolysis is ampicillinoic acid. (b) Polymer vesicle with embedded ionophores allowing Ca^{2+} ions to enter the vesicle where they react with phosphate ions to form calcium phosphate crystals. (c) The LamB protein serves as a receptor for the λ phage virus which can inject its DNA through the channel into the polymer vesicle. Taken from Mecke A. et al.[32]

For example, the channel protein OmpF was incorporated into poly(2-methyloxazoline)-co-poly(dimethylsiloxane)-co-poly(2-methyloxazoline) PMOXA-*co*-PDMS-*co*-PMOXA vesicular membrane which enables the transport of the ampicillin through the membrane and its subsequent hydrolysis by enzyme forming ampicillinoic acid[37] (Scheme 3, a). The

function of this nanoreactor can be regulated through activation or deactivation of the channels by simply changing the cross membrane potential which depends on the ionic strength of the solution. Similar principle was applied for mineralization within PMOXA-*co*-PDMS-*co*-PMOXA vesicles[58] (Scheme 3, b). Graff and coauthors showed that LamB channel proteins inserted into the PMOXA-*co*-PDMS-*co*-PMOXA vesicular membrane retained their activity and further served as a receptor for phage λ viruses. Thus, the phage λ viruses were able to recognize the receptors and "infect" the synthetic vesicles by injecting their DNA through the channels[38] (Scheme 3, c).

These were some examples of applications of polymer micelles and vesicles in biotechnology. However numerous steps must had to be performed prior to come to this stage, starting from synthetic strategies followed by complex analysis of the polymer self-assembly using different techniques. The synthesis of amphiphilic block copolymers is the key factor determining the structure, functionality and properties of the potential assemblies. Therefore a careful choice of the synthetic approach must be taken in order to obtain amphiphilic polymers with desired composition, molecular weight and polydispersity. The following chapter describes some commonly used synthetic techniques for the preparation of different types of amphiphilic copolymers.

1.2. Overview of synthetic approaches that are mostly used for the creation of amphiphilic block copolymers

The current approaches for the synthesis of amphiphilic block copolymers usually require "living" polymerization techniques, such as anionic,[59] cationic,[60] or group transfer polymerization.[61] The living polymerization approaches have the advantage of yielding polymers with narrow molecular weight distributions with predetermined degrees of polymerization that depend only on the molar ratio of monomer to initiator concentration. However, when one of the components can not be polymerized according to a living mechanism, macromonomer synthesis,[62, 63] or capping with special end-groups for restarting, chain transfer, or termination[64, 65] are also possible. For most synthetic procedures, high purity of reactants, tedious isolation protocols or/and use of protecting group chemistry is required.

All synthetic approaches were discussed and reviewed in details by Floudes et al.,[66] Gnanou et al.[67] and in review[68] as well. Some of the techniques involving sequential block growth by living polymerization are shortly presented below followed by a more extensive description of atom transfer radical polymerization (ATRP). The ATRP technique is being in focus since this approach was used in this research work for the preparation of the amphiphilic block copolymers in solution and at surfaces.

1.2.1. Anionic polymerization

Anionic polymerization was historically the first technique for the preparation of well-defined amphiphilic copolymers. This type of reaction is used for the polymerization of styrene, vinylpyridines, (meth)acrylates, butadiene and isoprene monomers. Some of the most common amphiphilic block copolymers contain a hydrophilic segments of poly(methacrylic acid) (PMAA) or poly(acrylic acid) (PAA), which were prepared by sequential living anionic polymerization of tert-butyl methacrylate (tBMA) or tert-butyl acrylate (tBA) respectively followed by elimination of tert-butyl protective groups.[69, 70] The micellization of poly(methyl methacrylate)-co-PAA,[71-73] poly(2-ethylhexyl acrylate)-co-PAA[74] and poly (hexyl or dodecyl methacrylate)-co-PAA[75] block copolymers prepared by this method was shown before. Andre et al. reported the synthesis of the thermo- and pH-responsive micelles after applying anionic polymerization of tBA and N,N-diethylacrylamide. The PAA-co-poly(N,N-diethylacrylamide) polymers reversibly formed spherical micelles having a poly(N,N-diethylacrylamide) core.[76] Apart from tBMA and tBA, other protected monomers were also used for the anionic polymerization and synthesis of amphiphilic block copolymers. Hence, Ruckenstein and Zhang demonstrated the application of three alkoxyethyl methacrylate monomers, 1-(ethoxy)ethyl methacrylate, 1-(butoxy)ethyl methacrylate and 1-(tert-butoxy)ethyl methacrylate, for anionic polymerization.[77] The protecting group, 1-(alkoxy)ethyl of each of the monomers, could be easily eliminated after copolymerization using a mild acidic environment. Morishima et al. reported the synthesis of amphiphilic PMMA-co-poly(N,N-dimethylaminostyrene) block copolymers using living anionic polymerization of trimethylsilyl methacrylate and N,N-dimethylaminostyrene monomers.[78] The trimethylsilyl ester groups in the block copolymer were quantitatively hydrolyzed by treatment with aqueous methanol at room temperature, yielding MMA sequences. The final block copolymer exhibited micellar properties in an aqueous solution. Using monomers with different protective groups, i.e. tBMA, 2-(trimethylsilyloxy)ethyl methacrylate, and 2-(perfluorobutyl)ethyl methacrylate, Ishizone et al. synthesized ABC

triblock copolymers with various block sequences.[79] The block copolymers were converted into amphiphilic systems by removing the trimethylsilyl protecting group to give a poly(2-hydroxyethyl methacrylate) block. These copolymers can also be regarded as precursors for triblock copolymers containing a PMAA block.

1.2.2. Cationic polymerization

A wide variety of diblock copolymers, ABA triblock copolymers[80, 81] and sequence-regulated oligomers[82-84] were prepared via living cationic polymerization of vinyl ethers[85] and isobutylenes.[86, 87] Patrickios et al. reported the synthesis of ABC triblock copolymers which exhibited a cloud point effect and micellization in aqueous solutions.[88] The self-assembly behavior of these amphiphilic block copolymers composed of methyl vinyl ether, ethyl vinyl ether and methyl tri(ethylene glycol) vinyl ether (MTEGVE) depended on the location of the hydrophilic MTEGVE block on the polymer chain. The dependence of the self-assembly on the block lengths was investigated by Armes and coworkers[89] using aqueous solutions of amphiphilic diblock copolymers composed of methyl tri(ethylene glycol) vinyl ether and isobutyl vinyl ether which were synthesized by living cationic polymerization. It is also possible to prepare amphiphilic vinyl ether block copolymers with glycoside moieties[90] using this polymerization technique.

1.2.3. Group transfer polymerization

Group transfer polymerization is a valuable method for the preparation of acrylate- and methacrylate-based amphiphilic block copolymers.[66, 91, 92] The reaction can be carried out at room temperature and in the presence of air. It is tolerant towards different functional groups, especially vinyl side chains which would otherwise polymerize during radical polymerization. Billingham and coworkers reported the synthesis of amphiphilic block copolymers containing a polyelectrolyte hydrophilic poly(2,2-dimethylaminoethyl) methacrylate part.[93-95] The micellization of polymers in aqueous media was investigated. Okano et al.[96] created a highly blood-compatible polymer surface with polystyrene-co-2-(hydroxyethyl) methacrylate block copolymers. If such blood compatibility can be introduced into a polymer with high gas permeability, a new high-performance artificial lung could be designed.

1.2.4. Atom transfer radical polymerization

Atom transfer radical polymerization (ATRP) is one of the most successful methods to polymerize styrenes, methacrylates, acrylates and a variety of other monomers in a controlled fashion, yielding polymers with high molecular weights and narrow polydispersities.[97] This technique allows preserving of the polymer functionalities and modeling of the polymer chain architecture, thus resulting in multifunctional polymers of different compositions and architectures such as block copolymers, multiarmed stars or hyperbranched polymers.[97]

Components of ATRP

ATRP is in many ways a complex reaction, which includes one or more (co)monomers, a transition metal complex in two or more oxidation states,[98] which can be composed of various counter ions and ligands, an initiator with one or more radically transferable atoms or groups and can additionally include an optional solvent, suspending media and various additives. All of the components present in the reaction medium can, and often do, affect the ATRP equilibrium.[99, 100]

The initiator molecule is typically an alkyl halide (R-X). In all of the published literature on ATRP this R-X molecule has been called the initiator, even though in contrast to a standard free radical polymerization initiator, this molecule is an inherently thermally stable entity and is incorporated into the final polymer. The halide is most frequently bromide or chloride, although iodide based initiators were reported.[101] Examples of halogenated compounds that were used as initiators in ATRP are carbon tetrachloride and chloroform, benzyl halides and α-halo esters.[102] The R-X molecule can be a mono functional initiator, a multifunctional initiator, i.e. it can either possess more than one initiating functionality or it can be used to introduce additional functionalities into the alpha-chain end; it can be a macroinitiator (a polymer containing initiator site), or initiators attached to a surface, either a particle, flat surface or fiber. The only requirement is the presence of the radical stabilizing substituents around the atom containing halogen. Also, the initiation step must be faster than/ equal to the propagation rate for a controlled polymerization.[103]

Several transition metals were applied in ATRP. Catalyst systems employing copper are mostly used for the polymerization; however a wide range of other metals can be applied for ATRP including iron,[104, 105] ruthenium,[106, 107] nickel,[108, 109] molybdenum,[110, 111] rhenium,[112] rhodium,[113] palladium,[114] osmium[115] and cobalt.[116]

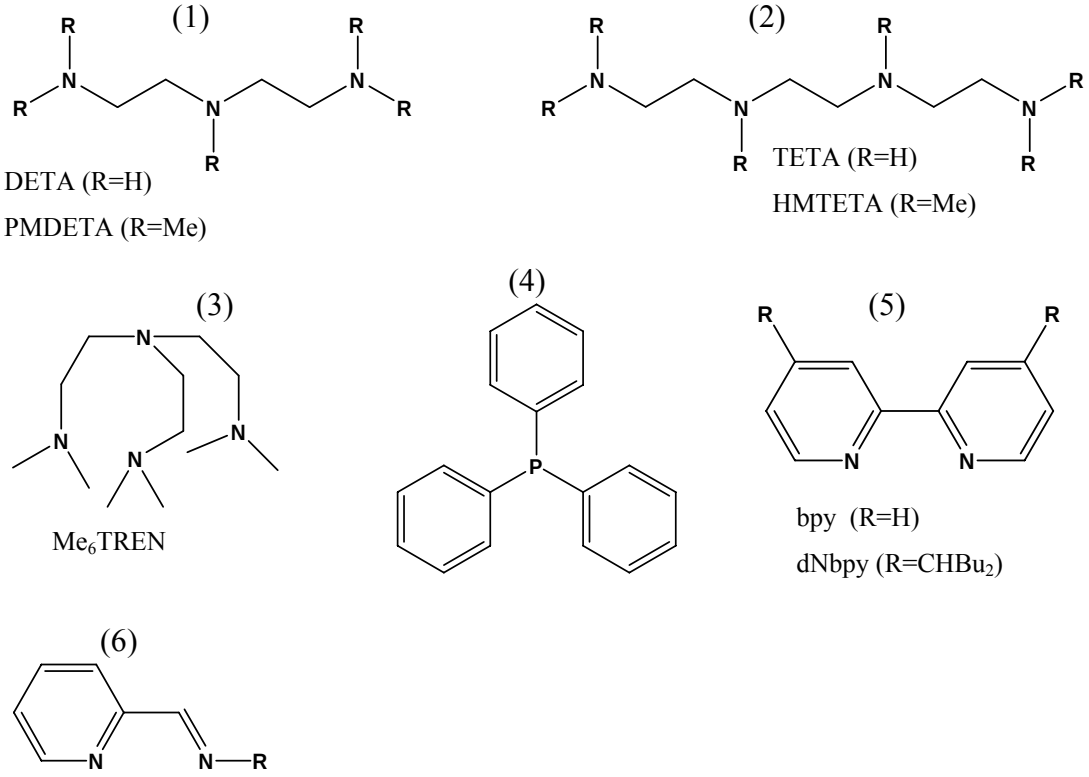

Figure 1. Examples of some ligands that are used in ATRP: (1) DETA-diethylenetriamine, PMDETA-N,N,N',N",N"-pentamethyldiethylenetriamine, (2) TETA-triethylenetetramine, HMTETA-1,1,4,7,10,10-hexamethyltriethylenetetramine, (3) Me6TREN-hexamethyltris[2 (dimethylamino)ethyl]amine, (4) triphenylphosphine, (5) bpy-2,2'-bipyridyne, dNbpy-4,4'-di(5-nonyl)-2,2'-bipyridine, (6) N-alkyl(2-pyridyl)methanimine.

To fine-tune the catalyst systems, a variety of ligands were developed that attenuate solubility, selectivity and/or reactivity of catalysts. For example, the use of 4,4'-alkyl-substituted bipyridynes resulted in the preparation of polymers with very low polydispersities ($M_n/M_w<1.1$).[117] Furthermore, linear aliphatic amines,[118] terpyridyl,[119] and picolyl[120] ligands provided catalysts that were more reactive than the 2,2'-bipyridyne (bpy) ligands originally employed for ATRP.[121] Phosphine-based ligands are also applied in the ATRP catalyst systems.[106, 104, 105] Figure 1 depicts the examples of commonly used ligands and their abbreviations.

ATRP is well-suited for the polymerization of styrenes,[122] methacrylates[123-126] and acrylates.[127-129] The power of this technique is its tolerance towards different functional groups of the monomer molecules. These functional monomers often contain donor atoms such as N or O, and have the potential to coordinate to the catalyst.[130] However, a protected monomer is still required during the ATRP process because acid monomers can poison the catalysts by coordinating to the transition metal.[131]

Mechanism of ATRP

In 1995 Matyjaszewski and Wang[121, 132] independently from Sawamoto et al.[106] developed this polymerization approach from redox catalized telomerization reactions[133, 134] and atom transfer radical addition (ATRA).[135]

ATRP is a catalytic process where a transition metal complex reversibly activates the dormant chains via a halogen atom transfer reaction[121, 106, 136-138] (Figure 2).

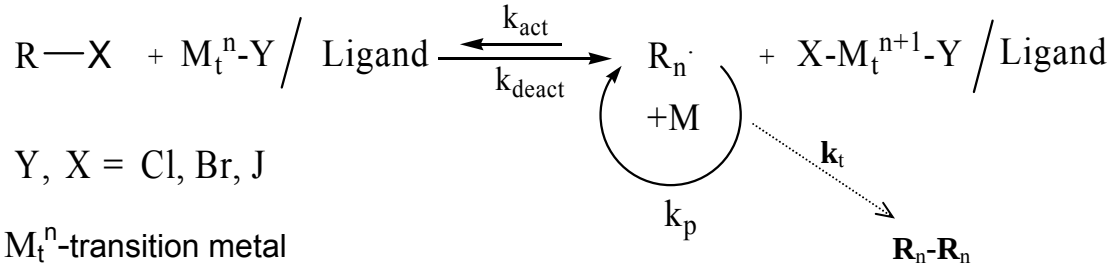

Figure 2. Schematic representation of the ATRP mechanism.

Thus, the transition metal catalyst (M_t^n-Y/Ligand) reacts with an alkyl halide initiator generating a radical and a transition metal complex by transfer of the halogen (X) to the catalyst. The bond between the alkyl and the halide is cleaved homolytically and a carbon-centered radical is formed on the alkyl[132] (Figure 3). As the radical propagates by addition of monomer (M), it is rapidly deactivated by reaction with the oxidized transition metal halide ($X\text{-}M_t^{n+1}$-Y/Ligand) to reform the original catalyst and an oligomeric alkyl halide. This process repeats itself with all chains growing in sequential steps, resulting in polymers

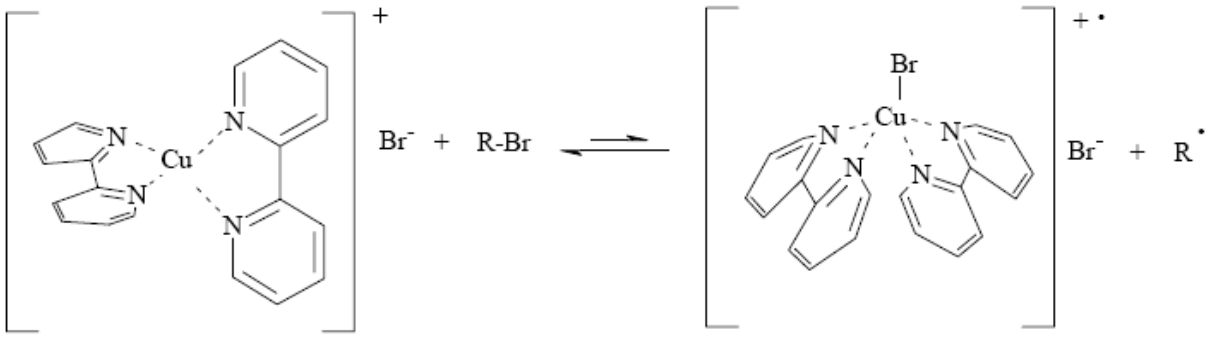

Figure 3. Example of the initiation reaction between alkyl bromide and a transition metal catalyst represented by a complex of Cu (I) with 2,2`-bipyridine ligand.

with molecular weights defined by $DP_n=\Delta[M]/[I]_0$, where $[I]_0$ is the concentration of original initiator (alkyl halide), DP is the degree of polymerization, and narrow molecular weight distributions, $M_w/M_n < 1,5$. The activity of the catalyst is correlated to the equilibrium constant (K_{eq}) defined by the ratio $K_{eq}=k_{act}/k_{deact}$, where k_{act} and k_{deact} are activation and deactivation rate constants respectively. In order to obtain a good control over the polymerization, the equilibrium must be strongly shifted towards the dormant species to limit termination between active species (k_t). Furthermore, deactivation of the active species must be fast enough, in comparison with propagation (k_p), to provide the same rate of growth for all chains and lead to a controlled/"living" behavior.[139] If deactivation is very slow or non-existent the polymerization becomes uncontrolled.[140] The reaction is termed controlled/"living" since termination reactions are not completely avoided.[132, 136] Therefore, the ATRP should be carefully distinguished from ideal living polymerizations as defined by Szwarc.[141] Taking into account the termination processes, the percentage of living chains capped by a halogen atom is less than 100%. Moreover, besides bimolecular termination, several side reactions may affect the chain-end functionality, which additionally reduce the number of living chains. Since a high portion of living chains is required for the preparation of well-defined block copolymers,[142] an accurate control over the chain-end functionality must be provided. Lutz et al. reported a significant decrease of the amount of bromine-functionalized chains during the increase of the monomer conversion for bulk ATRP of styrene.[143] The loss of functionality was divided into two steps: first, the functionality decreased linearly with the monomer conversion, and second, at very high conversions (>90%, i.e. long reaction times), the functionality decreased faster with the conversion. The authors experimentally proved that the quenching of the ATRP at the latest 47 % of styrene conversion provided 92% of end-functional polymer chains which could further serve as macroinitiators for the subsequent polymerization steps. This is one of the crucial features of ATRP when applied for the synthesis of block copolymers. In order to reduce the fraction of termination reactions and slow down the propagation rate, a low level of oxidized transition metal halide is usually injected.[144, 145]

Kinetics of ATRP

Based on the ATRP mechanism presented in Figure 2, two equations were proposed by Matyjaszewski et al.[122] (M-2) and by Fischer[146] (F-2) to describe the kinetics of ATRP.

$$K_{eq} = \frac{k_{act}}{k_{deact}} = \frac{[P_n^{\cdot}]\,[X\text{-}M_t^{n+1}\text{-}Y]}{[M_t^{n}\text{-}Y]\,[P_n\text{-}X]} \qquad (1)$$

$$\ln \frac{[M]_0}{[M]} = k_p\, K_{eq}\, [R\text{-}X]\, \frac{[M_t^{n}\text{-}Y]}{[X\text{-}M_t^{n+1}\text{-}Y]}\, t \qquad (M\text{-}2)$$

$$\ln \frac{[M]_0}{[M]} = \frac{3}{2}\, k_p\, ([R\text{-}X]_0\, [M_t^{n}\text{-}Y]_0)^{1/3} \left(\frac{K_{eq}}{3k_t}\right)^{1/3} t^{2/3} \qquad (F\text{-}2)$$

Equation (M-2) is based on the assumption that the termination step can be neglected and a fast pre-equilibrium is established, thus the value of k_p is constant throughout the reaction. According to M-2, the propagation rate (R_p) corresponds to a first-order reaction with respect to monomer [M], initiator [R-X] and activator [M_t^n-Y] concentrations. This equation explains the fact that the rate of ATRP in bulk is about four times greater than that conducted with 50 vol.% monomer solutions.[122] Thus, a reduction in the concentrations of both initiator and activator by a factor of two should result in a reduction of the overall rate by a factor of four. So far, the majority of the experimental results were analyzed according to Matyjaszewski's equation (M-2). Some data were in agreement with M-2 in terms of reaction orders for initiator and Cu (I),[122, 147, 148] while some others deviated to various extents.[149-151] The deviations were mostly assigned to the existence of "self-regulation" caused by the persistent radical effect in ATRP.[152] On the basis of the existence of this persistent radical effect, Fischer derived a kinetic equation for the ATRP (F-2). This equation was also proven to be applicable in some living radical polymerization systems.[153, 154] Zhang et al. experimentally verified both equations (M-2 and F-2) in Cu-mediated ATRP of methyl methacrylate.[155] The results obtained showed that initially added Cu(II) had strong effects on the kinetics of the ATRP depending on the $[Cu(II)]_0/[Cu(I)]_0$ ratio. When ≤10% of Cu(II) relative to Cu(I) was added at the beginning of the polymerization, the kinetics were described by Fischer's equation ($\ln([M]_0/[M]) \sim t^{2/3}$, F-2). The obtained reaction orders for initiator, Cu(I) and Cu(II) were close to or the same as those in Fischer's equation verifying the applicability of Fischer's equation in ATRP systems of lower activity. On the other hand, when $[Cu(II)]_0/[Cu(I)]_0 \geq 0.1$, the kinetics could be interpreted by Matyjaszewski's equation ($\ln([M]_0/[M]) \sim t$, M-2).

The polymerization rate was almost first order with respect to the concentration of the initiator and Cu(I) and inverse first order with respect to the concentration of Cu(II), suggesting that the "self-regulation" and radical termination becomes less important for ATRP process when enough Cu(II) is added at the beginning of the reaction. These results brought a great contribution to a better control of ATRP systems as well as an understanding of applicability of both kinetic equations for ATRP.

Some aspects of surface-initiated ATRP

As mentioned before, the ATRP initiator molecule can be attached to a planar surface, spherical particles, fibers, etc. In this case the polymerization proceeds from the surface and the final polymer chains are anchored on the support. Often, the control over the surface-initiated ATRP does not necessarily result from the application of conditions suitable for the ATRP in solution. Prucker and Rühe showed that the main differences between surface and solution polymerizations occur because of changes in termination reactions.[156] For some polymerizations from surfaces, termination is enhanced at elevated temperatures because of rapid initiation, and the film thickness can actually decrease with the reaction temperature.[157] Several studies of surface-initiated ATRP proved that the growth in polymer film thicknesses decreases with time, suggesting significant termination.[158-160] Matyjaszewski et al. simulated the growth of polymer chains by surface-initiated polymerization, considering the transfer of the monomer to the growing chains and changes in the polydispersity index with time.[161] The authors concluded that initiator coverage is a major factor in defining whether the growth in layer thickness depends linearly on the reaction time. However, that study did not consider the possibility of chain termination or the activation and deactivation reactions. Later, Kim et al. showed that there is a specific catalyst concentration that yields a maximum film thickness for a given polymerization time.[162] The optimal catalyst concentration depends on the particular ATRP system applied. They concluded that the polymerization at high catalyst concentration causes a high concentration of radicals and, therefore, rapid initial growth followed by early termination, whereas polymerization at low catalyst concentrations simply yields very little film growth. Interestingly, stirring of the solution also appears to enhance early termination processes. This was explained in terms of increased mobility of chain ends during stirring, which increases the possibility of radical coupling.[162]

The surface-initiated ATRP attracted much attention due to the possibility to create variety of polymer structures on different types of surfaces. This approach opens new perspectives for the engineering and modification of surfaces. Some examples of polymer composite materials are presented in the following chapter.

1.3. Solid-supported amphiphilic copolymer membranes: next step towards new „smart“ materials and biosensors

Amphiphilic copolymer membranes anchored to the solid substrates (so-called solid-supported membranes) gain an increasing interest in surface engineering and technology due to their similarity to biological membranes and ability to respond to external stimuli. While the complexity of biological membranes themselves and their interactions with intra- and extracellular networks make direct investigations of bioprocesses difficult, the artificial polymer model membranes can play an important role in unraveling the physical and chemical characteristics of membranes and membrane function.[163] Some examples of the successful polymer vesicle applications in biotechnology were shown in the first chapter. The tethering of the vesicles on solid supports could be an instrumental tool for the development of fluidic technologies for bioanalytics and diagnostics. The immobilization on surfaces offers the ability to easily isolate and array vesicles individually[164-166] or in groups,[167] to apply a wide range of surface sensitive techniques for the investigation of the vesicles and their content,[164] to create well-suited platforms for high-throughput experiments.[168] However most of the reported studies were performed on liposomes while anchoring of polymer vesicles on surfaces is rarely reported.

The situation is similar with solid-supported planar membranes. For almost 20 years, phospholipid bilayers deposited onto solid substrates were the only used experimental cell-surface models and allowed gaining insights into immune reactions and cell adhesion.[169-173] However, the membrane-substrate distance is usually not sufficiently large to avoid direct contact between transmembrane proteins incorporated in the lipid membrane and the solid surface (Scheme 4, (a)). This problem is particularly serious when working with cell-adhesion receptors, whose functional extracellular domains can extend to several tens of nanometers.[174] Another disadvantage of the lipid membranes is their weak air-stability which needs to be enhanced by additional chemical modifications.[175] The next steps to improve the quality of model membranes were the application of soft polymer materials as an

intermediate layer between the substrate and the lipid membrane.[176-178] Thus, the macromolecules were used as a "cushion"[177, 179, 180] or to tether the supported lipid bilayer[181-185] (Scheme 4, (b) and (c) respectively). This approach significantly improved the function of the lipid membranes as model surfaces. Nevertheless, it demands careful preparation and characterization of the complex lipid-polymer systems, prediction of the polymer-lipid interactions and still expansion of stability of the layers as well.

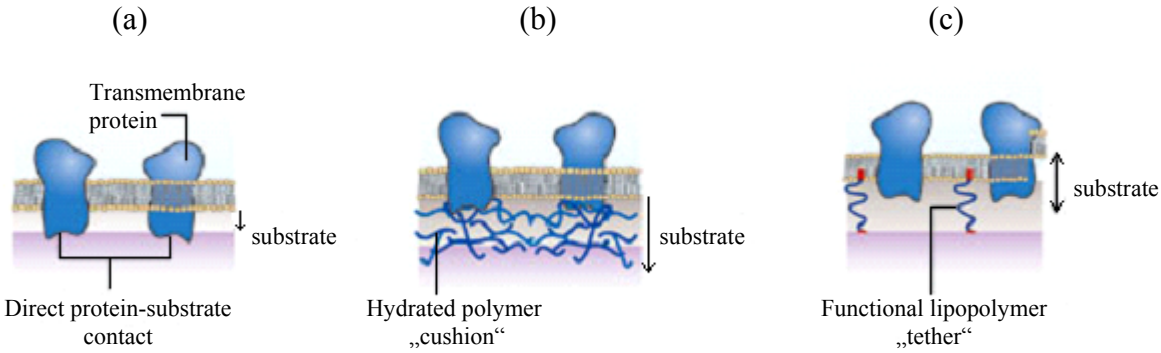

Scheme 4. Solid-supported membranes. Solid-supported lipid membrane (a), lipid membrane that is supported using a polymer cushion (b) or lipopolymer tethers (c). Transmembrane proteins are marked as blue objects across the membranes. Taken from Tanaka and Sackmann.[163]

Another method for the modeling of biological membranes involves the surface-attachment of amphiphilic block copolymer molecules into a film mimicking the structure of lipid bilayers.[186] Such an artificial polymer membrane does benefit from high stability and rather high thickness which allows incorporation of membrane proteins avoiding their contact with the substrate. The amphiphilic polymer membrane can be prepared by two different methods: physisorption and covalent attachment of the polymer to the substrate. The polymer physisorption normally involves adsorption of block copolymers onto a substrate, where one block has a strong affinity to the surface. However, this approach often results in copolymer membranes which are not stable toward solvent treatment and are not permanent structures.[187] Furthermore, it provides poor control over the polymer chain density and complications in the synthesis of suitable amphiphilic block copolymers. The covalent attachment of the polymer chains to the substrate can be achieved by either "grafting to" or "grafting from" techniques. The "grafting to" technique implies to anchor an end-functional polymer chain to the substrate containing suitable functional groups for covalent binding.[188] This method usually leads to polymer membranes with low grafting density of the chains due to diffusion problems of large macromolecules reaching a substrate. The "grafting from"

technique overcomes this problem and results in preparation of thick, covalently tethered polymer brushes with a high grafting density.[189] This method attracted a lot of attention since the "living" polymerization techniques were optimized for surface functionalization. Nowadays the "grafting from" approach and surface-initiated polymerization is the mostly applied method for the creation of solid-supported amphiphilic copolymer membranes. For the first time, the grafting of amphiphilic triblock copolymer from gold substrates, and subsequent analysis of the resulting brushes will be presented in this thesis.

The application of grafted amphiphilic copolymers for the development of "smart" (or adaptive, responsive) surfaces is widely reported. All these surfaces are responding reversibly to changes in the surrounding environment, such as temperature, [190-192] pH, [193-197] and solvent.[198-201] Boyes et al. applied surface-initiated ATRP for the synthesis of solvent responsive PS-co-PMA-co-PS and PMA-co-PS-co-PMA triblock copolymer brushes.[202] Treatment of the polymer brushes with block-selective solvents caused reversible changes in the water contact angles and surface topography (Figure 4).

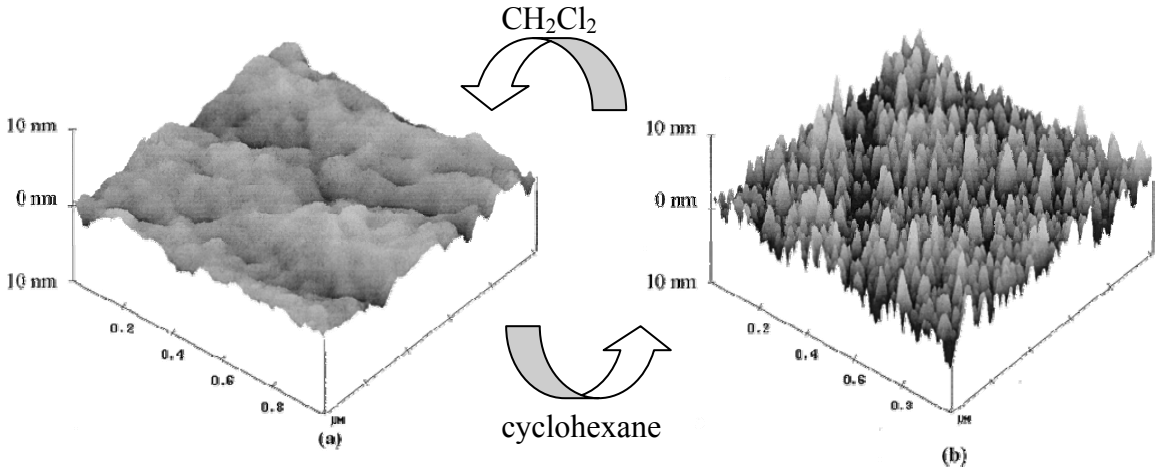

Figure 4. AFM images of PMA-co-PS-co-PMA brushes on SiO_2 substrate after treatment with CH_2Cl_2 (a) and cyclohexane (b). Taken from Boyes et al.[202]

When the polymer brushes were immersed into a good solvent for both PS and PMA blocks (CH_2Cl_2), the chains were stretched away from the interface (Scheme 5). If the same sample was then immersed in cyclohexane, a good solvent for PS only, the outer PMA segments migrated from the solvent interface and formed aggregates with both neighboring PMA blocks and PMA blocks tethered to the surface avoiding contact with solvent. Similar solvent adaptive responses were observed for PS-co-PAA,[203] PMMA-co-PDMAEMA-co-PMMA,[204] PS-co-PDMAEMA[205] and other[206, 207] copolymer brushes grown from

surfaces. The solvent response of amphiphilic copolymer brushes grafted onto surfaces will be presented in this thesis as well.

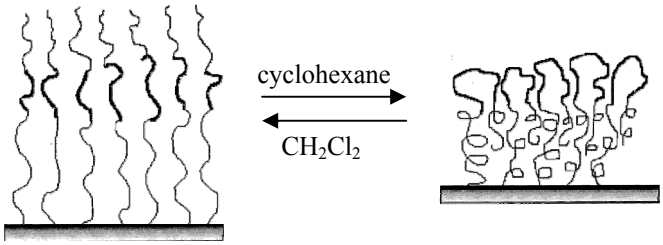

Scheme 5. Solvent response of surface-attached PMA-*co*-PS-*co*-PMA brushes.[202]

1.4. Scope of the thesis

Over the last decades, polymer science, biochemistry and biophysics developed in parallel. In polymer science, the focus shifted from the properties of bulk materials to the search of new functionalities by the design at the molecular level. In cell biology, the new methods of single molecule biophysics[208] enabled to study the behavior of biological macromolecules in their natural habitat allowing us to see how these molecular machines actually work. Meanwhile synthetic polymer chemistry has found an access to control over molecular architecture and function.[209] Obviously, synthesis with precise structural control is a key and achieving this goal in complex polymer systems is an important step for further developments and applications.

The aim of this research work is the synthesis of new methacrylate-based amphiphilic polymer architectures for the development of polymer biomimetic membranes in solutions and on surfaces. Up to now, the development of biomimetic block copolymer membranes was limited to the vesicular structures in solution while only a few reports on free-standing planar polymer layers can be found. Meanwhile, the current achievements in biotechnology and nanoengineering require stable solid-supported structures with precise architecture and tunable properties. In this respect, the "smart" polymer membranes are potential candidates for real applications. This work presents several approaches for the creation of solid-supported amphiphilic copolymer membranes.

Strategy

- ATRP was chosen for the polymer preparation since it allows synthesizing the same block copolymers both in solution and from surfaces by simply changing the structure of the initiator molecule. Besides, this approach provides covalent grafting of the polymer chains from the surfaces and allows a good control over the molecular weights and polydispersity.
- We aimed to synthesize macromolecules with amphiphilic properties to study their self-assembly in aqueous solutions. The hydrophobic n-butyl methacrylate and hydrophilic 2,2-dimethylaminoethyl methacrylate or 2-hydroxyethyl methacrylate monomers were chosen for the ATRP since the polyelectrolyte nature of the resulting poly(2,2-dimethylaminoethyl methacrylate) (PDMAEMA) could be used for the immobilization of the polymer self-assemblies on charged surfaces. The OH-groups of poly(2-hydroxyethyl methacrylate) (PHEMA) allows their chemical modifications at soft conditions and thus, tailoring of the properties of copolymer membrane for specific applications.
- The investigation of the self-assembly of polymer chains possessing different architecture (di- and triblock amphiphilic copolymers) and various hydrophilic-to-hydrophobic ratio could elucidate the effect of the chain structure on the macromolecular self-organization in aqueous solution.
- In order to develop solid-supported copolymer membranes, the immobilization of the resulting polymer vesicles consisting of polyelectrolyte PDMAEMA outer shell on different surfaces might be applied. Ideally the surface charge density of the chosen solid supports must vary in a broad range. However, other parameters like roughness of the substrates play also an important role for the immobilization of the vesicular structures. Finally, the mica, silicon oxide and graphite surfaces were chosen as a solid substrate for immobilization of the polymer vesicles. The density of negative charges decreases in a raw mica-SiO_2-graphite and all three substrates have a smooth surface.
- Further improvement of solid-supported amphiphilic copolymer membranes was based on the application of “grafting from” chemistry for the creation of covalently bound polymer chains onto the surfaces. The “grafting from” approach provides better control over the polymer growth allowing tailoring of the polymer membrane thickness and the density of the polymer brushes in a desired manner.

- To reach the final goal and create biomimetic copolymer membranes at surfaces, we planed to synthesized amphiphilic triblock copolymer brushes (PHEMA-PBMA-PHEMA) reproducing the hydrophilic-hydrophobic-hydrophilic structure of lipid bilayer. The optimized conditions for the initiator immobilization and surface-initiated ATRP found on the previously stage could be potentially used for the growth of triblock amphiphilic polymer brushes from gold supports. The presence of PHEMA blocks can give us a possibility to tune the properties of the membrane in a broad extent.

The investigation of polymer self-assemblies in solution is performed combining a variety of techniques such as light scattering, transmission electron microscopy (TEM), cryogenic TEM, atomic force microscopy and laser scanning microscopy. Functionalization of silicon and gold surfaces by amphiphilic copolymer brushes and subsequent surface analysis by contact angle measurement, X-ray photoelectron spectroscopy, ellipsometry, different types of infrared spectroscopy are applied and presented in the thesis.

Contribution to the field

For the first time, the present research offers a simple experimental approach to the preparation of solid-supported planar amphiphilic block copolymer membranes via the adsorption of polyelectrolyte copolymer vesicles; it is also the first report on the growth of amphiphilic triblock copolymer membranes from surfaces which is a step forward to the development of chemically and mechanically stable artificial biomembranes and a suitable platform for potential applications in biosensing. This thesis presents an opportunity to compare similar solid-supported polymer layers obtained either by “grafting to” or “grafting from” techniques.

1.5. References

[1] IUPAC. "Glossary of Basic Terms in Polymer Science". Pure Appl. Chem. 1996, 68, 2287-2311

[2] Hamley I. W. *Introduction to Block Copolymers* In *Developments in Block Copolymer Science and Technology,* Hamley I. W. Ed. ; Wiley 2004.

[3] Soo P. L., Eisenberg A. *J. Polym. Sci. B: Polym. Phys.* **2004**, *42*, 923.

[4] Zhang L., Eisenberg A. *J. Am. Chem. Soc.* **1996**, *118*, 3168.

[5] Allen C., Maysinger D., Eisenberg A. *Colloids Surf. B* **1999**, *16*, 3.

[6] Zhang L., Eisenberg A. *Science* **1995**, *268*, 1728.

[7] Zhang L., Eisenberg A. *Macromol. Symp.* **1997**, *113*, 221.

[8] Shen H., Eisenberg A. *Macromolecules* **2000**, *33*, 2561.

[9] Shen H., Eisenberg A. *J. Phys. Chem. B* **1999**, *103*, 9473.

[10] Yu Y., Zhang L., Eisenberg A. *Macromolecules* **1998**, *31*, 1144.

[11] Yu Y., Eisenberg A. *J. Am. Chem. Soc.* **1997**, *119*, 8383.

[12] Hauschild S., Lipprandt U., Rumplecker A., Borchert U., Rank A., Schubert R., Förster S. *Small* **2005**, *1(12)*, 1177.

[13] Choi H.-J., Brooks E., Montemagno C. D. *Nanotechnology* **2005**, *16*, 143.

[14] Yang J., Levy D., Deng W., Keller P., Li M.-H. *Chem. Commun.* **2005**, 4345.

[15] Yamamoto Y., Yasugi K., Harada A., Nagasaki Y., Kataoka K. *J. Controlled Release* **2002**, *82*, 359.

[16] Kjoniksen A.-L., Laukkanen A., Galant C., Knudsen K. D., Tenhu H., Nyström B. *Macromolecules* **2005**, *38*, 948.

[17] Schilli C. M., Zhang M., Rizzardo E., Thang S., Chong Y. K., Edwards K., Karlsson G., Müller A. H. *Macromolecules* **2004**, *37*, 7867.

[18] Shen H., Zhang L., Eisenberg A. *J. Phys. Chem. B* **1997**, *101*, 4697.

[19] Astafieva I., Zhong X. F., Eisenberg A. *Macromolecules* **1993**, *26*, 7339.

[20] Matsuoka H., Matsutani M., Mouri E., Matsumoto K. *Macromolecules* **2003**, *36*, 5321.

[21] Förster S., Hermsdorf N., Böttcher C., Lindner P. *Macromolecules* **2002,** *35*, 4096.

[22] Rager T., Meyer W. H., Wegner G., Mathauer K., Mächtle W., Schrof W., Urban D. *Macromol. Chem. Phys.* **1999**, *200*, 1681.

[23] Matsuoka H., Maeda S., Kaewsaiha P., Matsumoto K. *Langmuir* **2004**, *20*, 7412.

[24] Matsumoto K., Ishizuka T., Harada T., Matsuoka H. *Langmuir* **2004**, *20*, 7270.

[25] Kaewsaiha P., Matsumoto K., Matsuoka H. *Langmuir* **2005**, *21*, 9938.

[26] Zhang L., Eisenberg A. *J. Polym. Sci. B: Polym. Phys.* **1999**, *37*, 1469.

[27] Terreau O., Luo L., Eisenberg A. *Langmuir* **2003**, *19*, 5601.

[28] Drolet F., Fredrickson G. H. *Phys. Re. Lett.* **1999**, *83*, 4317.

[29] Bohbot-Raviv Y., Wang Z.-G. *Phys. Re. Lett.* **2000**, *85*, 3428.

[30] Vriezema, D. M.; Aragone's, M. C.; Elemans, J. A. A. W.; Cornelissen, J. J. L. M.; Rowan, A. E.; Nolte, R. J. M. *Chem. Rev.* **2005**, *105*, 1445.

[31] Förster S., Antonietti M. *Adv. Mater.* **1998**, *10(3)*, 195.

[32] Mecke A., Dittrich C., Meier W. *Soft Matter* **2006**, *2*, 751.

[33] Discher B. M., Won Y. Y., Ege D. S., Lee J. C. M., Bates F. S., Discher D. E., Hammer D. A. *Science* **1999**, *284*, 1143.

[34] Najafi F., Sarbolouki M. N. *Biomaterials* **2003**, *24*, 1175.

[35] Kwon G. S. *Crit. Rev. Ther. Drug* **1998**, *15*, 481.

[36] Nardin C., Hirt T., Leukel J., Meier W. *Langmuir* **2000**, *16*, 1035.

[37] Nardin C., Widmer J., Winterhalter M., Meier W. *Eur. Phys. J. E* **2001**, *4*, 403.

[38] Graff A., Sauer M., Van Gelder P., Meier W. *Proc. Natl. Acad. Sci. U. S. A.* **2002**, *99*, 5064.

[39] Rijcken C. J. F., Soga O., Hennink W. E., van Nostrum C. F. *J. Controlled Release* **2007**, *120*, 131.

[40] Bader H., Ringsdorf H., Schmidt B. *Angew. Makromol. Chem.* **1984**, *123/124*, 457.

[41] Allen C., Maysinger D., Eisenberg A. *Colloids Surf., B Biointerface* **1999**, *16*, 3.

[42] Adams M. L., Lavasanifar A., Kwon G. S. *J. Pharm. Sci.* **2003**, *92*, 1343.

[43] Lavasanifar A., Samuel J., Kwon G. S. *Adv. Drug Deliv. Rev.* **2002**, *54*, 169.

[44] Jones M. C., Leroux J. C. *Eur. J. Pharm. Biopharm.* **1999**, *48*, 101.

[45] Torchilin V. P. *J. Controlled Release* **2001**, *73*, 137.

[46] Mathot F., van Beijsterveldt L., Preat V., Brewster M., Arien A. *J. Controlled Release* **2006**, *111*, 47.

[47] Sant V. P., Smith D., Leroux J.-C. *J. Controlled Release* **2005**, *104*, 289.

[48] Yokoyama M., Kwon G. S., Okano T., Sakurai Y., Seto T., Kataoka K. *Bioconjug. Chem.* **1992**, *3*, 295.

[49] Rapoport N. *Int. J. Pharm.* **2004**, *277*, 155.

[50] Shuai X., Merdan T., Schaper A. K., Xi F., Kissel T. *Bioconjug. Chem.* **2004**, *15*, 441.

[51] Liggins R. T., Burt H. M. *Adv. Drug Deliv. Rev.* **2002**, *54*, 191.

[52] Nishiyama N., Okazaki S., Cabral H., Miyamoto M., Kato Y., Sugiyama Y., Nishio K., Matsumara Y., Kataoka K. *Cancer. Res.* **2003**, *63*, 8977.

[53] Nishiyama N., Kato Y., Sugiyama Y., Kataoka K. *Pharm. Res.* **2001**, *18*, 1035.

[54] Lin W. J., Juang L. W., Lin C. C. *Pharm. Res.* **2003**, *20*, 668.

[55] Djordjevic J., Barch M., Uhrich K. E. *Pharm. Res.* **2005**, *22*, 24.

[56] Rösler A., Vandermeulen G. W. M., Klok H.-A. *Adv. Drug Deliv. Rev.* **2001**, *53*, 95.

[57] Cerritelli S., Velluto D., Hubbell J. A. *Biomacromolecules* **2007**, *8*, 1966.

[58] Sauer M., Haefele T., Graff A., Nardin C., Meier W. *Chem. Commun.* **2001**, *23*, 2452.

[59] Szwarc M. *Adv. Polym. Sci.* **1983**, *49*, 1.

[60] Kennedy J. P., Ivan B. *Designed polymers by carbocationic macromolecular engineering*, Hanser Verlag 1991.

[61] Brittain W. J. *Rubber Chem. Technol.* **1992**, *65(3)*, 580.

[62] Tezuka Y. *Prog. Polym. Sci.* **1992**, *17*, 471.

[63] Meijs G. F., Rizzardo E. *J. Macromol. Sci. Rev.* **1990**, *C30*, 305.

[64] Chung R. P. T., Solomon D. H. *Prog. Org. Coat.* **1992**, *21*, 227.

[65] Riess G., Hurtrez G., Bahadur P. In *Encyclopedia of polymer science and engineering,* 2nd ed.; Ed. by Mark H. F., Bikales N. M., Overberger C. G., Menges G. Wiley: New York **1985**.

[66] Hadijichristidis N., Pispas S., Floudas G. *Block Copolymers by Group Transfer Polymerization;* In *Block Copolymers,* Hadijichristidis N., Pispas S., Floudas G. Eds.; Wiley 2003, p. 65.

[67] Taton D., Gnanou Y. *Guidelines for Synthesizing Block Copolymers;* In *Block Copolymers in Nanoscience,* Lazzari M., Liu G., Lecommandoux S. Eds.; Wiley-VCH 2007, p. 9.

[68] Förster S., Antonietti M. *Adv. Mater.* **1998**, *10(3)*, 195.

[69] Hautekeer J.-P., Varshney S. K., Fayt R., Jacobs C., Jerome R., Teyssie P. *Macromolecules* **1990**, *23*, 3893.

[70] Ramireddy C., Tuzar Z., Prochazka K., Webber S. E., Munk P. *Macromolecules* **1992**, *25*, 2541.

[71] Rager T., Meyer W. H., Wegner G., Winnik M. A. *Macromolecules* **1997**, *30*, 4911.

[72] Rager T., Meyer W. H., Wegner G. *Macromol. Chem. Phys.* **1999**, *200*, 1672.

[73] Rager T., Meyer W. H., Wegner G., Mathauer K., Machtle W., Schrof W., Urban D. *Macromol. Chem. Phys.* **1999**, *200*, 1681.

[74] Kriz J., Plestil J., Tuzar Z., Pospisil H., Brus J., Jakes J., Masar B., Vlcek P., Doskocilova D. *Macromolecules* **1999**, *32*, 397.

[75] Kriz J., Brus J., Plestil J., Kurkova D., Masar B., Dybal J., Zune C., Jerome R. *Macromolecules* **2000**, *33*, 4108.

[76] Andre X., Zhang M., Müller A. H. E. *Macromol. Rapid Commun.* **2005**, *26*, 558.

[77] Ruckenstein E., Zhang H. *Macromolecules* **1998**, *31*, 9127.

[78] Morishima Y., Hashimoto T., Itoh Y., Kamachi M., Nozakura S.-I. *J. Polym. Sci.: Polym. Chem.* **2003**, *20*, 299.

[79] Ishizone T., Sugiyama K., Sakano Y., Mori H., Hirao A., Nakahama S. *Polym. J.* **1999**, *31*, 983.

[80] Higashimura T., Aoshima S., Sawamoto M. *Makromol. Chem., Macromol. Symp.* **1986**, *3*, 99.

[81] Sawamoto M., Aoshima S., Higashimura T. *Makromol. Chem., Macromol. Symp.* **1988**, 1*3/14*, 513.

[82] Minoda M., Sawamoto M., Higashimura T. *Polym. Bull.* **1990**, *23*, 133.

[83] Minoda M., Sawamoto M., Higashimura T. *Macromolecules* **1990**, *23*, 4889.

[84] Minoda M., Sawamoto M., Higashimura T. *J. Polym. Sci. A: Polym. Chem.* **1993**, *31*, 2789.

[85] Miyamoto M., Sawamoto M., Higashimura T. *Macromolecules* **1984**, *17*, 265.

[86] Faust R., Kennedy J. P. *Polym. Bull.* **1986**, *15*, 317.

[87] Faust R., Kennedy J. P. *J. Polym. Sci. A: Polym. Chem. Ed.* **1987**, *25*, 1847.

[88] Patrickios C. S., Forder C., Armes S. P., Billingham N. C. *J. Polym. Sci. A: Polym. Chem.* **1996**, *34*, 1529.

[89] Forder C., Armes S. P., Billingham N. C. *Polym. Bull.* **1995**, *35*, 291.

[90] Yamada K., Yamaoka K., Minoda M., Miyamoto T. *J. Polym. Sci. A: Polym. Chem.* **1997**, *35*, 255.

[91] Gabor A. H., Ober C. K. *Chem. Mater.* **1996**, *8(9)*, 2272.

[92] Brittain W. *Rubber. Chem. Technol.* **1992**, *65*, 580.

[93] Baines F. L., Billingham N. C., Armes S. P. *Macromolecules* **1996**, *29*, 3416.

[94] Baines F. L., Armes S. P., Billingham N. C., Tuzar T. *Macromolecules* **1996**, *29*, 8151.

[95] Su T. J., Styrkas D. A., Thomas R. K., Baines F. L., Billingham N. C., Armes S. P. *Macromolecules* **1996**, *29*, 6892.

[96] Okano T., Nishiyama S., Shinohara I., Akaike T., Sakurai Y., Kataoka K., Tsuruta T. *J. Biomed. Mater. Res.* **1981**, *15*, 393.

[97] Coessens V., Pintauer T., Matyjaszewski K. *Prog. Polym. Sci.* **2001**, *26*, 337.

[98] Matyjaszewski K., Coca S., Gaynor S. G., Wei M., Woodworth B. E. *Macromolecules* **1998**, *31*, 5967.

[99] Braunecker W. A., Matyjaszewski K. *Prog. Polym. Sci.* **2007**, *32*, 93-146.

[100] Tsarevsky N. V., Braunecker W. A., Matyjaszewski K. *J. Organomet. Chem.* **2007**, *692*, 3212.

[101] Matyjaszewski K., Jo S. M., Paik H.-J., Shipp D. A. *Macromolecules* **1999**, *32*, 6431.

[102] Matyjaszewski K., Xia J. *J. Chem. Rev.* **2001**, *101*, 2921.

[103] Matyjaszewski K., Wang J. L., Grimaud T., Shipp D. A. *Macromolecules* **1998**, *31*, 1527.

[104] Matyjaszewski K., Wei M., Xia J., McDermott N. E. *Macromolecules* **1997**, *30*, 8161.

[105] Ando T., Kamigaito M., Sawamoto M. *Macromolecules* **1997**, *30*, 4507.

[106] Kato M., Kamigaito M., Sawamoto M., Higashimura T. *Macromolecules* **1995**, *28*, 1721.

[107] Simal F., Demonceau A., Noels A. F. *Angew. Chem., Int. Ed.* **1999**, *38*, 538.

[108] Granel C., Dubois P., Jerome R., Teyssie P. *Macromolecules* **1996**, *29*, 8576.

[109] Uegaki H., Kotani Y., Kamigaito M., Sawamoto M. *Macromolecules* **1997**, 30, 2249.

[110] Brandts J. A. M., van der Geijn P., van Faassen E. E., Boersma J., van Koten G. *J. Organomet. Chem.* **1999**, *584*, 246.

[111] Le Grognec E., Claverie J., Poli R. *J. Am. Chem. Soc.* **2001**, *123*, 9513.

[112] Kotani Y., Kamigaito M., Sawamoto M. *Macromolecules* **1999**, 32, 2420.

[113] Moineau G., Granel C., Dubois P., Jerome R., Teyssie P. *Macromolecules* **1998**, 31, 542.

[114] Lecomte P., Drapier I., Dubois P., Teyssie P., Jerome R. *Macromolecules* **1997**, 30, 7631.

[115] Braunecker W. A., Itami Y., Matyjaszewski K. *Macromolecules* **2005**, *38*, 9402.

[116] Wang B., Zhuang Y., Luo X., Xu S., Zhou X. *Macromolecules* **2003**, *36*, 9684.

[117] Matyjaszewski K., Patten T., Xia J., Abernathy T. *Science* **1996**, *272*, 866.

[118] Matyjaszewski K., Xia J. H. *Macromolecules* **1997**, *30*, 7697.

[119] Kickelbick G., Matyjaszewski K. *Macromol. Rapid Commun.* **1999**, *20*, 341.

[120] Xia J., Matyjaszewski K. *Macromolecules* **1999**, *32*, 2434.

[121] Wang J.-S., Matyjaszewski K. *J. Am. Chem. Soc.* **1995**, *117*, 5614.

[122] Matyjaszewski K., Patten T. E., Xia J. *J. Am. Chem. Soc.* **1997**, *119*, 674.

[123] Beers K. L., Boo S., Gaynor S. G., Matyjaszewski K. *Macromolecules* **1999**, *32*, 5772.

[124] Kimani S. M., Moratti S. C. *J. Polym. Sci. A : Polym. Chem.* **2005**, *43*, 1588.

[125] Narrainen A. P., Pascual S., Haddleton D. M. *J. Polym. Sci. A : Polym. Chem.* **2002**, *40*, 439.

[126] Rakhmatullina E., Braun T., Chami M., Malinova V., Meier W. *Langmuir* **2007**, *23*, 12371.

[127] Davis K. A., Matyjaszewski K. *Macromolecules* **2000**, *33*, 4039.

[128] Wang G., Yan D. *J. Appl. Polym. Sci.* **2001**, *82*, 2381.

[129] Ravi P., Wang C., Tam K. C., Gan L. H. *Macromolecules* **2003**, *36*, 173.

[130] Lad J., Harrisson S., Mantovani G., Haddleton D. M. *Dalton Trans.* **2003**, 4175.

[131] Mori H., Müller A. H. E. *Prog. Polym. Sci.* **2003**, *28*, 1403.

[132] Wang J.-S., Matyjaszewski K. *Macromolecules* **1995**, *28*, 7901.

[133] Boutevin B., Maubert C., Mebkhout A., Pietrasanta Y. J. *J. Polym. Sci. A : Polym. Chem.* **1981**, *19*, 499.

[134] Boutevin B. *J. Polym. Sci. A : Polym. Chem.* **2000**, *38*, 3235.

[135] Curran D. P. *Synthesis* **1988**, 489.

[136] Patten T. E., Matyjaszewski K. *Adv. Mater.* **1998**, *10*, 901.

[137] Patten T. E., Matyjaszewski K. *Acc. Chem. Res.* **1999**, *32*, 895.

[138] Matyjaszewski K. *Chem. Eur. J.* **1999**, *5*, 3095.

[139] Greszta D., Mardare D., Matyjaszewski K. *Macromolecules* **1994**, *27*, 638.

[140] Matyjaszewski K. *J. M. S.-Pure Appl. Chem.* **1997**, *A34*, 1785.

[141] Szwarc M. *Nature* **1956**, *178*, 1168.

[142] Davis K., Matyjaszewski K. *Adv. Polym. Sci.* **2002**, *159*, 1.

[143] Lutz J.-F., Matyjaszewski K. *J. Polym. Sci. A : Polym. Chem.* **2005**, *43*, 897.

[144] Matyjaszewski K., Tang W. *Macromolecules* **2005**, *38*, 2015.

[145] Tokuchi K., Ando T., Kamiaito M., Sawamoto M. *J. Polym. Sci. A: Polym. Chem.* **2000**, *38*, 4735.

[146] Fischer H., *J. Polym. Sci. A: Polym. Chem.* **1999**, *37*, 1885.

[147] Wang J. L., Grimaud T., Matyjaszewski K. *Macromolecules* **1997**, *30*, 6507.

[148] Haddleton D. M., Crossman M. C., Dana B. H., Duncalf D. J., Heming A. M., Kukulj D., Shooter A. J. *Macromolecules* **1999**, *32*, 2110.

[149] Davis K. A., Paik H. J., Matyjaszewski K. *Macromolecules* **1999**, *32*, 1767.

[150] Percec V., Barboiu B., Kim H. J. *J. Am. Chem. Soc.* **1998**, *120*, 305.

[151] Pascual S., Coutin B., Tardi M., Polton A., Vairon J. P. *Macromolecules* **1999**, *32*, 1432.

[152] Fischer H. *Macromolecules* **1997**, *30*, 5666.

[153] Ohno K., Tsujii Y., Miyamoto T., Fukuda T. *Macromolecules* **1998**, *31*, 1064.

[154] Lutz J. F., Lacroix-Desmazes P., Boutevin B. *Macromol. Rapid Commun.* **2001**, *22*, 189.

[155] Zhang H., Klumperman B., Ming W., Fischer H., van der Linde R. *Macromolecules* **2001**, *34*, 6169.

[156] Prucker O., Rühe J. *Macromolecules* **1998**, *31*, 602.

[157] Minko S., Sidorenko A., Stamm M., Gafijchuk G., Senkovsky V., Voronov S. *Macromolecules* **1999**, *32*, 4532.

[158] Ejaz M., Ohno K., Tsujii Y., Fukuda T. *Macromolecules* **2000**, *33*, 2870.

[159] Jones D. M., Huck W. T. S. *Adv. Mater.* **2001**, *13*, 1256.

[160] Xiao D., Wirth M. J. *Macromolecules* **2002**, *35*, 2919.

[161] Matyjaszewski K., Miller P. J., Shukla N., Immaraporn B., Gelman A., Luokala B. B., Siclovan T. M., Kickelbick G., Vallant T., Hoffmann H., Pakula T. *Macromolecules* **1999**, *32*, 8719.

[162] Kim J.-B., Huang W., Miller M. D., Baker G. L., Bruening M. L. *J. Polym. Sci. A: Polym. Chem.* **2003**, *41*, 386.

[163] Tanaka M., Sackmann E. *Nature* **2005**, *437*, 656.

[164] Christensen S. M., Stamou D. *Soft Matter* **2007**, *3*, 828.

[165] Michel R., Reviakine I., Sutherland D., Fokas C., Csucs G., Danuser G., Textor M. *Langmuir* **2002**, *18*, 8580.

[166] Renault J. P., Bernard A., Bietsch A., Michel B., Bosschar H. R., Delamarche E., Kreiter M., Hecht B., Wild U. P. *J. Phys. Chem. B* **2003**, *107*, 703.

[167] Städler B., Falconnet D., Pfeiffer I., Höök F., Vörös J. *Langmuir* **2004**, *20*, 11348.

[168] Salaita K., Wang Y. H., Fragala J., Vega R. A., Liu C., Mirkin C. A. *Angew. Chem. Int. Ed.* **2006**, *45*, 7220.

[169] Brian A. A., McConnell H. M. *Proc. Natl. Acad. Sci. U. S. A.* **1984**, *81*, 6159.

[170] Erb E.-M., Tangemann K., Bohrmann B., Müller B., Engel J. *Biochemistry* **1997**, *36*, 7395.

[171] Kloboucek A., Behrisch A., Faix J., Sackmann E. *Biophys. J.* **1999**, *77*, 2311.

[172] Qi S. Y., Groves J. T., Chakraborty A. K. *Proc. Natl. Acad. Sci. U. S. A.* **2001**, *98,* 6548.

[173] Tamm L. K., McConnell H. M. *Biophys. J.* **1985**, *47*, 105.

[174] Sackmann E. *Science* **1996**, *271*, 43.

[175] Daniel S., Albertorio F., Cremer P. S. *MRS Bulletin* **2006**, *31*, 536.

[176] Wagner M. L., Tamm L. K. *Biophys. J.* **2001**, *61*, 266.

[177] Sackmann E., Tanaka M. *Trends Biotechnol.* **2000**, *18*, 58.

[178] Knoll W., Frank C. W., Heibel C., Naumann R., Offenhäusser A., Rühe J., Schmidt E. K., Shen W. W., Sinner A. *Rev. Mol. Biotechnol.* **2000**, *74*, 137.

[179] Nissen J., Gritsch S., Wiegand G., Rädler J. O. *Eur. Phys. J. B* **1999**, *10*, 335.

[180] Tanaka M., Rehfeldt F., Schneider M. F., Mathe G., Albersdörfer A., Neumaier K. R., Purrucker O., Sackmann E. *J. Phys. Cond. Matt.* **2005**, *17*, S649.

[181] Lang H., Duschl C., Vogel H. *Langmuir* **1994**, *10*, 197.

[182] Schiller S. M., Naumann R., Lovejoy K., Kunz H., Knoll W. *Angew. Chem. Int. Ed. Engl.* **2003**, *42*, 208.

[183] Wagner M. L., Tamm L. K. *Biophys. J.* **2000**, *79*, 1400.

[184] Purrucker O., Förtig A., Jordan R., Tanaka M. *Chem. Phys. Chem.* **2004**, *5*, 327.

[185] Purrucker O., Förtig A., Ludke K., Jordan R., Tanaka M. *J. Am. Chem. Soc.* **2005**, *127*, 1258.

[186] Nardin C., Winterhalter M., Meier W. *Langmuir* **2000**, *16*, 7708.

[187] Alexandridis P. *Curr. Opin. Colloid and Interface Sci.* **1996**, *1*, 490.

[188] Mansky P., Liu Y., Huang E., Russell T. P., Hawker C. *Science* **1997**, *275*, 1458.

[189] Zhao B., Brittain W. J. *Prog. Polym. Sci.* **2000**, *25*, 677.

[190] Ista L.K., Mendez S., Perez-Luna V.H., Lopez G.P. *Langmuir* **2001**, *17***,** 2552.

[191] Takei Y.G., Aoki T., Sanui K., Ogata N., Sakurai Y., Okano T. *Macromolecules* **1994**, *27* 6163.

[192] Zhang M.M., Liu L., Zhao H.Y., Yang Y., Fu G.Q., He B.L. *J. Colloid Interface Sci.* **2006**, *301*, 85.

[193] Julthongpiput D., Lin Y.H., Teng J., Zubarev E.R., Tsukruk V.V. *Langmuir* **2003**, *19*, 7832.

[194] Hester F., Olugebefola S.C., Mayes A.M. *J. Membr. Sci.* **2002**, *208*, 375.

[195] Tjipto E., Quinn J.F., Caruso F. *Langmuir* **2005**, *21*, 8785.

[196] Jiang Y.G., Wang Z.Q., Yu X., Shi F., Xu H.P., Zhang X. *Langmuir* **2005**, *21*, 1986.

[197] Wilson M.D., Whitesides G.M. *J. Am. Chem. Soc.* **1988**, *110*, 8718.

[198] Minko S., Usov D., Goreshnik E., Stamm M. *Macromol. Rapid Commun.* **2001**, *22*, 206.

[199] Zhao B., Brittain W.J. *Macromolecules* **2000**, *33*, 8813.

[200] Lupitskyy R., Roiter Y., Tsitsilianis C., Minko S. *Langmuir* **2005**, *21*, 8591.

[201] Zhao B., Brittain W.J., Zhou W.S., Cheng S.Z.D. *J. Am. Chem. Soc.* **2000**, *122*, 2407.

[202] Boyes S. G., Brittain W. J., Weng X., Cheng S. Z. D. *Macromolecules* **2002**, *35*, 4960.

[203] Zhu Y., Shi M., Wu X., Yang S. *J. Colloid Interface Sci.* **2007**, *315*, 580.

[204] Huang W., Kim J.-B., Baker G. L., Bruening M. L. *Nanotechnology* **2003**, *14*, 1075.

[205] Hu D., Cheng Z., Zhu J., Zhu X. *Polymer* **2005**, *46(18)*, 7563.

[206] Cheng G., Böker A., Zhang M., Krausch G., Müller A. H. E. *Macromolecules* **2001**, *34*, 6883.

[207] Minko S. *Grafting on solid surfaces: „grafting to“ and „grafting from“ methods;* In *Polymer surfaces and interfaces: characterization, modification and applications*, Stamm M. Ed.; Springer Berlin Heidelberg **2008**, p. 215.

[208] Conroy R. S., Danilowicz C. *J. Contemp. Phys.* **2004**, *45*, 277.

[209] Barron A. E., Zuckermann R. N. *Curr. Opin. Chem. Biol.* **1999**, *3*, 681.

2. Self-organization behavior of methacrylate-based amphiphilic di- and triblock copolymers

Ekaterina Rakhmatullina[1], Thomas Braun[2], Mohamed Chami[3], Violeta Malinova[1], Wolfgang Meier[1*]

[1] Department of Chemistry, University of Basel, Klingelbergstrasse 80, CH-4056

[2] Department of Physics, University of Basel, Klingelbergstrasse 82, CH-4056

[3] Biozentrum, University of Basel, Klingelbergstrasse 70, CH-4056

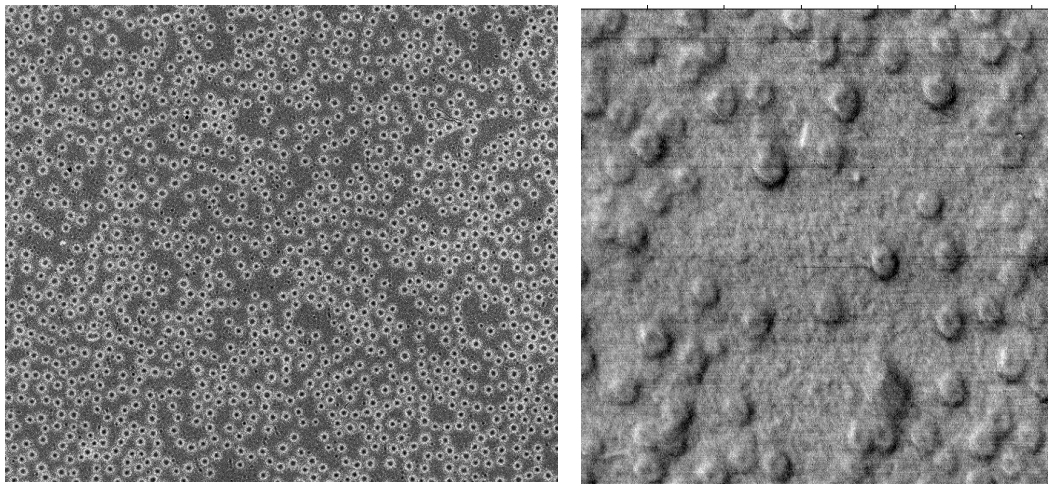

Published in: *Langmuir* **2007**, *23*, 12371.

2.1. Introduction

Amphiphilic macromolecules with precisely structured architectures are one of the most challenging and rewarding areas of polymer chemistry. They tend to self-assemble in aqueous media or at interfaces to form micro- or nanostructures with a wide range of potential applications in cosmetics, medical diagnostics and biotechnology.[1-5] Besides, amphiphilic polymer brushes on solid supports are used for surface structuring[6] and creation of "smart"surfaces.[7] A big advantage of block copolymer assemblies is their improved stability in comparison with self-organized structures from low molecular weight amphiphiles. Furthermore, by introducing certain chemical groups, tailoring of the polymer self-assembly properties for specific applications is possible.[8]

The simplest self-assembled structures are micelles, where the polymer hydrophobic parts form a micellar core in aqueous media; whereas the hydrophilic chains comprise the shell and stabilize the micelles.[9-13] Amphiphilic polymers can, however, form a wide range of morphologies including compound micelles,[14] vesicles,[15,16] tubes[17] or lyotropic liquid crystalline phases.[18, 19] Numerous studies were performed trying to establish the relationship between the type of self-assembled structure and the degree of chain stretching, the strength of interactions between blocks (Flory-Huggins parameter), polydispersity of the polymer chains, interfacial tension between the core and the solvent outside of the core and copolymer composition.[20,21] Some theories might be used in future to predict the type of polymer self-assembly.[22] Nevertheless, the self-assembly of every new amphiphilic block copolymer must be experimentally evaluated prior usage for a specific application. Especially a determination of the inner structure of the assemblies can demand a variety of different techniques in cooperation.

The self-organization of macromolecules combining a neutral hydrophobic block with a charged hydrophilic block can further be influenced by varying the charge density of the polyelectrolyte chain.[23,24] Such structures are attractive regarding various applications.[25,26] Di- and triblock amphiphilic copolymers composed of hydrophobic (B) PBMA and hydrophilic (A) PDMAEMA blocks (Scheme 1) are one example of polyelectrolyte architectures. These polymers were prepared via ATRP by Haddleton et al. and their micellization process was described briefly.[27] Our objective was to perform more comprehensive investigations on the self-assembly behavior of these molecules using a combination of light scattering techniques and diverse microscopy tools. In order to determine how the chain hydrophilicity influences the copolymer self-assembly, molecules

with different length of the hydrophilic block (A) were synthesized. We also established different types of self-organization for di- and triblock copolymers and found that changes in temperature induced reorganization of the copolymer self-assemblies in aqueous solution. A mechanism of this process is proposed.

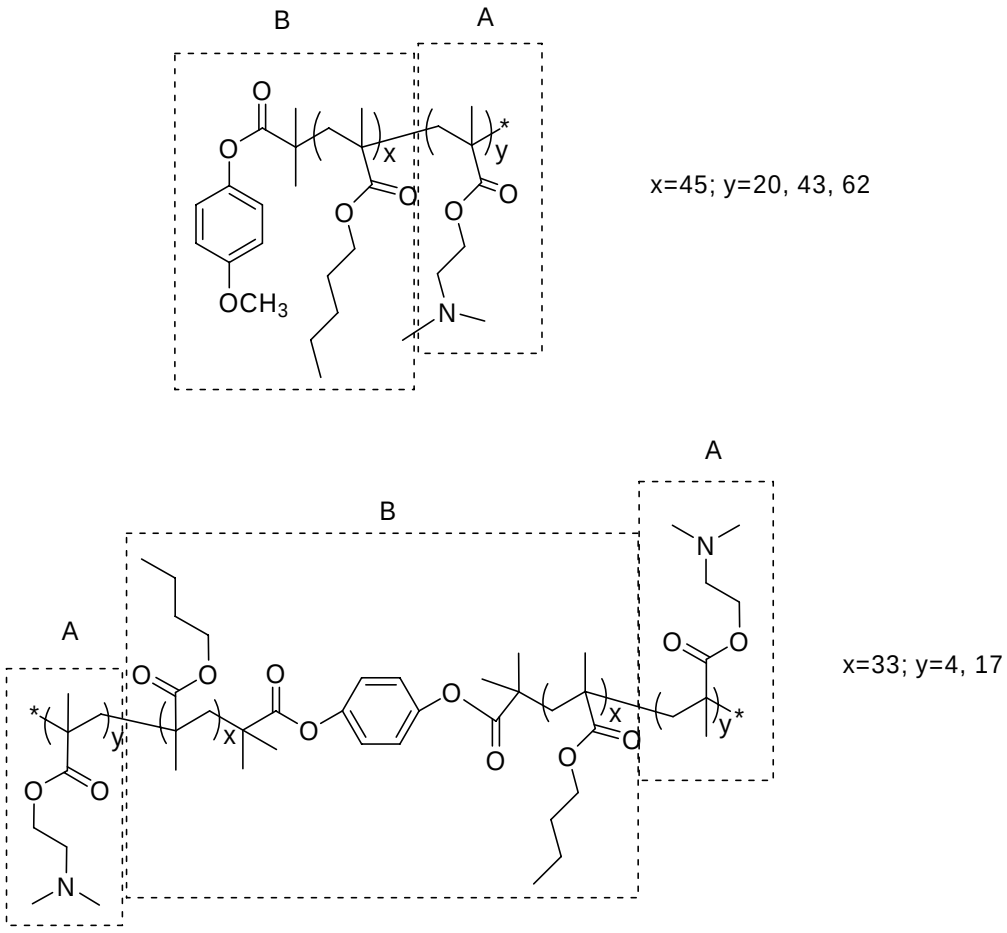

Scheme 1. Chemical structures of di- and triblock copolymers (A-hydrophilic PDMAEMA block, B-hydrophobic PBMA block with initiator fragment).

2.2. Experimental Section

2.2.1. Materials

All chemicals needed for the synthesis of the copolymers were prepared and purified as described by Haddleton et al.27 Alexa Fluor® 488 C5-maleimide was received from Molecular Probes Inc. Sepharose 4B and Dowex® Marathon® MSC (H) ion-exchange resin

were obtained from Sigma-Aldrich. Regenerated cellulose ultrafiltration membranes, NMWL=10000, 5000 and filters Durapore-PVDF were acquired from Millipore corporation.

2.2.2. Methods

^{1}H NMR

Spectra were recorded with 400.1300 MHz Varian Unity 400NMR spectrometer, with a sweep width of 8278.146 Hz and a 22° pulse width of 2.96 μs.

Gel permeation chromatography (GPC)

GPC analysis of polymer molecular weights was performed using Agilent Technologies GPC instrument with a ODS Hypersil column (5 μm) and polystyrene standards to establish a universal calibration curve. All molecular weights were corrected in according to polymethacrylate standards as described by Mori.[28] A refractive index detector was applied for sample detection. Tetrahydrofurane was used as a solvent.

Vapour pressure osmometry (VO)

A Knauer vapour pressure osmometer calibrated to toluene solvent was applied for molecular weight detection. Several copolymer solutions with different concentrations were analysed and the results were extrapolated to zero concentration to obtain the final number average molecular weights.

Negative-stain transmission electron microscopy (NS-TEM)

NS-TEM images were recorded with a Hitachi H-8000 transmission electron microscope at 200 kV and nominal magnification of 50'000 x on Kodak SO-163 films. 3.5 μl of 0,5 wt.% aqueous solution of the corresponding copolymer was adsorbed for 1 min onto glow discharged (20s) carbon film-coated copper grids, washed once with distilled water and stained with 2% uranyl acetate.

Cryoelectron microscopy (Cryo-EM)

Cryo-EM was done on the Philips CM200-FEG electron microscope with a Gatan 626 cryo-holder. Electron micrographs were recorded at accelerating voltage of 200 kV and a magnification of 50000 x, using a low-dose system and defocus values equal to -3 μm. Micrographs were performed on Kodak SO-163 films. A 4 μl aliquot of the polymer sample

(0.5 wt.%) were adsorbed for 1 min onto holey-carbon film grids (Quantifoil, Germany), blotted with Whatman 4 filter paper and frozen into liquid ethane at -178 °C. Frozen grids were transferred onto the microscope and imaged.

Confocal laser scanning microscopy (LSM) and fluorescence correlation spectroscopy (FCS)

Studies were performed with a Zeiss 510 Confocor 2 setup equipped with an argon-ion laser (maximum power 30 mW). 488-nm line of the argon-ion laser was used for the excitation of the Alexa Fluor® 488 C5-maleimide dye. FCS autocorrelation curves were obtained by exciting a small amount (5 μl) of aqueous sample, which was added to a rigid sample holder made of quartz glass (Lab-Tek, NUNC), using the 488 nm argon laser in combination with a suitable dichroic mirror and a longpass filter enabling transmission above 505 nm. Improvement of signal to noise ratio of autocorrelation curves was achieved by averaging 5 measurements, each 10 seconds long. Samples were prepared by dropping dimethylsulfoxide solution of Alexa Fluor® 488 C_5-maleimide to the copolymer aqueous solution (1 wt.%) to get a final concentration of the dye 10^{-6} M. The mixture was kept overnight and passed through a column of Sepharose 4B prior to measurements to remove the free dye.

Static and Dynamic Light Scattering (SLS and DLS)

DLS studies were carried out using a commercial goniometer (ALV-Langen) equipped with He-Ne laser (λ=633 nm) at scattering angles between 30° and 150°. An ALV-5000/E correlator calculates the photon intensity autocorrelation function g^2 (t). The copolymers were dissolved in bidistilled water containing 0.5 M NaCl (solutions had pH=8, see 2.5). The addition of salt screened the electrostatic charge interactions between the polyelectrolyte PDMAEMA blocks. The solutions were sonicated and left to equilibrate for 24h. The samples were prepared by filtering the solutions through 0.45 μm filter (Millex Durapore-PVDF, Millipore) into the quartz cells. These cells were mounted in a thermostatic optical matching vat with a temperature accuracy of T=0.02 K. The experiments were performed at T=293 K. Samples with concentrations of 0.2 wt.%, 0.4 wt.% and 0.6 wt.% were measured for each copolymer.

The refractive index increment d*n*/d*c* was obtained at the corresponding temperature and wavelength of the light scattering experiments by using a commercial ALV-DR-1 differential refractometer.

The data of DLS measurements were analyzed using a regularized fit for AB and ABA samples. SLS data were analyzed according to the method proposed by Zimm.[29]

Atomic force microscopy (AFM)

Tapping mode AFM was performed using PycoLE System, Molecular Imaging, and silicon nitride cantilevers, k=42 N/m, at scan rate 1lines/s. Aqueous solutions of the copolymers (0.5 wt.%) were deposited on silicon substrates and left for 2 minutes. The samples were washed three times with bidistilled water and dried at room environment. Different positions of the sample were monitored. All experiments were done at room temperature.

Cloud point temperature (CPT)

CPT of the copolymer aqueous solutions was determined using Safas UV spectrophotometer (Monaco) at a wavelength 300 nm and heating rate 2°C/min.

2.2.3. Synthesis of PBMA block (I)

The first PBMA hydrophobic block was prepared as described in literature[27] using mono- and difunctional initiators. The polymerization reaction was terminated at low monomer conversion in order to preserve the Br-end functionality of the polymer chains.[30] We improved, however, the purification procedure in order to obtain polymers with narrow polydispersity which is important for the self-assembly of the final copolymers. Passing the polymer solution through a column with basic alumina was not sufficient enough to get rid of the copper ions completely. After passage through the column the solvent was evaporated and the polymers were dissolved in ethanol and stirred with Dowex® Marathon® MSC (H) ion-exchange resin for 24 hours. Then the polymer solution was passed through a paper filter and purified furthermore by ultrafiltration through a regenerated cellulose membrane (Millipore, NMWL: 5000) to remove any unreacted monomer and oligomer chains. Finally the polymer was precipitated in cold methanol (-50°C), and dried in vacuo. ^{1}H NMR ($CDCl_3$), δ (ppm): 0.86 (3H, CH_3), 1.38 (2H, CH_2), 1.59 (2H, CH_2), 3.94 (2H, CH_2), 6.88 (2H, 2CH), 6.96 (2H, 2CH).

2.2.4. Copolymerization of DMAEMA (II)

Di- and triblock copolymers (AB and ABA correspondingly) were synthesized with mono- and difunctional PBMA macroinitiators as described in literature.[27] As mentioned above, the polymerization reaction was terminated at low monomer conversion. Additionally, we

performed more purification steps in order to remove the copper ions from the final copolymers and decrease their polydispersity. Each block copolymer reaction mixture was passed through a column with basic alumina, the solvent was evaporated and the copolymer was dissolved in ethanol and stirred with Dowex® Marathon® MSC (H) ion-exchange resin for 24 hours. Then the polymer solution was passed through paper filter and further purified by ultrafiltration through regenerated cellulose membrane (Millipore, NMWL: 10000) to get rid of unreacted monomer and oligomer chains. Finally the copolymers were precipitated into cold isopropanol (-55°C), filtered and dried in vacuo. ^{1}H NMR ($CDCl_3$) δ (ppm): 0.86 (3H, CH_3, PBMA), 1.38 (2H, CH_2, PBMA), 1.59 (2H, CH_2, PBMA), 2.29 (6H, $2CH_3$, PDMAEMA), 2.58 (2H, CH_2, PDMAEMA), 3.94 (2H, CH_2, PBMA), 4.12 (2H, CH_2, PDMAEMA).

Following the polymerization procedure described by Haddleton et al.[27] and the purification steps discussed above, block copolymers with different lengths of PDMAEMA block and low polydispersity indexes were synthesized.

2.2.5. Preparation of copolymer self-assemblies in aqueous solution

Polymer solutions with different concentrations were prepared by stirring the corresponding amount of polymer in distilled water overnight at room temperature. Prior investigation the solutions were filtered through 0.8 μm filter (Millex Durapore-PVDF, Millipore). The aqueous solutions had a slightly basic pH (pH=8) due to the tertiary amine groups in PDMAEMA block (PDMAEMA, pKa= 7.3[31]).

2.3. Results and discussion

2.3.1. Characterization of AB and ABA copolymers.

^{1}H NMR analysis

^{1}H NMR confirmed the chemical structures of the polymers and was also used to determine the degree of polymerization. The initiator molecule containing a p-methoxyphenolic ring was intentionally chosen due to the possibility to identify the aromatic signal in the "empty" part (6-7ppm) of the spectrum. This allowed us to calculate the degree of polymerization based on initiator/polymer peaks integration (Table1).

GPC and vapour pressure osmometry results

Number average molecular weight (M_n) and polydispersity index (PDI) of the polymers were determined by GPC and are shown in Table 1. The PDIs of all samples were in the range of 1.1-1.2 showing lower polydispersity than the one reported before.[27] A good agreement between GPC and ^{1}H NMR results was observed in the case of triblock copolymers and difunctional PBMA macroinitiator (i.e. entry 5-7, Table 1) pointing to accurately established polymer compositions. The size of PDMAEMA blocks (4 and 18 monomer units respectively) was defined as a difference between the molecular weights of ABA and PBMA macroinitiator precursor measured by GPC. The obtained values were in agreement with ^{1}H NMR analysis (5 and 16 units correspondingly). Hence, the copolymer compositions were calculated as average values from the two methods (Table 1).

No.	M_n, g/mol			PDI*	Polymer composition**	
	GPC	^{1}H NMR	VO		Targeted DP***	Experimental DP
1	6810	6000	6700	1.1	A_0B_{54}	A_0B_{45}
2	9360	9200	9700	1.1	$A_{30}B_{45}$	$A_{20}B_{45}$
3	13120	12700	13600	1.1	$A_{50}B_{45}$	$A_{43}B_{45}$
4	16000	15800	16520	1.1	$A_{70}B_{45}$	$A_{62}B_{45}$
5	9900	10100	-	1.2	A_0B_{80}****	A_0B_{66}****
6	11190	11600	-	1.2	$A_6B_{66}A_6$	$A_4B_{66}A_4$
7	15170	15500	-	1.2	$A_{25}B_{66}A_{25}$	$A_{17}B_{66}A_{17}$

Table 1. Estimation of polymer molecular weights and compositions.

* Average values measured by GPC

** Molecular mass contribution of the initiator fragments (193 g·mol^{-1} for diblock copolymer and 408 g·mol^{-1} for triblock copolymers) was taken into account. For estimation of the polymer composition the average of the molecular weights given by the methods was used. A-hydrophilic PDMAEMA block and B-hydrophobic PBMA part.

*** at 30 % conversion

**** PBMA block prepared from difunctional initiator

In case of diblock copolymers a small discrepancy between GPC and ^{1}H NMR data was observed. Therefore we applied vapour pressure osmometry (VO) for more accurate estimation of the copolymer composition (Table 1). The number average molecular weights calculated by VO coincided well with the GPC data. For final calculations of the polymer composition, the average from the values given by GPC and VO were taken into account. Thus 45 BMA monomer units were included into PBMA macroinitiator chain that gave rise to a polymerization of 20, 43 and 62 DMAEMA monomer units (entry 2-4, Table 1) respectively.

2.3.2. Self-assembly in aqueous solutions

Light scattering (DLS and SLS)

Dynamic light scattering (DLS) measurements revealed two populations of structures in aqueous solutions of diblock copolymers $A_{20}B_{45}$, $A_{43}B_{45}$ and $A_{62}B_{45}$ (Table 2). Most probably they corresponded to micelles (hydrodynamic radii of 8, 12, 15 nm) (Scheme 2) and larger assemblies (hydrodynamic radii of 77, 89, 102 nm). This assumption was also supported by the relatively high polydispersity indexes (PDIs) of all diblock copolymer samples (0.28-0.30, Table 2).

No.	Polymer composition	R_h, nm		PDI	ρ parameter*
		1st fraction	2nd fraction		
1	$A_{20}B_{45}$	8	77	0.28	2.0
2	$A_{43}B_{45}$	12	89	0.30	1.8
3	$A_{62}B_{45}$	15	102	0.28	1.9
4	$A_4B_{66}A_4$	-	56	0.16	1.1
5	$A_{17}B_{66}A_{17}$	-	59	0.18	1.1

Table 2. Light scattering analysis of di- and triblock self-assemblies in aqueous solutions. AB and ABA are di- and triblock copolymers consisting of A-hydrophilic PDMAEMA block and B-hydrophobic PBMA block.

* ρ parameter was obtained by the ratio R_g/R_h . ρ parameters (entries 1-3) were calculated using R_h of the second fractions.

The average hydrodynamic radius (R_h) of the polymer aggregates clearly increased with an increase of the polymer chain length which was in a good agreement with the data published before.[27] It was interesting to compare the experimentally found sizes of the self-assemblies with the theoretical lengths estimated for fully stretched copolymer chains (C-C bonds 1,5 Å, 109.28° angle). Thus, the lengths of fully stretched $A_{20}B_{45}$, $A_{43}B_{45}$ and $A_{62}B_{45}$ polymer molecules must be 17.1, 22.1 and 27.4 nm accordingly. For micelles, the theoretical radius corresponds to the length of one polymer chain approximately. Thus, an increase in the polymer chain length of A block from 20 to 43 units must result in 5 nm larger micelles of $A_{43}B_{45}$ than $A_{20}B_{45}$. Analogically, a subsequent increase in the chain length from $A_{43}B_{45}$ to $A_{62}B_{45}$ must cause an increase in the micelle size of additional 5.3 nm. Comparing these calculations with the experimental data, we found a good agreement between theoretical and experimental data although some differences occurred. These differences might be related to variations in the R_h (DLS) due to the water shell which can grow non-linearly with the length of the hydrophilic PDMAEMA block. Nevertheless, we can conclude that despite the hydration effect, the polymer chains had a rather stretched conformation in solution since the experimental and theoretical radii were very close to each other. We did not observe the same correlation between the PDMAEMA length and the size of triblock copolymer assemblies. Only one type of self-organized structures with an average R_h of 56 nm ($A_4B_{66}A_4$) and 59 nm ($A_{17}B_{66}A_{17}$) and low PDI of 0.16-0.18 (entry 4,5, Table 2) were detected. Theoretically, the sizes of completely stretched $A_4B_{66}A_4$ and $A_{17}B_{66}A_{17}$ molecules correspond to 18.5 and 24.2 nm. However, the experimentally found R_h (56 and 59 nm) was rather too big for micellar structures. On the other hand, formation of aggregates should result in higher PDIs than the one measured. Therefore, we believed that another type of self-assembly was most likely formed in case of triblock copolymers.

Furthermore, the static light scattering (SLS) results also supported a different morphology of AB and ABA particles. The radius of gyration (R_g) and the R_h from DLS were found to be nearly identical for ABA assemblies, thus leading to a ratio $\rho=R_g/R_h$ of 1.1 (entries 4, 5; Table 2). This so called ρ-parameter is a structure-sensitive property reflecting the radial density distribution of the scattering particle.[32, 33] A ratio of $\rho=1$ is characteristic for hollow spheres.[34, 35] The higher ρ values for AB assemblies (entries 1-3, Table 2) could be due to the broader polydispersity of the particles and/or different self-organization of AB chains.

Although the light scattering data do not give complete information concerning the nature of the polymer self-assemblies, one can conclude that di- and triblock copolymers self-organized into different types of structures in aqueous solutions. The micelles presented in

the diblock copolymer solutions could further aggregate forming a second fraction of particles that increased the PDI. In contrary, the existence of only one population of triblock copolymer self-assemblies led to PDIs similar to those observed for lipid vesicles.[36, 37]

Interestingly, though $A_{20}B_{45}$ contains a nearly the same hydrophilic fraction as $A_{17}B_{66}A_{17}$ copolymer (the ratio between the molecular weights of the hydrophilic block and the whole macromolecule are 0.32 and 0.35 for $A_{20}B_{45}$ and $A_{17}B_{66}A_{17}$ correspondingly), it does not exhibit the same type of self-assembly. Presumably, in the case of PBMA-co-PDMAEMA type of block copolymers the self-assembly in aqueous media is controlled by the chain architecture (i.e. diblock or triblock).

In a previous report[27] independent from the preparation procedure, $PBMA_{36}$-$PDMAEMA_{63}$ copolymer self-organized in acidic aqueous solutions into assemblies of comparable sizes. Notably, also two populations were detected by DLS. Since the $A_{62}B_{45}$ copolymer had similar molecular composition to $PBMA_{36}$-$PDMAEMA_{63}$ discussed by authors, we performed DLS studies of acidic solution of this copolymer but no differences in self-assembly behavior compared to basic solution were found. No differences for the other AB and ABA copolymers were observed as well. Since the hydrophobic-to-hydrophilic ratio and the chain length of our ABA triblock copolymers differed from the one presented in the reference,[27] their self-assembly was not compared.

To the best of our knowledge, no further investigations of the inner structure of the polymer aggregates were reported. Hence, we applied different types of microscopy in order to elucidate the nature of the aggregates.

Negative-stain transmission electron microscopy (NS-TEM)

To observe the shape and the size distribution of the self-assembled structures, we performed NS-TEM studies (Figure 1). The polymer solutions were adsorbed on a carbon coated TEM grid and negatively stained by uranyl acetate. The images showed an existence of spherical particles with diameters in the range of 30-60 nm for diblock copolymer self-assemblies (Figure1, **D**, **E**, **F**) and 40-50 nm for ABA copolymers (Figure 1, **B**, **C**). A second population of smaller micelles was present in the case of AB polymers. Only one type of uniformly sized structures were found however for ABA triblock copolymers (Figure 1, **A**). This observation coincided with the low polydispersity index for triblock copolymer assemblies measured by DLS. The smaller sizes of the particles given by NS-TEM than those measured by DLS are not surprising since the solvation effect in NS-TEM measurements is eliminated.

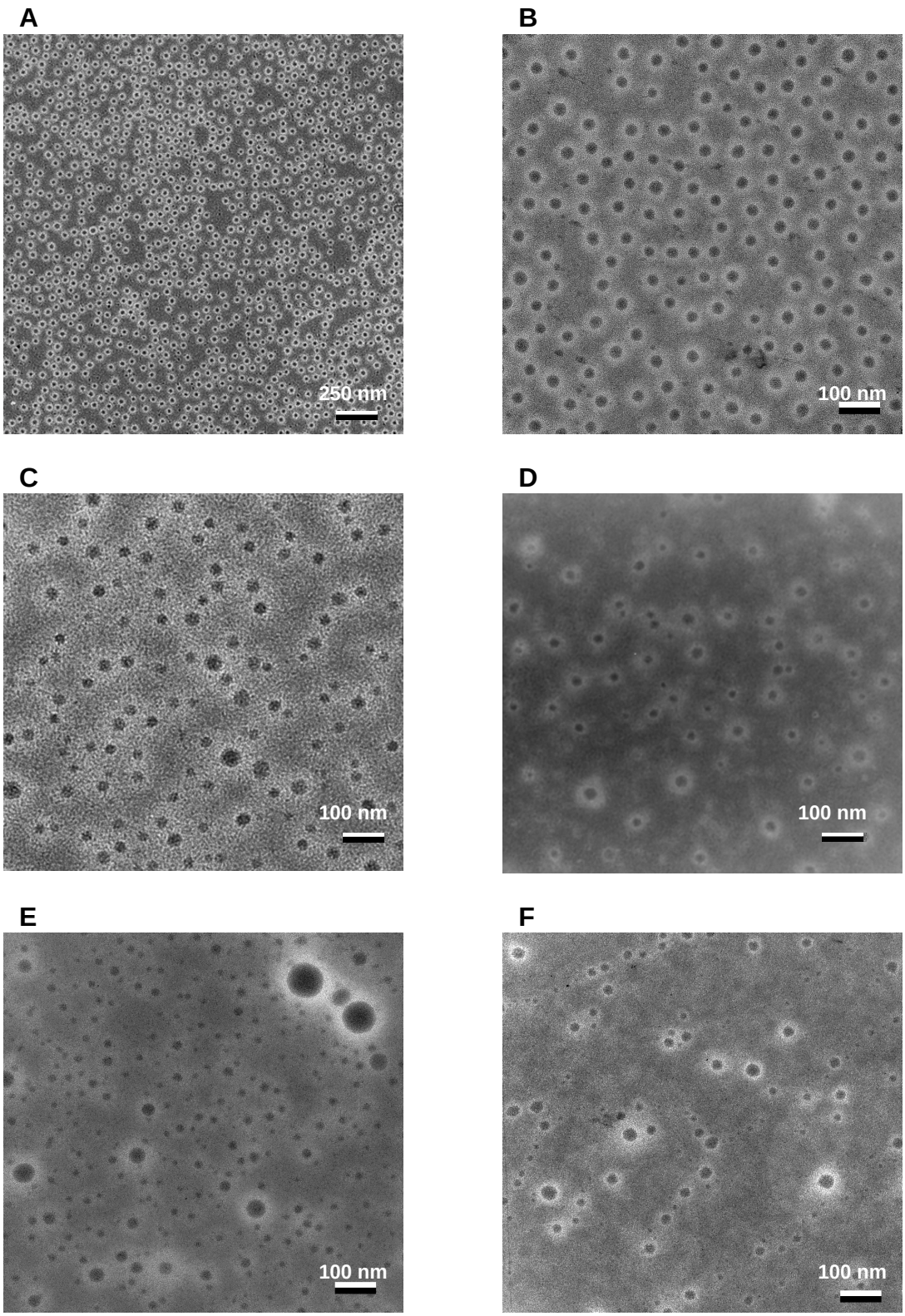

Figure 1. TEM images of polymer self-assemblies (samples were negative stained with uranyl acetate): A- an overview of $A_4B_{66}A_4$, B-$A_4B_{66}A_4$, C-$A_{17}B_{66}A_{17}$, D-$A_{62}B_{45}$, E-$A_{43}B_{45}$, and F-$A_{20}B_{45}$.

As was already discussed, the solvation effect of the PDMAEMA polyelectrolyte block can influence significantly the DLS results. Thus a dependence of the hydrodynamic radius on PDMAEMA block length in AB copolymer system was detected. This dependence was not, however, observed on NS-TEM images. Another factor that could contribute the different particle sizes detected by NS-TEM and DLS is the sample preparation. DLS measurements were carried out in solutions while deposition of the polymer self-assemblies onto the carbon grid implied sample drying that could cause shrinkage of the particles and thus smaller radii detected by NS-TEM. It should also be noted that during the preparation procedure particles can be flattened on the TEM grids due to the adsorption forces. These effects we expect to be more serious for AB compound micelles that represent aggregates of micelles with high polydispersity which were presumably less stable than ABA vesicles. Therefore, we do not discuss the absolute structural parameters. These effects are not expected in the cryo-EM.

Cryoelectron microscopy (Cryo-EM)

Figure 3 represents cryo-EM images of the diblock ($A_{43}B_{45}$) and triblock ($A_4B_{66}A_4$) copolymers embedded in a thin water film. We observed spherical self-assemblies of $A_{43}B_{45}$ copolymer with sizes ranging from 60 to 100 nm, which is in agreement with the polydispersity given by DLS. The uniform density inside the spheres is a sign that they are filled,[38, 39] pointing most probably to compound micelles (Scheme 2). Interestingly, the cryo-EM data revealed bigger sizes of the diblock self-assemblies than those shown by NS-TEM. The differences in the particle size can be explained by the assumption discussed above, namely that, in addition to the drying effect, the deposition of the particles on the TEM grid induce deformation of the self-assemblies. The cryo-EM images of the triblock copolymer solution (Figure 2, **B**) revealed homogeneously distributed self-assemblies composed of 25-30 nm spheres and "hairs" with lengths of about 15 nm around them (Figure 2, **B**, arrows). Furthermore, a magnified image clearly showed a thin shell around the spheres (Figure 2, **C**), which is a characteristic for vesicular membranes (Scheme 2).[40, 41]

It was surprising to observe such small vesicles since a small diameter means rather high curvature of the sphere. Hence we suppose that some copolymer chains aggregated outside of the vesicle or had a conformation at which they form so called "hairs" out of the vesicular membrane in order to stabilize the self-assembled system. Similar observations were recently reported for vesicles consisting of polystyrene-co-polyacrylic acid chains.[22]

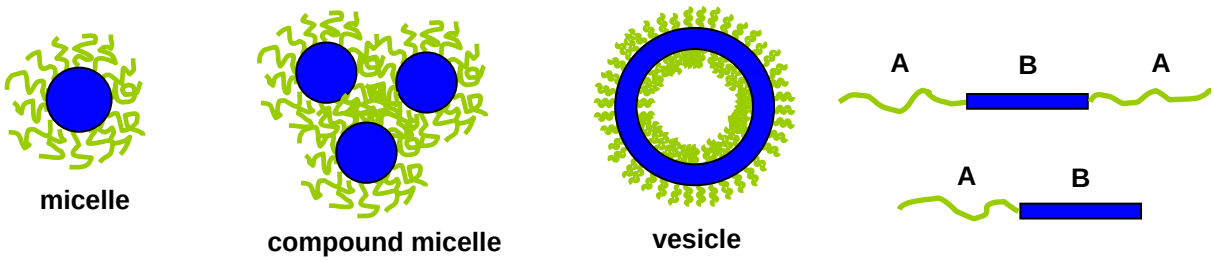

Scheme 2. Different types of self-assemblies: micelles, compound micelles, vesicles.

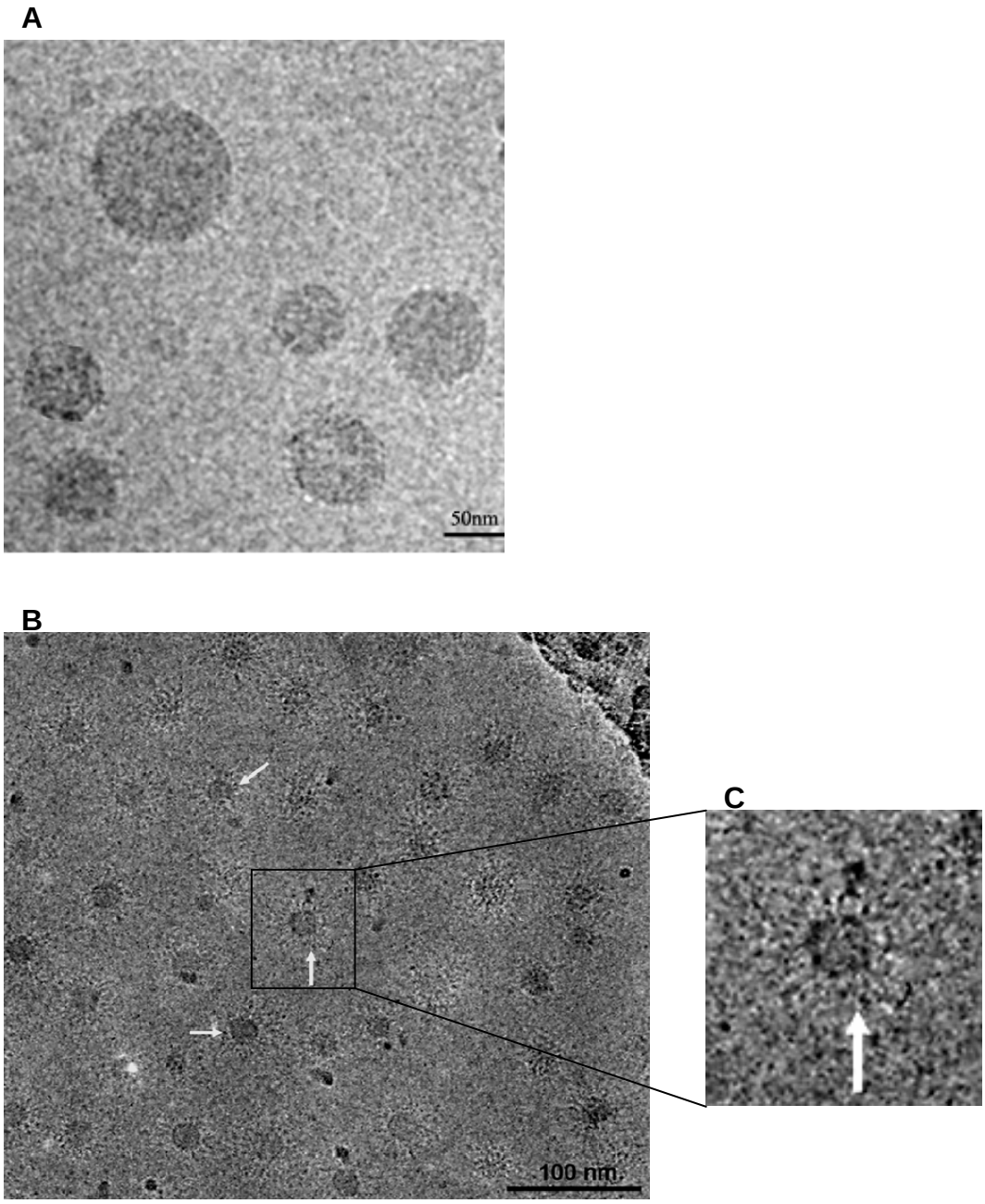

Figure 2. Cryo-EM images of $A_{43}B_{45}$ (A) and $A_4B_{66}A_4$ (B) copolymer self-assemblies.

The nature of these "hairs" is not yet clear to us, therefore further experiments to clarify their structure will be carried out in future. The overall size of triblock self-assemblies (spheres plus "hairs") was around 50 nm that is in agreement with NS-TEM results. Apparently, no significant changes occurred during sample preparation for NS-TEM measurements. This observation indicates that the morphology of the di- and triblock self-assemblies reflects different behaviour of the particles on the grid surface. Like for the case of diblock copolymer self-assemblies, the sizes of triblock copolymer particles given by cryo-EM appeared to be smaller than those measured with DLS. This variation was expected due to thick layer of water molecules around partly charged PDMAEMA chains.

Atomic force microscopy (AFM)

Additional information about the nature of the polymer self-assemblies was given by AFM. Similar results were obtained for $A_4B_{66}A_4$ and $A_{17}B_{66}A_{17}$ copolymer self-assemblies. Figure 3, **A** represents collapsed spheres of $A_4B_{66}A_4$ assemblies. All structures were approximately of the same size and had similar "M" profile shape, meaning that always the central part of the particle was settled down. This shape of dried self-assemblies is known for polymer vesicles[42,43] (Scheme 2) and results from evaporation of the inner water from the polymer spheres during sample drying causing a collapse of the central part. The crumpled vesicles had a diameter of 80-90 nm and height of 4-5 nm that corresponded to the diameter-to-height ratio around 20. Such a ratio is characteristic for the collapsed hollow structures.[35,44] However one should note that the vesicles were most probably flattened on the surface and inserted into a polymer film or another layer of vesicles below them as appeared from the phase images. This certainly influenced their sizes, and therefore we did not use AFM for further estimation of the self-assemblies dimensions. It is interesting to note that monitoring of the sample during two weeks after preparation did not reveal further deformation of the vesicles.

In contrary to triblock copolymer vesicles, the diblock copolymer self-assemblies showed different behavior (Figure 3, **B**). AB block copolymers formed a polymer film on the silicon substrate where spherical particles preferably stayed intact. No spherical particles on the silicon surface out of this film were detected. Imaging of the sample over weeks did not reveal any collapses or deformations of the self-assemblies. The cross-section profiles showed a spherical shape which is known for block copolymer assemblies containing no inner water.[45]

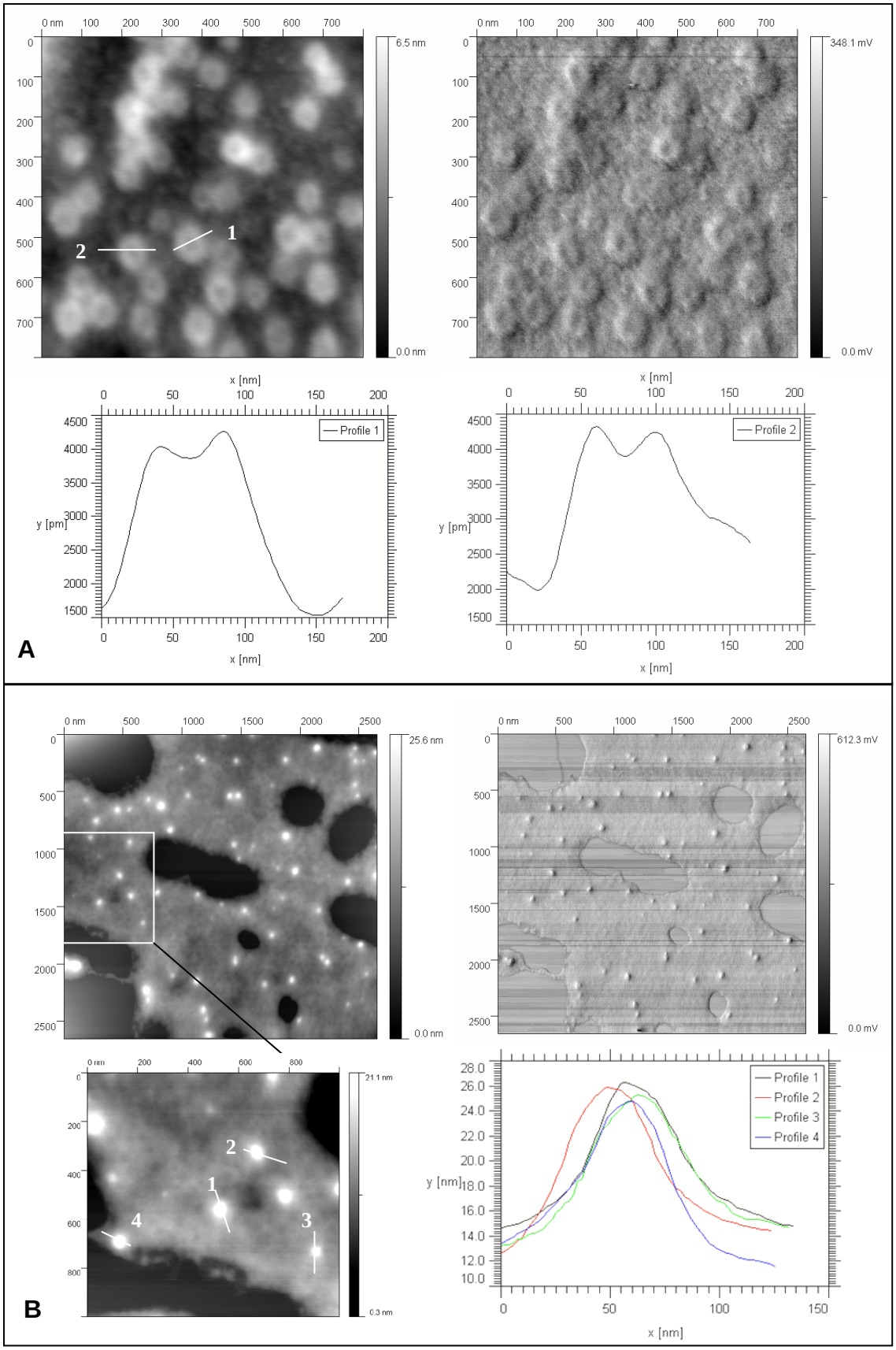

Figure 3. Tapping mode AFM analysis of $A_4B_{66}A_4$ (A) and $A_{20}B_{45}$ (B) self-assemblies on silicon substrate.

Hence, the AFM results indicated once again that the diblock copolymers formed compound micelles in aqueous media while the triblock copolymers self-aggregated into vesicular structures.

2.3.3. Cloud point effect

It is well known that some block copolymers, especially those containing cationic monomer units, polyethylene glycol blocks or polyalkylene oxide fragments reveal a cloud point effect.[46-50] The temperature response of the system is individual in each case and depends on parameters such as copolymer architecture, hydrophilic-to-hydrophobic ratio and others.[51] In our case, it was found that all copolymer aqueous solutions turned cloudy above a certain temperature that indicated an existence of a cloud point. Furthermore, the cloud point temperature (CPT) was different for different copolymers at the same concentration. Figure 4 illustrates the tendency of CPT to increase with increasing the hydrophilicity of the polymers. This tendency can be related to the solvation of the polymer molecule in aqueous solutions. Correspondingly, higher hydrophilicity of the polymer chain leads to a better solvation of the whole molecule and the CPT is shifted towards higher values.

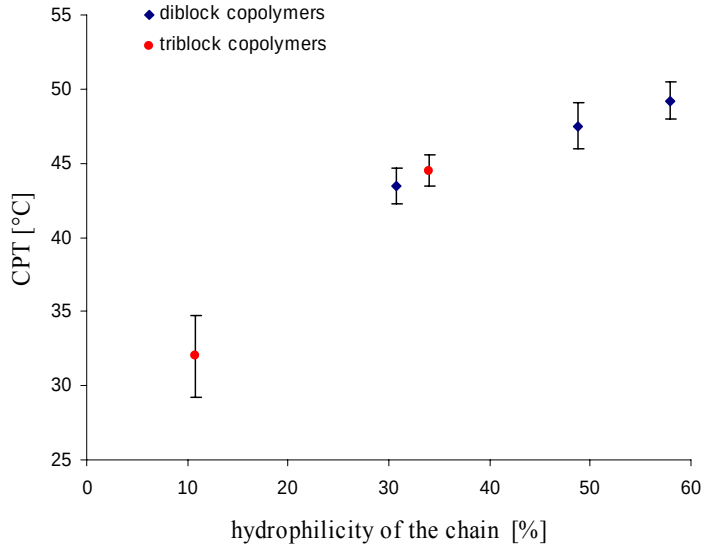

Figure 4. Dependence of the CPT on the polymer hydrophilicity. The hydrophilicity of the chain was calculated as a ratio between the molecular weight of the hydrophilic part and the molecular weight of the whole copolymer chain.

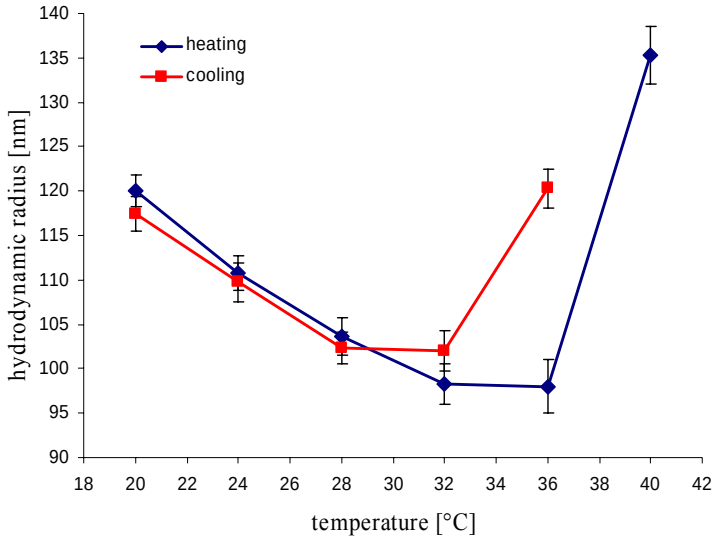

Figure 5. Dependence of the hydrodynamic radius on temperature in heating-cooling cycle ($PBMA_{45}$-$PDMAEMA_{20}$).

More detailed investigation of the polymer response to changes in temperature was performed with DLS (Figure 5). An aqueous solution of $PBMA_{45}$-$PDMAEMA_{20}$ was monitored during a heating-cooling cycle. For each measurement the system was equilibrated for 40 minutes. A slow decrease of the hydrodynamic radius was observed during heating until the solution became milky (36°C) followed by a sharp increase of the radius. The observed temperature induced changes were fully reversible in the range of 20°C - 30°C (Figure 5). Most likely, heating led to shrinking of the micelles (Scheme 3, ***a***) and, probably, desolvation of the hydrophilic block that resulted in "collapse" of the hydrophilic chains on the particle surface and therefore decrease of the sizes. Further heating (higher than 36°C) caused large increase of the R_h as well as PDI up to 0,4-0,5. We assume that the heating above 36°C initiated interchain association of the particles leading to the formation of large aggregates (Scheme 3, ***b***) and probably globules, which was accompanied by an increase in the polydispersity index. We observed a hysteresis effect during heating-cooling cycle in the temperature region where aggregation occurred, i.e. above 35°C (Figure 5). The same processes were found for aqueous solutions of ABA triblock copolymers.

Similar temperature induced changes in self-assembly were described for other copolymers,[52,53] though the majority of researchers reported increasing of the hydrodynamic radius during heating or jump in its value at temperature close to the cloud point.[54-56]

Remarkably, the copolymer self-assemblies repeated their temperature response every heating-cooling cycle, showing that these physical processes are reproducible.

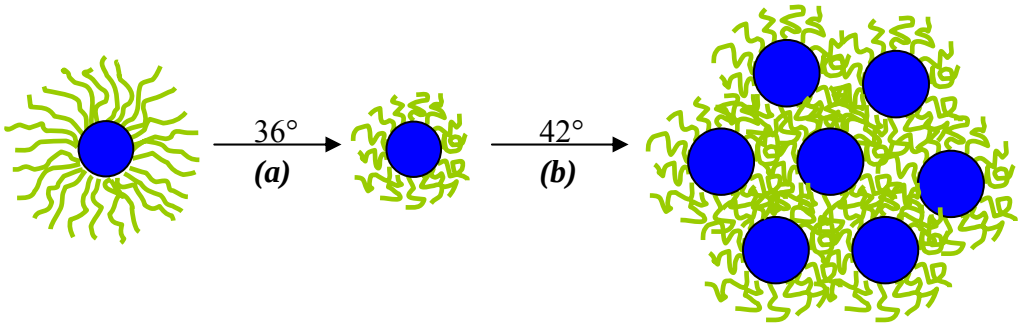

Scheme 3. Temperature induced reorganization of diblock polymer self-assemblies (shrinkage **(a)**, followed by interchain association upon additional heating **(b)**).

2.3.4. Confocal laser scanning microscopy (LSM) and fluorescence correlation spectroscopy (FCS)

LSM and FCS were used for additional characterization of the system. Alexa Fluor® 488 C_5-maleimide was incorporated into di- and triblock copolymer self-assemblies in aqueous solutions. Alexa Fluor® 488 C_5-maleimide penetrates into the hydrophilic part of the self-assemblies and can also interact with the PDMAEMA block via charge interactions. FCS measurements were performed in order to estimate the sizes of particles. Using this method we detected self-organized structures of di- and triblock copolymers with sizes from 40-70 nm applying the minimal laser intensity (8% from maximum power). It was found that the intensity of the laser at the constant exposure time had a strong influence on the particle sizes which might be related to the cloud point effect of these copolymer systems. We suppose that the laser impact led to a local heating followed by shrinkage of the copolymer assemblies. Thus, higher laser intensity induced more significant shrinkage and smaller radii of particles were detected respectively. In our opinion these observations are an indirect support for the suggested temperature-induced reorganization in the copolymer systems observed with DLS. LSM images gave an evident proof for the proposed mechanism of the cloud point effect. We observed the presence of huge agglomerates after heating of the copolymer solution (Figure 6, **A**). These dense agglomerates sedimented on the surface of the support and disappeared after cooling of the sample (Figure 6, **B**).

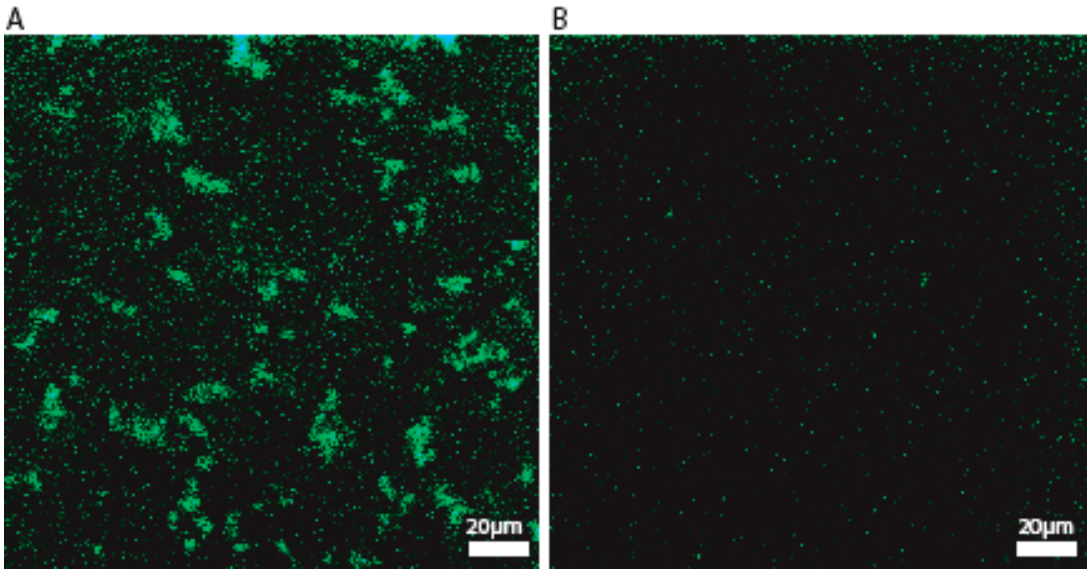

Figure 6. LSM image of PBMA45-PDMAEMA43 self-assemblies in aqueous solution (Alexa Fluor® 488 C5-maleimide dye): A–heating (50°C), B-cooling (20°C) (focus on the surface).

2.4. Summary

Amphiphilic di- and triblock copolymers with different ratio of hydrophobic to hydrophilic blocks and narrow polydispersity distribution were prepared by ATRP. The copolymer compositions were accurately established comparing data from GPC, ^{1}H NMR and VO.

Using a combination of different methods we showed that the diblock copolymers self-assembled in aqueous solution into micelles and compound micelles while triblock copolymers formed vesicular structures. Additionally, cryo-EM analysis showed that polymer chains oriented outside of the vesicles which might stabilize the self-assembly. Though the hydrophilic-to-hydrophobic ratio of the $A_{20}B_{45}$ and $A_{17}B_{66}A_{17}$ copolymers were similar, they exhibited different type of self-assembly. Apparently, the copolymer architecture (di- or triblock) plays important role for the macromolecular self-organization. DLS measurements revealed a dependence of the average hydrodynamic radius on PDMAEMA block length in case of diblock copolymers. However analysis of the dry samples did not show the same tendency which might be an indication for significant interaction between water molecules and polyelectrolyte PDMAEMA chains.

All block copolymers exhibited a cloud point effect which can be important information for future application of these macromolecules. We demonstrated that the cloud point

temperature raised as hydrophilicity of the chain increased. Thus, the hydrophobic-hydrophilic balance of the polymer chains contributes to the stability of the self-assembled structures. Moreover, we monitored a change of the hydrodynamic radius during heating-cooling cycle of the copolymer aqueous solutions. It was found by DLS, FCS and LSM that the heating caused shrinkage of the PDMAEMA block, while additional heating above CPT led to a subsequent aggregation. Furthermore, cooling of the system resulted in the reversible process.

These results illustrating the self-assembly behaviour of PBMA-PDMAEMA di- and triblock copolymers might be useful information for further studies towards their application.

2.5. Acknowledgement

The authors thank Per Rigler, Department of Chemistry, University of Basel, for the FCS measurements. This work was supported by NCCR Nanoscale Science, Swiss National Science Foundation and MRTN-CT-2003-505027.

2.6. References

[1] Kwon, G. S.; Kataoka, K. *Adv. Drug Deliv. Rev.* **1995**, *16*, 295.

[2] Kwon, G. S.; Okano, T. *Adv. Drug Deliv. Rev.* **1996**, *21*, 107.

[3] Kwon, G. S. *Crit. Rev. Ther. Drug* **1998**, *15*, 481.

[4] Discher, D. E.; Eisenberg, A. *Science* **2002**, *297*, 967.

[5] Nasseau, M.; Boublik, Y.; Meier, W.; Terhalter, M.; Fournier, D. *Biotechnol. Bioeng.* **2001**, *75*, 615.

[6] Rakhmatullina, E.; Braun, T.; Kaufmann, T.; Spillmann, H.; Malinova, V.; Meier, W. *Macromol. Chem. Phys.* **2007**, *208*, 1283.

[7] Huang, W.; Kim, J.-B.; Baker, G.; Bruening, M.L. *Nanotechnology* **2003**, *14*, 1075.

[8] Vriezema, D. M.; Aragone's, M. C.; Elemans, J. A. A. W.; Cornelissen, J. J. L. M.; Rowan, A. E.; Nolte, R. J. M. *Chem. Rev.* **2005**, *105*, 1445.

[9] Dai, S.; Ravi, P.; Tam, K. C.; Mao, B. W.; Gan, L. H. *Langmuir* **2003**, *19*, 5175.

[10] Yamamoto, Y.; Yasugi, K.; Harada, A.; Nagasaki, Y.; Kataoka, K. *J.Controlled. Release* **2002**, *82*, 359.

[11] Weaver, J. V. M.; Bannister, I.; Robinson, K. L.; Bories-Azeau, X.; Armes, S. P. *Macromolecules* **2004**, *37*, 2395.

[12] Antonietti, M.; Förster, S.; Hartmann, J.; Oestreich, S. *Macromolecules* **1996**, *29*, 3800.

[13] Patrickios, C. S.; Forder, C.; Armes, S. P.; Billingham, N. C. *J. Polym. Sci. A: Polym. Chem.* **1997**, *35*, 1181.

[14] Cameron, N. S.; Eisenberg, A.; Brown, G. R. *Biomacromolecules* **2002**, *3(1)*, 124.

[15] Nardin, C.; Hirt, T.; Leukel, J.; Meier, W. *Langmuir* **2000**, *16*, 1035.

[16] Zhu, J.; Jiang, Y.; Liang, H.; Jiang, W. *J. Phys. Chem. B* **2005**, *109(18)*, 8619.

[17] Grumelard, J.; Taubert, A.; Meier, W. *Chem. Commun.* **2004**, 1462.

[18] Ivanova, R.; Lindman, B.; Alexandridis, P. *Adv. Colloid Interface Sci.* **2001**, *89-90*, 351.

[19] Wang, L.; Chen, X.; Chai, Y.; Hao, J.; Sui, Z.; Zhuang W.; Sun, Z. *Chem. Commun.* **2004**, 2840.

[20] Zhang, L.; Eisenberg, A. *Polym. Adv. Technol.* **1998**, *9*, 677.

[21] Soo, P. L.; Eisenberg, A. *J. Polym. Sci. B: Polym. Phys.* **2004**, *42*, 923.

[22] Luo, L.; Eisenberg, A. *J. Am. Chem. Soc.* **2001**, *123*, 1012.

[23] Sun, Q.; Tong, Z.; Wang, C.; Ren, B.; Liu, X.; Zeng, F. *Polymer* **2005**, *46(13)*, 4958.

[24] Klitzing, R.; Wong, J. E.; Jaeger, W.; Steitz, R. *Curr. Opinion in Colloid and Interface Sci.* **2004**, *9*, 158.

[25] Szczubiaska, K.; Jankowska, M.; Nowakowska, M. J. *Mater. Sci.: Materials in Medicine* **2003**, *14(8)*, 699.

[26] Pefferkorn, E.; Varoqui, R.; Benoit, H. *J. Appl. Polym. Sci.* **2003**, *19(10)*, 2929.

[27] Narrainen, A. P.; Pascual, S.; Haddleton, D. M. *J. Polym. Sci. A, Polym. Chem.* **2002**, *40*, 439.

[28] Mori, S. *J. Liquid Chromatogr.* **1990**, *13*, 1719.

[29] Tanford, D. *Physical Chemistry of Macromolecules*, Wiley: New York, 1961; p. 287.

[30] Bednarek, M.; Biedron T.; Kubisa, P. *Macromol. Chem. Phys.* **2000**, *201*, 58.

[31] Jakes, J. *Czech. J. Phys.* **1988**, *B38*, 1305.

[32] Burchard, W. In *Physical techniques for the study of food biopolymers*; Ross-Murphy, S. B., Ed.; Blackie Academics and Professional: New York, 1994; p. 151.

[33] Riegel, I. C.; de Bittencourt, F. M. O.; Eisenberg, A.; Petzhold, C. L.; Samios, D. *Pure Appl. Chem.* **2004**, *76(1)*, 123.

[34] Wu, C.; Zhou, S. Q. *Phys. Rev. Lett.* **1996**, *77*, 3053.

[35] Xie, D.; Jiang, M.; Zhang, G.; Chen, D. *Chem. Eur. J.* **2007**, *13*, 3346.

[36] Hunter, D. G. and Frisken, B. J. *Biophysical J.* **1998**, *74*, 2996.

[37] Lasic, D. D. *Liposomes: from physics to applications*, Elsevier science publishers B. V., 1993; p. 195.

[38] Radowski, M. R.; Shukla, A.; von Berlepsch, H.; Böttcher, C.; Pickaert, G.; Rehage, H.; Haag, R. *Angew. Chem. Int. Ed.* **2007**, *46*, 1265.

[39] Colombani, O.; Ruppel, M.; Burkhardt, M.; Drechsler, M.; Schumacher, M.; Gradzielski, M.; Schweins, R.; Müller, A. H. E. *Macromolecules* **2007**, *40*, 4351.

[40] Hamley, I. W. *Nanotechnology* **2003**, *14*, R39.

[41] Photos, P. J.; Bacakova, L.; Discher, B.; Bates, F. S.; Discher, D. E. *J. Controlled Release* **2003**, *90*, 323.

[42] Seo, S. H.; Chang, J. Y.; Tew, G. N. *Angew. Chem. Int. Ed.* **2006**, *45*, 7526.

[43] Dominguez-Gutierrez, D.; Surtchev, M.; Eiser, E.; Elsevier, C. J. *Nano Lett.* **2006**, *6(2)*, 145.

[44] Wang, Y.; Zhang, J.; Wang, Z.; Wang, Z.; Yang, B. *Colloids and Surfaces A: Physicochem. Eng. Aspects* **2007**, *292*, 159.

[45] Katsampas, I.; Roiter, Y.; Minko, S.; Tsitsilianis, C. *Macromol. Rapid Commun.* **2005**, *26*, 1371.

[46] Liu, X-M.; Yang, Y-Y.; Leong, K. W. *J. Colloid and Interface Sci.* **2003**, *266*, 295.

[47] Li, C.; Tang, Y.; Armes, S. P.; Morris, C. J.; Rose, S. F.; Lloyd, A. W.; Lewis, A. L. *Biomacromolecules* **2005**, *6(2)*, 994.

[48] Ma, Y.; Tang, Y.; Billingham, N. C.; Armes, S. P.; Lewis A. L.; Lloyd A. W. & Salvage J. P. *Macromolecules* **2003**, *36*, 3475.

[49] Soga, O.; van Nostrum, C. F.; Ramzi, A.; Visser, T.; Soulimani, F. *Langmuir* **2004**, *20*, 9388.

[50] Neradovic, D.; Soga, O.; van Nostrum, C.F.; Hennik, W. E. *Biomaterials* **2004**, *25*, 2409.

[51] Dimitrov, P.; Rangelov, S.; Dworak, A.; Tsvetanov, C.B. *Macromolecules* **2004**, *37*, 1000.

[52] Cai, Y.; Tang, Y.; Armes, S. P. *Macromolecules* **2004**, *37(26)*, 9728.

[53] Verbrugghe, S.; Laukkanen, A.; Aseyev, V.; Tenhu, H.; Winnik, F. M.; Du Prez, F. E. *Polymer* **2003**, *44*, 6807.

[54] Rangelov, S.; Dimitrov, P.; Tsvetanov, C. B. *J. Phys. Chem. B* **2005**, *109*, 1162.

[55] Kjoniksen, A.; Laukkanen, A.; Galant, C.; Knudsen, K. D.; Tenhu, H.; Nystriom, B. *Macromolecules* **2005**, *38(3)*, 948.

[56] Liu, X-M.; Pramoda, K. P.; Yang, Y-Y.; Chow, S. Y.; He, C. *Biomaterials* **2004**, *25*, 2619.

3. Solid Supported Block Copolymer Membranes through Interfacial Adsorption of Charged Block Copolymer Vesicles

Ekaterina Rakhmatullina[1], Wolfgang Meier[1]

[1] Department of Chemistry, University of Basel, Klingelbergstrasse 80, CH-4056

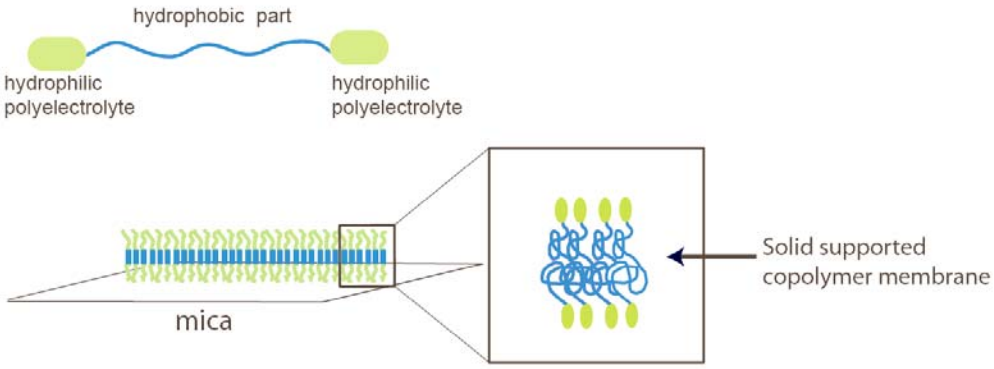

Published in: *Langmuir* **2008,** *24,* 6254

3.1. Introduction

Amphiphilic block copolymers offer unique possibilities for the structural control of materials at the nanoscopic length scale. Compared to other amphiphiles such as surfactants and lipids, their self-assembly is often more tolerant towards introduction of different chemical groups which allows tailoring of the polymer self-assembly properties for specific applications.[1] This can, for example, be exploited to stabilize or destabilize the macromolecules or the corresponding superstructures in a controlled manner.[2]

Depending on the chemical constitution, block length ratio, concentration and molecular architecture, amphiphilic block copolymers can aggregate into micelles,[3-5] vesicles,[6-12] tubes,[13] membranes[14] and liquid crystalline phases.[15] Block copolymer membranes and vesicles can serve as model systems of biological membranes, that even allow the reconstitution of integral membrane proteins.[16-18] Previous experiments showed that inserted membrane proteins seem to be stabilized and protected inside the polymer membranes.[17] In this context it should be noted that despite various stabilization strategies applied during the last decades,[19-25] the more commonly used phospholipid membranes[26-29] frequently lack the necessary chemical and mechanical stability for long-term technical applications. In contrast to lipid membranes, the block copolymer membranes' physical properties, like membrane thickness, permeability fluidity and stability can conveniently be tailored via their molar mass and chemical constitution.[30] These possibilities potentially allow preparing air-stable polymer membrane systems that could, for example, be interesting for odorant sensing. Such biosensor applications usually require a controlled and reproducible immobilization of either defect-free planar membrane structures or intact vesicles on solid supports. The type of supported structure that might be formed from a vesicular dispersion is directly related to the mechanical stability of the vesicles and the strength of the interactions between the aggregates and the surface. This was extensively investigated for lipid vesicles using different analytical techniques including impedance spectroscopy,[31] surface plasmon resonance,[32-34] surface plasmon fluorescent spectroscopy,[34] quartz crystal microbalance with dissipation monitoring[35-37] and atomic force microscopy.[37-41] However, the organization of the amphiphilic polymer vesicles on the solid supports has rarely been studied so far.[42]

Here we used AFM investigations to study the interactions of block copolymer vesicles with three different model surfaces. Since our long-term goal is the development of air-stable, solid supported membrane systems, a major focus of our experiments was on dry samples. The vesicles were based on an amphiphilic poly(2,2-dimethylaminoethyl methacrylate)-

block-poly(n-butyl methacrylate)-block-poly(2,2-dimethylaminoethyl methacrylate) (PDMAEMA-PBMA-PDMAEMA) triblock copolymer (Scheme 1).

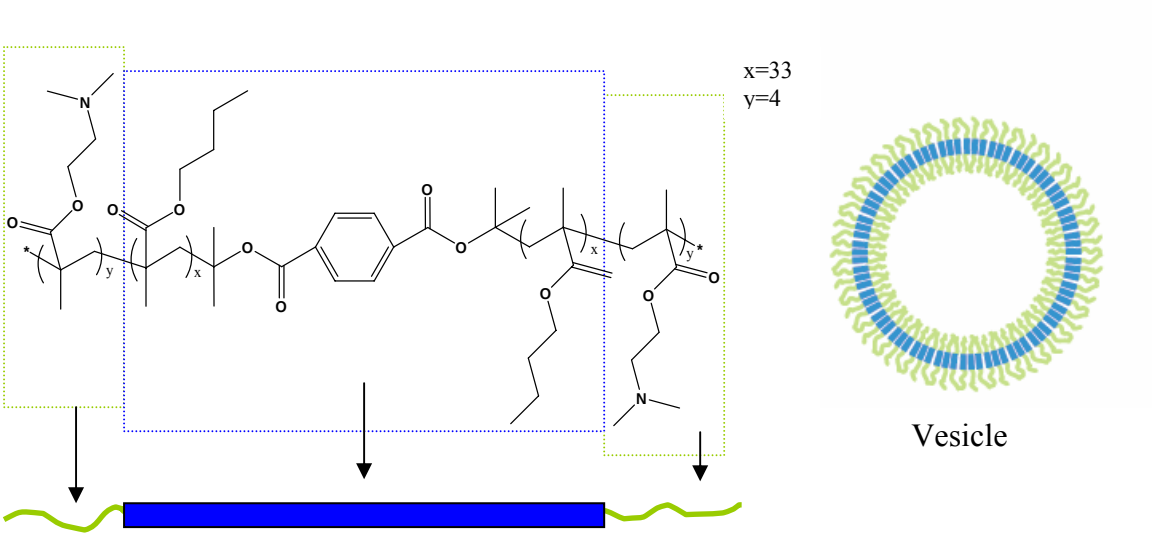

Scheme 1. The chemical composition of the amphiphilic triblock $PDMAEMA_4$-$PBMA_{66}$-$PDMAEMA_4$ copolymer (left) and the structure model of the vesicular self-assemblies (right).

A detailed description of the copolymer synthesis and the characterization of its self-assembly behavior in aqueous solution were reported before.[43] Since the hydrophilic PDMAEMA end blocks are polycationic (pKa= 7.3[44]), the outer surface of the resulting vesicles is positively charged.[45-47] This allows using electrostatic interactions in order to immobilize vesicles on negatively charged surfaces. The surface roughness can significantly influence the process of molecular organization,[48, 49] therefore we used three types of molecularly smooth supports for our experiments, i.e. graphite (HOPG), silicon oxide and muscovite mica, which mainly differed in their polarity and charge density. While HOPG is hydrophobic and chemically inert, the muscovite mica ($KAl_2(Si_3AlO_{10})(F, OH)_2$) surface is strongly hydrophilic and has a high density of negative surface charges.[50, 51] The silicon oxide surface is only weakly anionic, and its surface charge density increases with increasing pH.[52] This trend is also directly reflected in contact angle measurements (see Table 1). To avoid roughening of the surface we applied a rather mild cleaning procedure for the silicon oxide substrate. Hence, some carbon contaminants might still be present on the surface, thus resulting in a rather high contact angle (see Table 1) Note, that we kept all other parameters,

such as temperature (22°±1C) and pH of the solutions (pH=8.0) constant throughout the AFM experiments.

Analyzed sample	Contact angle value, °
Cleaved mica	3.0±0.2
Mica, covered by copolymer membrane	49.3±1.7
Silicon oxide	39.9±2
HOPG	87.5±2

Table 1. Wetting properties of different surfaces.*

* Bidistilled water was used for the contact angle measurements

3.2. Experimental Section

3.2.1. Materials

Poly (2,2-dimethylaminoethyl methacrylate)-block-poly(n-butyl methacrylate)-block-poly(2,2-dimethylaminoethyl methacrylate) ($PDMAEMA_4$-$PBMA_{66}$-$PDMAEMA_4$) was synthesized and characterized as described earlier.[43] The number average molecular weight of the copolymer was 11200 g/mol and the polydispersity index was relatively low (1.2) as a result of the atom transfer radical polymerization followed by a complex purification procedure.[43]

Ethanol (absolute, 99.8%) was obtained from Fluka. Mica was received from BAL-TEC AG. Polished silicon wafers were purchased from GRINM Semiconductor Materials Co. Highly oriented pyrolytic graphite (HOPG) SPI-3 grade was obtained from Schaefer AG. 0.8 μm filters Durapore-PVDF were acquired from Millipore corporation.

3.2.2. Methods

Atomic force microscopy (AFM)

Tapping mode AFM analysis of the samples was performed using PycoLE system, Molecular Imaging, and silicon nitride cantilevers, k=42 N/m, scan rate 1 line/s. Images were recorded in height, amplitude and phase modes with a size of 512 x 512 pixels. Height images were

flattened and plane adjusted. All measurements were performed on the height images; however, some processes were visible with better contrast in the phase mode.

An aqueous solution of block copolymer was deposited on the corresponding substrate and left for two minutes. The samples were washed three times with bidistilled water to remove the wetting layer of the polymer solution, and then dried at room temperature. Different areas of the sample were monitored. Experiments were performed in the dry state, at an average air humidity of 40-50% and temperature of 22±1°C.

Fourier Transform Infrared spectroscopy (FTIR)

FTIR measurements were acquired using a FTIR-8400S spectrophotometer, Shimadzu. Spectra were recorded with 128 scans for the blank mica surface and the sample, with 2 cm^{-1} resolution.

Contact angle determination

All measurements were performed using the plate method with a Tensiometer K100MK2, Krüss Gmbh. Bidistilled water was applied for the analysis. The presented results were taken as average values from three measurements.

Ellipsometry

Film thickness was determined using a spectroscopic multi-angle ellipsometer (SENTECH SE 850-STE, Sentech Instruments Gmbh) measuring at three angles (45°, 55°, and 65°). Measurements were carried out on the samples in dry state and at room temperature.

Dynamic Light Scattering

DLS studies were carried out using a commercial goniometer (ALV-Langen) equipped with He-Ne laser (λ=633 nm) at scattering angles between 30° and 150°. An ALV-5000/E correlator calculates the photon intensity autocorrelation function $g^2(t)$. The cell was mounted in thermostatic optical matching vat with a temperature accuracy of T=0.02 K. Experiments were performed at T=293 K.

3.2.3. Substrate preparation

Muscovite mica, silicon wafers and HOPG surfaces were used for the AFM investigations.

Mica and HOPG slides were cleaved and applied directly for the analysis. Silicon wafers were cleaned with ethanol and bidistilled water and dried in the nitrogen stream.

3.2.4. Preparation of the copolymer vesicles

50 mg of the block copolymer was dissolved in 500 mg of ethanol. This solution was added dropwise into bidistilled water to obtain 10 ml of final copolymer dispersion. Two different concentrations were prepared by further dilution of this copolymer dispersion in bidistilled water. All samples were filtered through 0.8 μm filter (Millex Durapore-PVDF, Millipore) prior to investigation. Dynamic light scattering measurements were performed for each sample just before AFM experiments in order to check that only one fraction of vesicles with a narrow polydispersity was present in the solution.

The aqueous dispersion of the vesicles had a pH=8.0 (PDMAEMA, pKa= 7.3[44]). To investigate the influence of pH changes on the adsorption behavior of the polymer vesicles (see supporting information), the pH of the dispersions was adjusted in a range from pH = 5 to 9 by addition of HCl or NaOH, respectively.

3.3. Results and discussion

Self-assembly behavior of the $PDMAEMA_4$-$PBMA_{66}$-$PDMAEMA_4$ copolymer was reported before.[43] Briefly, this amphiphilic copolymer self-organized in aqueous solution into small vesicles with a diameter of 45-50 nm as determined from cryo- transmission electron microscopy (cryo-TEM) and transmission electron microscopy (TEM) images. Dynamic light scattering analysis (DLS) showed only one fraction of self-assemblies with a hydrodynamic radius of 56 nm and a polydispersity index of 0.16,[43] which was similar to that of lipid vesicles.[53, 54]

Since our block copolymers are amphiphilic polyelectrolytes we expected the interactions between the vesicles and the substrates to be dominated by electrostatic forces. In our experiments the strength of this interaction was mostly determined by the nature of the substrates as other parameters were constant. The charge density of the surfaces and their hydrophilicity decreased as: mica-SiO_2-HOPG (Table 1). Theoretically, the equilibrium of interchain interactions and forces between macromolecules and substrates determines the integrity of the vesicles on the particular surface.

All measurements were carried out on dried samples since we aimed to obtain air-stable solid-supported block copolymer structures. Particularly for mica and silicon oxide surfaces control experiments with wet samples did not show significantly different surface structures,

thus confirming the stability of the immobilized polymer superstructures upon drying (see supporting information for a representative example, Figure 2).

3.3.1. Block copolymer vesicles on HOPG

Cleaved HOPG was the most hydrophobic of the applied surfaces (contact angle of 87.5°, Table 1) and electrically neutral. Therefore, we did not expect attractive interactions between the outer hydrophilic polyelectrolyte shell of the block copolymer vesicles and the hydrophobic surface.

In order to observe the behavior of the polymer vesicles we covered the HOPG surface with vesicle dispersions containing 0.1 wt.% and 0.5 wt.% polymer, respectively. Afterwards, the surfaces were rinsed with bidistilled water, dried and analyzed by AFM. The images of the samples prepared by deposition of the 0.1 wt.% and 0.5 wt.% vesicular dispersions showed no difference. Therefore, we present here only samples where a 0.5 wt.% vesicular dispersion was used for the analysis.

Figure 1, A, D, shows the AFM images of the deposited block copolymer on the HOPG substrate. The images revealed that the surface was covered by an inhomogeneous polymer film containing spherical objects with a diameter around 100 nm and many holes. Within the holes the surface showed the same roughness as the original bare HOPG (Figure 1, B) indicating that in these areas no adsorption of the polymer occurred. Around the holes, a smooth rim about 20 nm broad with a mean thickness of 1.5±0.04 nm was found. The thickness of the rims was measured as an average from 22 cross-section profiles taken from the analysis of different sample areas (see Supporting information, Table 1). Figure 1, C shows the cross section profiles of two rims as representative examples. Remarkably, the thickness of the block copolymer membrane in vesicles was previously estimated around 4-5 nm.[43] This implies that the 1.5±0.04 nm rims presumably consisted of a block copolymer monolayer in which the hydrophobic PBMA blocks were adsorbed onto the hydrophobic graphite while the hydrophilic end blocks were pointing upwards. Indeed, the presence of the copolymer vesicles on top of the film indicated that its upper part was hydrophilic, i.e. the PDMAEMA groups were oriented outside of the layer (Scheme 2, A).

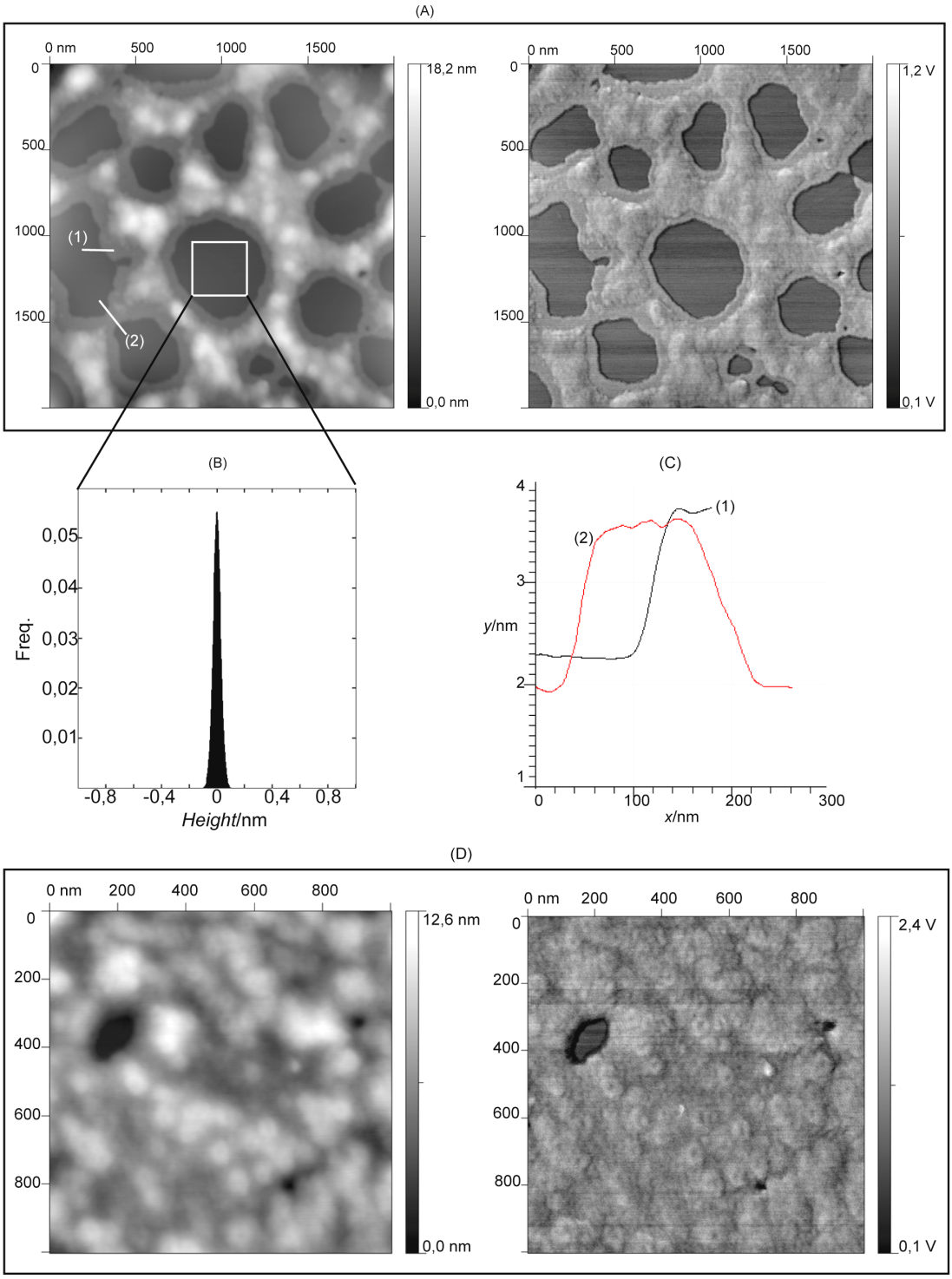

Figure 1. Copolymer self-organization on the HOPG substrate. (A) Overview, topography (left) and phase (right) modes are presented. The HOPG substrate is only partially covered by copolymer material. The "holes" are surrounded by rim-like copolymer structures. (B) Surface histogram of the uncovered part of the substrate demonstrates a low surface roughness identical to the bare HOPG substrate. (C) Typical cross section profiles of the periphery rims. The average thickness of the rims was 1.5±0.04 nm (see Supporting information). (D) Zoom in the surface area covered by copolymer material represents round structures that are collapsed in their central part (left-topography mode, right-phase). The collapsed copolymer vesicles are visible with better contrast in the phase mode (right).

Since a fully stretched triblock copolymer molecule would have a length of 18.5 nm (C-C bonds, 1.5 Å, 109.28°), a film thickness of 1.5 nm presumably corresponds to a strongly adsorbed PBMA middle block adopting a flat, "pancake" like conformation on the surface (Scheme 2, A). It should be noted that the vesicular structures were restricted to the areas covered by the copolymer layer (see Figure 1, D). It seems that a direct contact between the PDMAEMA brushes on the surface of the vesicles and the HOPG substrate was not favorable and led to reassembly of the macromolecules to a block copolymer monolayer. This monolayer provided a more hydrophilic PDMAEMA surface that allowed immobilization of intact vesicles.

The incomplete coverage of the surface was most probably induced upon dehydration of the PDMAEMA blocks during the drying process and resulted in surface patterns that strongly resembled a dewetting phenomenon. The dry patches on the surface grew over a time scale of several days and after 6 days the film was completely transformed into droplet like structures (see Supporting information, Figure 1). Similar behavior was recently reported for other polymer films.[55-57]

3.3.2. Block copolymer vesicles on silicon oxide

As shown in Table 1, silicon oxide is hydrophilic with a contact angle of 39.9°. At neutral pH the surface is slightly charged,[58] with a charge density of 0.15 e^-/nm^2.[59] Since the copolymer chains are weakly cationic due to partial protonation of the PDMAEMA blocks, we expected electrostatic interactions between the vesicles and the substrate to become more important.

Deposition of a 0.1 wt.% vesicular dispersion on the SiO_2 surface resulted in the adsorption of intact vesicles. Figure 2, B, represents vesicular structures distributed on the surface. A more detailed examination of the surface around the particles revealed that its roughness was identical to that of the clean SiO_2 substrate (Figure 2, C, D). Obviously, the adsorbed copolymer vesicles remained morphologically intact at this concentration even in the dry state (Scheme 2, B). This allowed us to perform a more accurate characterization of the vesicular structures that is presented below.

During the drying process the vesicles must collapse as a result of the water evaporation from their inner cavity. Hence, the height of the collapsed vesicles on the surface must correspond to twice the membrane thickness of the vesicle in solution.[60] Indeed AFM had already been previously used to determine the thickness of vesicular walls with a vertical resolution of below 1 nm.[61-63]

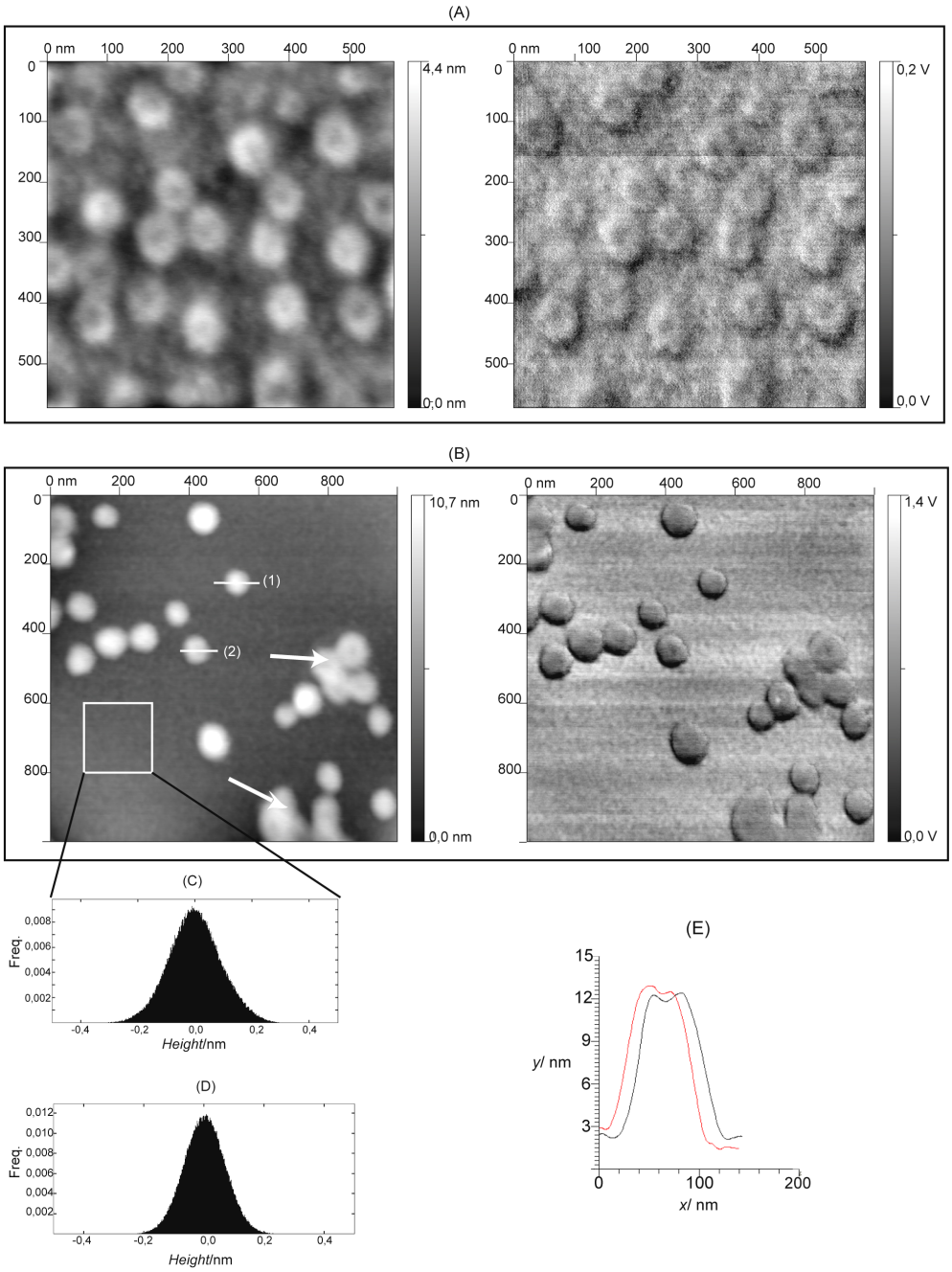

Figure 2. AFM images of the silicon oxide substrate after deposition of the vesicular dispersions. (A) Deposition of the 0.5 wt. % dispersion on the SiO_2 surface. Image (left-topography mode, right-phase) reveals numerous collapsed copolymer vesicles (donut-like structures, see text). The surface roughness of the background as well as the phase information indicates that the vesicles are adsorbed onto a polymer film. (B) Copolymer vesicles on the silicon oxide surface deposited from the 0.1 wt.% dispersion (left-topography mode, right-phase). Arrows on the image point at the fusion of the vesicles that are close to each other. (C) Surface histogram of the sample area uncovered by vesicles. White frame shows the region of interest taken for the histogram analysis. (D) Histogram of the clean silicon oxide wafer that was used for the AFM experiments. (E) Typical cross section profiles of the copolymer vesicles on SiO_2 surface. The mean height of the collapsed vesicles was 9.4±0.1 nm (see Supporting information).

We analyzed the cross section profiles of collapsed vesicles and determined their average height to be 9.4±0.1 nm (See Supporting information, Table 2). Figure 2, E shows two representative examples of profiles across the intact vesicles on the SiO_2 surface. The diameter of the collapsed vesicles was found around 100 nm, which results in a diameter-to-height ratio of about 10. This ratio is typical for the collapsed hollow spheres on surfaces.[64,65] Since the determined height corresponds to a twice that of a vesicular wall (Scheme 2, B), the thickness of an individual vesicle membrane must correspond to half of that value, i.e. ca 4.7 nm. It has to be emphasized that this value correlates well with cryo-TEM data of the same system[43] that showed 4-5 nm thick membranes for vesicular structures in solution.

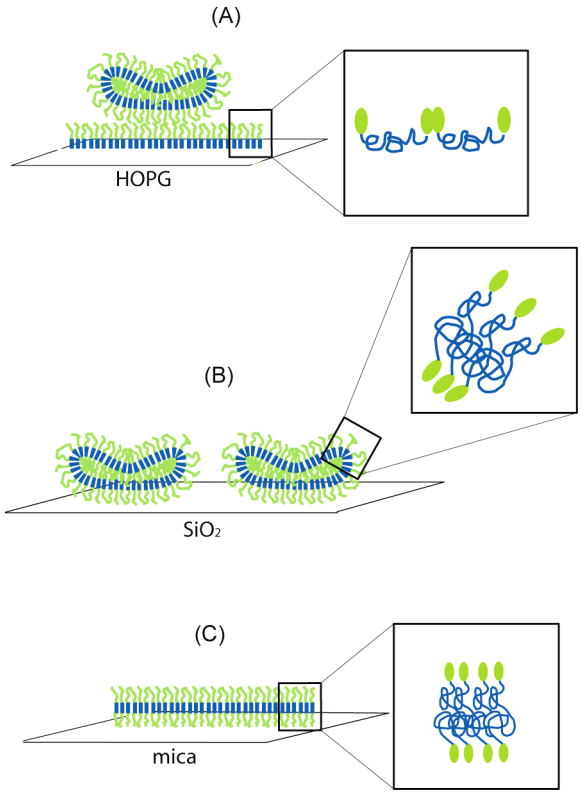

Scheme2. Models of the copolymer self-organization on different substrates. (A) HOPG, (B) silicon oxide, (C) mica. This scheme does not depict the dimensions of the objects.

A closer inspection of Figure 2, B, (topography image, arrows) revealed that in areas with tightly packed vesicles the particles started to fuse to larger aggregates. Similar behavior is

known from surface immobilized liposomes constituted from the natural lipids where this process finally may result in the formation of a planar, solid-supported lipid bilayer.[66]

To test whether this might also be the case in our system, we carried out experiments with vesicle dispersions having a higher concentration. For a concentration of 0.5 wt.%, AFM revealed not only collapsed vesicles but also an additional continuous block copolymer layer into which these vesicles were partially embedded (Figure 2, A). The surface histogram of the background layer (data are not presented) showed an increase of the surface roughness compared to that of the silicon oxide wafer (Figure 2, D). This film is presumably a (multi)layer of supported block copolymer membranes that resulted from fusion of block copolymer vesicles.

3.3.3. Block copolymer vesicles on mica

Mica had the most hydrophilic surface among our applied systems (contact angle of 3°, Table 1) and the highest negative charge density (~ 2 e^-/nm^2,[67]). Deposition of a 0.1 wt.% vesicular dispersion on mica surface led to the formation of a smooth homogeneous copolymer film. By screening the whole surface of the sample, we could not detect any defects (e. g. holes) in the film or intact vesicular structures. Figure 3, A shows a 5 x 5 μm overview of the sample where only continuous film is visible in topography and phase mode. FTIR measurements confirmed the presence of a block copolymer film on mica (Figure 4). A peak of the carbonyl group at 1730 cm^{-1} and signals of the CH, CH_2 and CH_3 groups in the range of 2765-2965 cm^{-1} can clearly be attributed to the methacrylate polymer chains on the surface. Moreover, the surface histograms showed that the roughness of the copolymer film significantly increased (Figure 3, B) compared to the „molecularly smooth“ mica surface (Figure 3, C). This observation was in good agreement with recently reported data on block copolymer membranes that were generated by a surface initiated polymerization.[68] The increase of the surface roughness can be explained by the block copolymer polydispersity and organization of the polymer chains within the film.[68] The formation of a less hydrophilic block copolymer layer was also reflected by contact angle measurements that revealed an increase from 3.0° (cleaved mica) to 49.3°, i.e. a value that is close to that of previous measurements on block copolymer films with the same hydrophobic (PBMA) and hydrophilic (PDMAEMA) blocks.[68]

This complete reorganization of the copolymer chains from vesicular structures towards a planar membrane indicated that in this system the electrostatic interactions between charged PDMAEMA blocks and the mica surface were much stronger than the interchain interactions

responsible for the integrity of the vesicles. The same tendency was reported by Zhao and coworkers for diblock phosphorylcholine copolymers.[58] According to the previous reports on lipid vesicles,[69, 70] we can assume that the $PDMAEMA_4$-$PBMA_{66}$-$PDMAEMA_4$ copolymer vesicles started to fuse and disrupt on the negatively charged mica surface and finally formed a continuous stable solid supported membrane. In this case the thickness of the copolymer membrane should directly correlate to the thickness of the vesicular walls. The homogeneity of the film allowed us to use ellipsometry to measure the thickness of the membrane. The average thickness was found to be 3.9±0.3 nm. As was mentioned above, the thickness of the $PDMAEMA_4$-$PBMA_{66}$-$PDMAEMA_4$ membranes obtained from cryo-TEM images was around 4-5 nm,[43] i.e. in agreement with ellipsometry data. A possible model of the copolymer self-organization on mica is represented in Scheme 2, C.

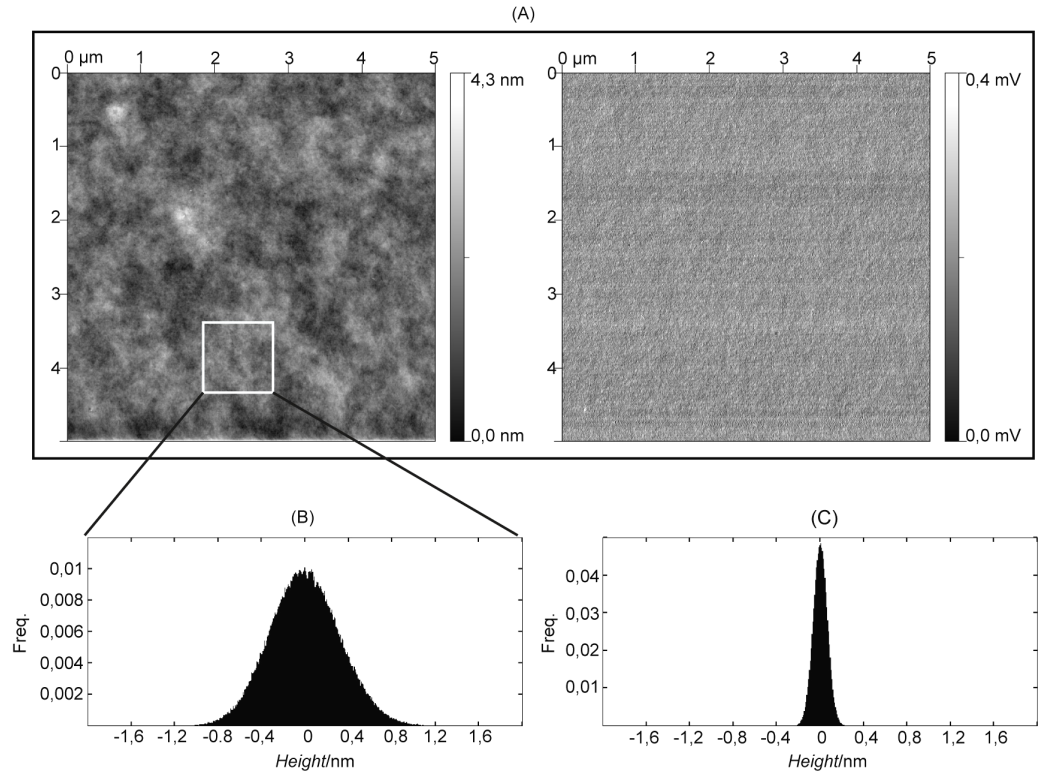

Figure 3. Self-assembly of the copolymer chains on freshly cleaved mica. (A) Copolymer membrane on mica (left-topography mode, right-phase), obtained by deposition of the 0.1 wt.% vesicular dispersion onto the mica substrate. A large 5 µm x 5 µm area of the sample is presented to demonstrate that the continuous copolymer film is defect-free. Surface histogram of the mica surface after (B) and before (C) deposition of the vesicles demonstrates increase of the surface roughness.

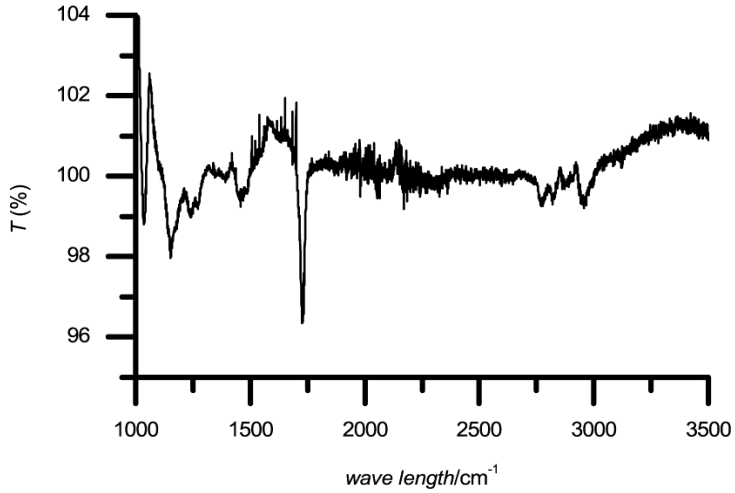

Figure 4. FTIR spectrum of the copolymer membrane on mica. Spectrum recorded using 128 scans and cleaved mica as a blank substrate. A peak of the carbonyl group at 1730 cm-1 and signals of the CH, CH_2 and CH_3 groups in the range of 2765-2965 cm-1 belong to the methacrylate polymer chains on the surface.

Remarkably, the theoretical length of the completely stretched $PDMAEMA_4$-$PBMA_{66}$-$PDMAEMA_4$ molecule is around 18.5 nm (1.5 Å C-C bonds, 109.28°), that is much longer than the experimental thickness of the membrane (3.9±0.3 nm). Hence we assume that the polymer chains adopt a coiled conformation inside the self-organized layer although we cannot exclude completely stretched chains that are tilted towards the mica surface. Certainly a more detailed investigation is necessary to elucidate the conformation of the polymer chains.

Similar to previous experiments, we deposited a 0.5 wt.% block copolymer dispersion on mica. Also at this concentration the polymers formed a planar supported membrane structure on the surface. The surface histogram of this polymer film (Figure 5, C) showed a similar roughness as the polymer membrane (Figure 3, B) obtained by deposition of a 0.1 wt. % vesicular dispersion. In addition we detected intact block copolymer vesicles partially embedded into this layer (Figure 5, A). Like in the experiments on SiO_2, the vesicles displayed a "M"-like profile (Figure 5, B) due to the evaporation of the inner water during sample drying. Furthermore, the height profile showed collapsed spheres with heights ranging from 1.5-4.0 nm indicating that the vesicles are partially buried within a (multi) layer of fused vesicles below with only their upper 'caps' sticking out of this film. Indeed, we discovered that some of them tended to fuse together (Figure 5, A, arrows) which supported our suggestion of multilayer formation at high concentrations.[71, 72]

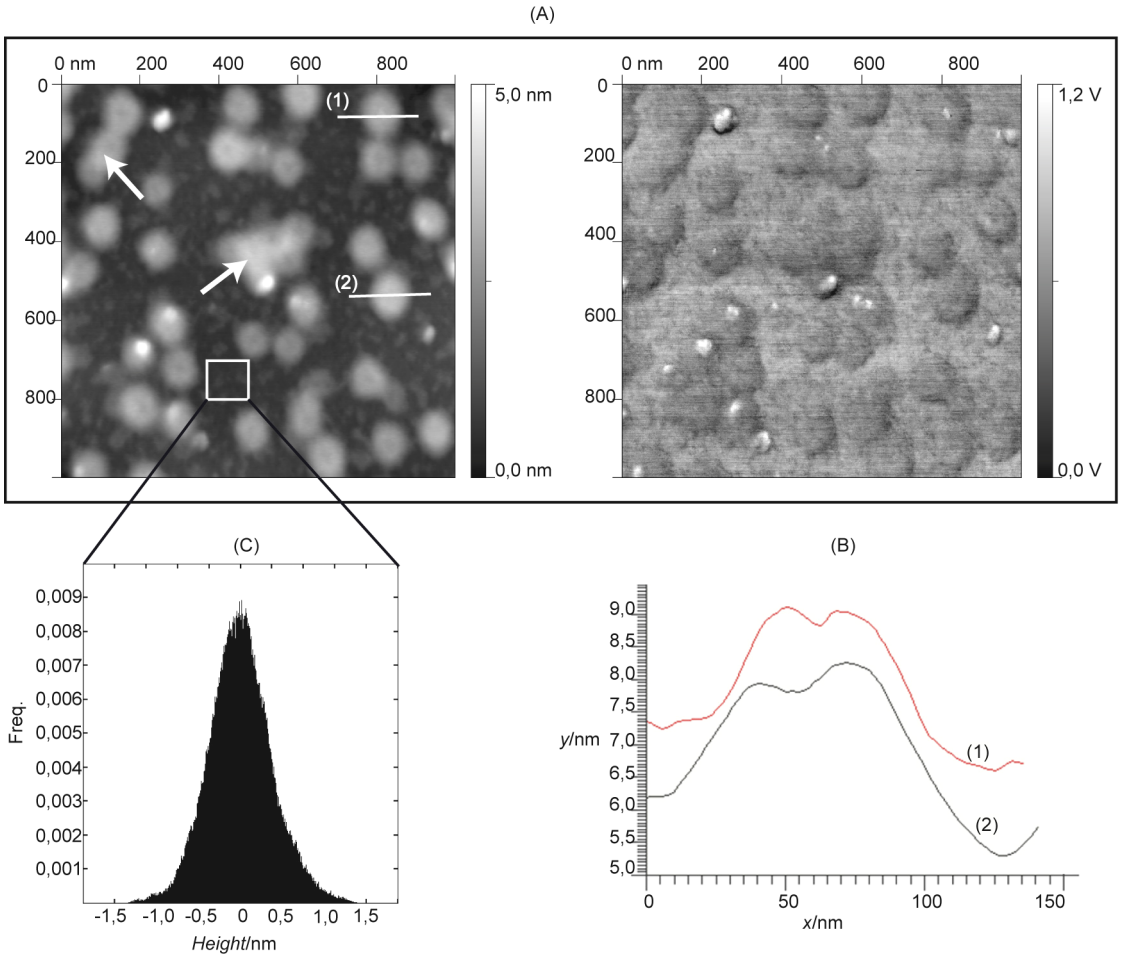

Figure 5. (A) AFM image (left-topography, right-phase) of the mica surface after deposition of 0.5 wt.% copolymer dispersion. Arrows point relatively large aggregates of fused vesicles. (B) Typical cross section analysis shows the "M"-like profile and the height of the collapsed vesicles embedded into the film below. (C) Surface histogram of the vesicle free area indicates surface roughness similar to the one of the polymer membrane obtained after application of the 0.1 wt.% vesicular dispersion.

Similar to previous experiments, we deposited a 0.5 wt.% block copolymer dispersion on mica. Also at this concentration the polymers formed a planar supported membrane structure on the surface. The surface histogram of this polyme Since our vesicles contain a polyelectrolyte (PDMAEMA) layer we varied the pH of their aqueous dispersions to influence the adsorption behaviour. Therefore we performed the control experiments in a pH range from 5 to 9 that corresponds to the 'physiologic regime' relevant for the desired biosensing applications. The polymer vesicular self-assemblies are known to be stable in the chosen solution pH range.[43] For all substrates investigated no significant pH influence on the adsorption behavior of the polymer vesicles was detected. The only exception was deposition

onto the silicon oxide, where at pH = 5 the density of adsorbed vesicles seemed to be slightly increased (see supporting information, Figures 3 and 4). However, we cannot exclude that more acidic (pH <5) or basic (pH> 9) conditions might have a stronger influence on the adsorption behavior.

3.4. Conclusion

We monitored the self-organization of $PDMAEMA_4$-$PBMA_{66}$-$PDMAEMA_4$ triblock copolymer vesicles on HOPG, silicon oxide and mica substrates. Not surprisingly, depending on the substrate properties and corresponding interactions the adsorption of the polymers led to different surface structures.

Reorganization of the copolymer chains from vesicular structure towards the planar 1.5±0.04 nm thick film occurred on the HOPG surface. However, upon drying the film starts to disrupt and 'dewet' and finally forms small droplets on the surface. This is presumably a result of the dehydration of the hydrophilic PDMAEMA blocks.

On SiO_2 and mica the electrostatic interactions between the positively charged PDMAEMA blocks of the polymers and the negatively charged surfaces resulted in the adsorption of vesicles. We observed formation of a planar supported membrane with a thickness of 3.9±0.3 nm on mica surface in analogy to the more well-known solid-supported lipid bilayers. In contrast to HOPG on both other substrates the morphology of the immobilized polymer nanostructures proved to be rather insensitive towards the drying process. According to our AFM images the films are defect free even in the dry state, which might be a result of the high mechanical stability of block copolymer membranes. To our knowledge this is the first report of such solid-supported, biomimetic block copolymer membranes. The film thickness was in good agreement with the dimensions of the vesicular walls obtained from cryo-TEM measurements on vesicle dispersions formed by the same polymers. Moreover, we noted that the polymer chains within the membrane presumably adopted a coiled conformation. This is in contrast to similar membrane structures formed by a surface initiated living radical polymerization where the polymer chains had strongly stretched conformation.[68] The latter was a result of the high grafting density of the polymer chains. It should be noted that the reported system offers for the first time the possibility to directly compare similar block copolymer membranes formed by "grafting to" and "grafting from" techniques.

Interestingly, in the case of SiO_2 substrate that has a lower surface charge density the onset of vesicle fusion and further layer formation requires a higher polymer concentration than on

mica where already deposition of the 0.1 wt.% vesicular dispersion yielded a homogenous, smooth supported membrane.

Our experiments were in good agreement with the well-known adsorption behavior of phospholipid vesicles on solid substrates[34, 41, 73] and allowed us for the first time to prepare solid-supported block copolymer membranes. It has to be emphasized that in contrast to phospholipids the major focus of research in the field of block copolymer membranes is still on vesicular structures and up to now only very few reports on planar membrane structures can be found in the literature.[74, 75]

Together with the versatility of polymer chemistry that allows convenient modification of the chemical constitution, the block length and even the molecular architecture of individual blocks or the whole polymer system, we believe that such surface-immobilized polymer membrane structures could find large interest as model systems for biological membranes or as supports for the development of new types of air-stable (bio-) sensors.

3.5. Acknowledgements

The authors thank Dr. Katarzyna Kita-Tokarczyk and Dr. Thomas Braun for their help in preparation of this manuscript, Dr. Teresa de los Arcos and Dr. Laurent Marot for the access to the ellipsometer. This work was supported by NCCR Nanoscale Science, Swiss National Science Foundation and MRTN-CT-2003-505027.

3.6. References

[1] Vriezema, D. M.; Aragone's, M. C.; Elemans, J. A. A. W.; Cornelissen, J. J. L. M.; Rowan, A. E.; Nolte, R. J. M. *Chem. Rev.* **2005**, *105*, 1445.

[2] Mecke, A.; Dittrich, C.; Meier, W. *Soft Matter* **2006**, *2*, 751.

[3] Antonietti, M.; Förster, S.; Hartmann, J.; Oestreich, S. *Macromolecules* **1996**, *29*, 3800.

[4] Dai, S.; Ravi, P.; Tam, K. C.; Mao, B. W.; Gan, L. H. *Langmuir* **2003**, *19*, 5175.

[5] Patrickios, C. S.; Forder, C.; Armes, S. P.; Billingham, N. C. *J. Polym. Sci. A: Polym. Chem.* **1997**, *35*, 1181.

[6] Discher, D. E.; Eisenberg, A. *Science* **2002**, *297*, 967.

[7] Pata, V.; Dan, N. *Biophys. J.* **2003**, *85*, 2111.

[8] Photos, P. J.; Bacakova, L.; Discher, B.; Bates, F. S.; Discher, D. E. *J. Controlled Release* **2003**, *90*, 323.

[9] Harris, J. K.; Rose, G. D.; Bruening, M. L. *Langmuir* **2002**, *18*, 5337.

[10] Nardin, C.; Hirt, T.; Leukel, J.; Meier, W. *Langmuir* **2000**, *16*, 1035.

[11] Nardin, C.; Widmer, J.; Winterhalter, M.; Meier, W. *Eur. Phys. J. E* **2001**, *4*, 403.

[12] Stoenescu, R.; Meier, W. *Chem. Commun.* **2002**, *24*, 3016.

[13] Grumelard, J.; Taubert, A.; Meier, W. *Chem. Commun.* **2004**, 1462.

[14] Black, C. T.; Ruiz, R.; Breyta, G.; Cheng, J. Y.; Colburn, M. E.; Guarini, K. W.; Kim, H.-C.; Zhang, Y. *IBM J. Res. & Dev.* **2007**, *51(5)*, 605.

[15] Wang, L.; Chen, X.; Chai, Y.; Hao, J.; Sui, Z.; Zhuang, W.; Sun, Z. *Chem. Commun.* **2004**, 2840.

[16] Graff, A.; Sauer, M.; Gelder, P. V.; Meier, W. *Proc. Natl. Acad. Sci. U. S. A.* **2002**, *99*, 5064.

[17] Nardin, C.; Thoeni, S.; Widmer, J.; Winterhalter, M.; Meier, W. *Chem. Commun.* **2000**, 1433.

[18] Stienescu, R.; Graff, A.; Meier, W. *Macromol. Biosci.* **2004**, *4*, 930.

[19] Munro, J. C.; Frank, C. W. *Langmuir* **2004**, *20*, 3339.

[20] Munro, J. C.; Frank, C. W. *Langmuir* **2004**, *20*, 10567.

[21] Kim, K.; Shin, K.; Kim, H.; Kim, C.; Byun, Y. *Langmuir* **2004**, *20*, 5396.

[22] Morigaki, K.; Schonherr, H.; Frank, C. W.; Knoll, W. *Langmuir* **2003**, *19*, 6994.

[23] Morigaki, K.; Baumgart, T.; Jonas, U.; Offenhäusser, A.; Knoll, W. *Langmuir* **2002**, *18*, 4082.

[24] Tanaka, M.; Sackmann, E. *Nature* **2005**, *437*, 656.

[25] Wagner, M. L.; Tamm, L. K. *Biophys. J.* **2000**, *79*, 1400.

[26] McConnell, H. M.; Watts, T. H.; Weis, R. M.; Brian, A. A. *Biochim. Biophys. Acta* **1986**, *864*, 95.

[27] Sackmann, E. *Science* **1996**, *271*, 43.

[28] Groves, J. T.; Boxer, S. G. *Acc. Chem. Res.* **2002**, *35*, 149.

[29] Cremer, P. S.; Yang, T. L. *J. Am. Chem. Soc.* **1999**, *121*, 8130.

[30] Kita-Tokarczyk, K.; Grumelard, J.; Haefele, T.; Meier, W. *Polymer* **2005**, *46(11)*, 3540.

[31] Steinem, C.; Janshoff, A.; Ulrich, W.-P.; Sieber, M.; Galla, H.-J. *Biochim. Biophys. Acta* **1996**, *1279*, 169.

[32] Williams, L. M.; Evans, S. D.; Flynn, T. M.; Marsh, A.; Knowles, P. F.; Bushby, R. J.; Boden, N. *Langmuir* **1997**, *13*, 751.

[33] Cooper, M. A.; Try, A. C.; Carroll, J.; Ellar, D. J.; Williams, D. H. *Biochim. Biophys. Acta* **1998**, *1373*, 101.

[34] Tawa, K.; Morigaki, K. *Biophys. J.* **2005**, *89*, 2750.

[35] Keller, C. A.; Kasemo, B. *Biophys. J.* **1998**, *75*, 1397.

[36] Reimhult, E.; Höök, F.; Kasemo, B. *J. Chem. Phys.* **2002**, *117*, 7401.

[37] Richter, R.; Mukhopadhyay, A.; Brisson, A. *Biophys. J.* **2003**, *85*, 3035.

[38] Reviakine, I.; Brisson, A. *Langmuir* **2000**, *16*, 1806.

[39] Muresan, A. S.; Lee, K. Y. C. *J. Phys. Chem. B* **2001**, *105*, 852.

[40] Schönherr, H.; Johson, J. M.; Lenz, P.; Frank, C. W.; Boxer, S. G. *Langmuir* **2004**, *20*, 11600.

[41] Hughes, T.; Strongin, B.; Gao, F. P.; Vijayvergiya, V.; Busath, D. D. *Biophys. J.* **2004**, *87*, 311.

[42] Su, Y.-I. *J. Colloid Interface Sci.* **2005**, *292*, 271.

[43] Rakhmatullina, E. ; Braun, T.; Chami, M. ; Malinova, V. ; Meier, W. *Langmuir* **2007**, *23*, 12371.

[44] Jakes, J. *Czech. J. Phys.* **1988**, *B38*, 1305.

[45] Haensler, J.; Szoka, F. C. *J. Bioconjugate Chem.* **1993**, *4*, 372.

[46] Bielinska, A.; Kukowska-Latallo, J. F.; Johnson, J.; Tomalia, D. A.; Baker, J. R. *Nucleic Acids Res.* **1996**, *24*, 2176.

[47] Tang, M. X.; Redemann, C. T.; Szoka, F. C. *J. Bioconjugate Chem.* **1996**, *7*, 703.

[48] Douglas, J. F. *Macromolecules* **1989**, *22*, 3707.

[49] Blunt, M.; Barford, W.; Ball, R. *Macromolecules* **1989**, *22*, 1458.

[50] Itami, K.; Fujitani, H. *Colloids and Surfaces A: Physicochem. Eng. Aspects* **2005**, *265*, 55.

[51] Scales, P. J.; Grieser, F.; Healy, T. W. *Langmuir* **1990**, *6(3)*, 582.

[52] Shin, Y.; Roberts, J. E.; Santore, M. M. *J. Colloid Interface Sci.* **2002**, *247*, 220.

[53] Hunter, D. G.; Frisken, B. J. *Biophysical J.* **1998**, *74*, 2996.

[54] Lasic, D. D. *Liposomes: from physics to applications;* Elsevier science publishers B. V., 1993; p. 195.

[55] Leonard, D. N.; Russell, P. E.; Smith, S. D.; Spontak, R. J. *Macromol. Rapid Commun.* **2002**, *23*, 205.

[56] Gu, X.; Raghavan, D.; Douglas, J. F.; Karim, A. *J. Polym. Sci. B: Polym. Phys.* **2002**, *40(24)*, 2825.

[57] Volegova, I. A.; Buzin, A. I. *Polym. Sci. A.* **2007**, *49(9)*, 1014.

[58] Zhao, X.; Zhang, Z.; Pan, F.; Ma, Y.; Armes, S. P.; Lewis, A. L.; Lu, J. R. *Langmuir* **2005**, *21*, 9597.

[59] Butt, H.-J. *Nanotechnology* **1992**, *3*, 60.

[60] Uzun, O.; Xu, H.; Jeoung, E.; Thibault, R. J.; Rotello, V. M. *Chem. Eur. J.* **2005**, *11*, 6916.

[61] Li, S. L.; Palmer, A. F. *Langmuir* **2004**, *20*, 7917.

[62] Reviakine, I.; Brisson, A. *Langmuir* **2000**, *16*, 1806.

[63] Egawa, H.; Furusawa, K. *Langmuir* **1999**, *15*, 1660.

[64] Wang, Y.; Zhang, J.; Wang, Z.; Wang, Z.; Yang, B. *Colloids and Surfaces A: Physicochem. Eng. Aspects* **2007**, *292*, 159.

[65] Xie, D.; Jiang, M.; Zhang, G.; Chen, D. *Chem. Eur. J.* **2007**, *13*, 3346.

[66] Jass, J.; Tjärnhage, T.; Puu, G. *Biophys. J.* **2000**, *79*, 3153.

[67] Pastre, D.; Pietrement, O.; Fusil, S.; Landousy, F.; Jeusset, J.; David, M.; Hamon, L.; Cam, E. L.; Zozime, A. *Biophys. J.* **2003**, *85*, 2507.

[68] Rakhmatullina, E.; Braun, T.; Kaufmann, T.; Spillmann, H.; Malinova, V.; Meier, W. *Macromol. Chem. Phys.* **2007**, *208*, 1283.

[69] Cha, T.; Guo, A.; Zhu, X.-Y. *Biophys. J.* **2006**, *90*, 1270.

[70] Jackson, S.; Reboiras, M.; Lyle, I. G.; Jones, M. N. *Faraday Discuss. Chem. Soc.* **1986**, *86*, 291.

[71] Knecht, V.; Marrink, S.-J. *Biophys. J.* **2007**, *92*, 4254.

[72] Malinin, V. S.; Frederik, P.; Lentz, B. R. *Biophys. J.* **2002**, *82*, 2090.

[73] Nardin, C.; Winterhalter, M.; Meier, W. *Langmuir* **2000**, *16*, 7708.

[74] Ho, D.; Chu, B.; Schmidt, J. J.; Brooks, E. K.; Montemagno, C. D. *IEEE Transactions on Nanotechnology* **2004**, *3(2)*, 256.

[75] Nardin, C.; Winterhalter, M.; Meier, W. *Langmuir* **2000**, *16*, 7708.

3.7. Supporting information

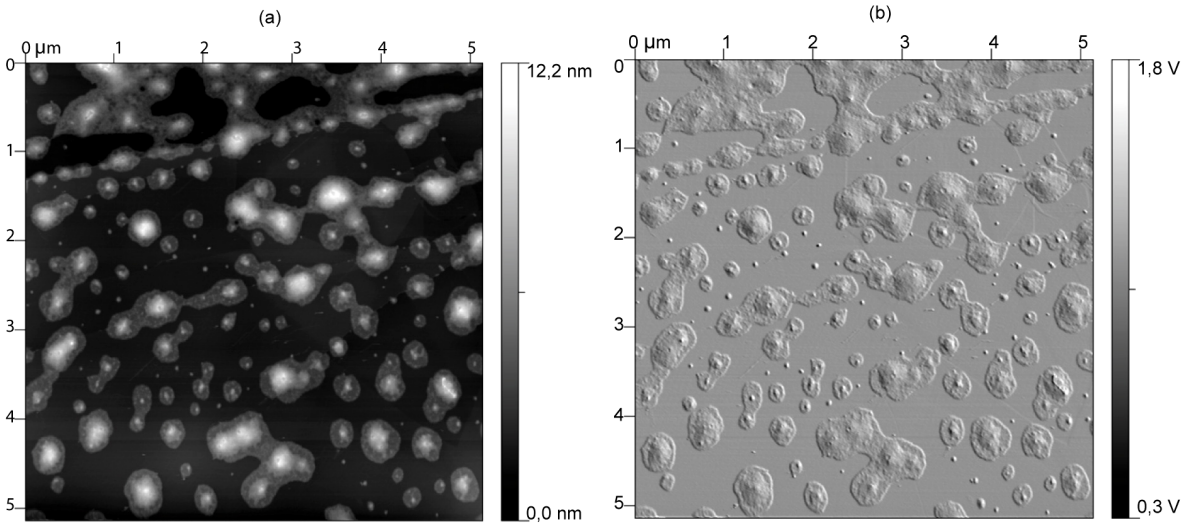

Figure 1. AFM image (topography mode (a) and phase (b)) of the polymer material on the HOPG surface six days after sample preparation.

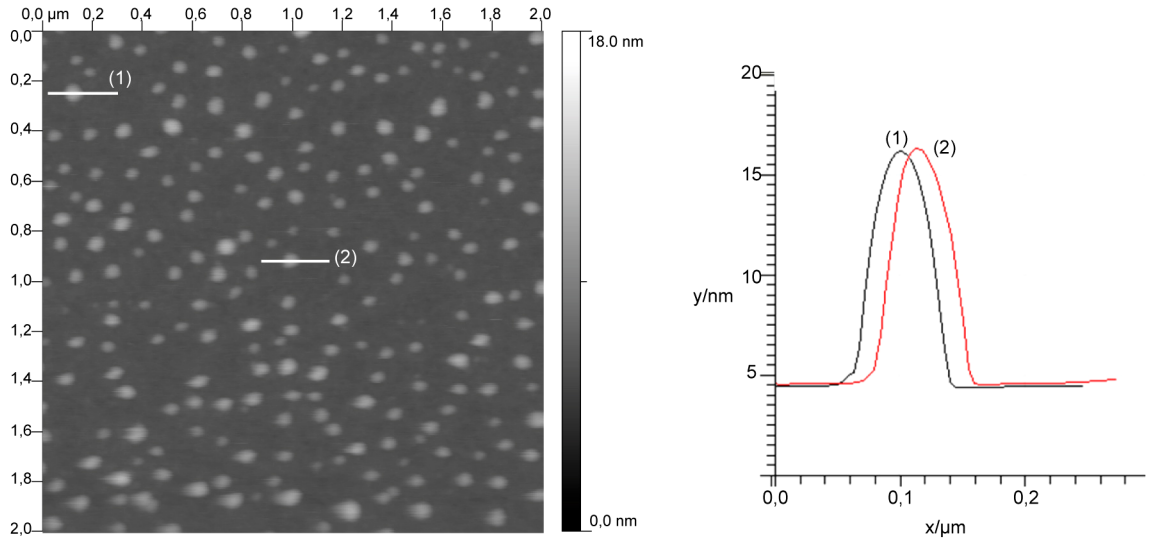

Figure 2. AFM measurement in liquid. Copolymer vesicles deposited onto SiO_2 substrate (topography mode-left) from 0.1 wt.% vesicular dispersion. Right image demonstrates the cross-section profiles of two vesicles on the surface. The shape of the peaks reveals spherical particles without deformations indicating that vesicles have inner water inside their cavity. The diameter to height ratio corresponds to flattened vesicles on the surface.

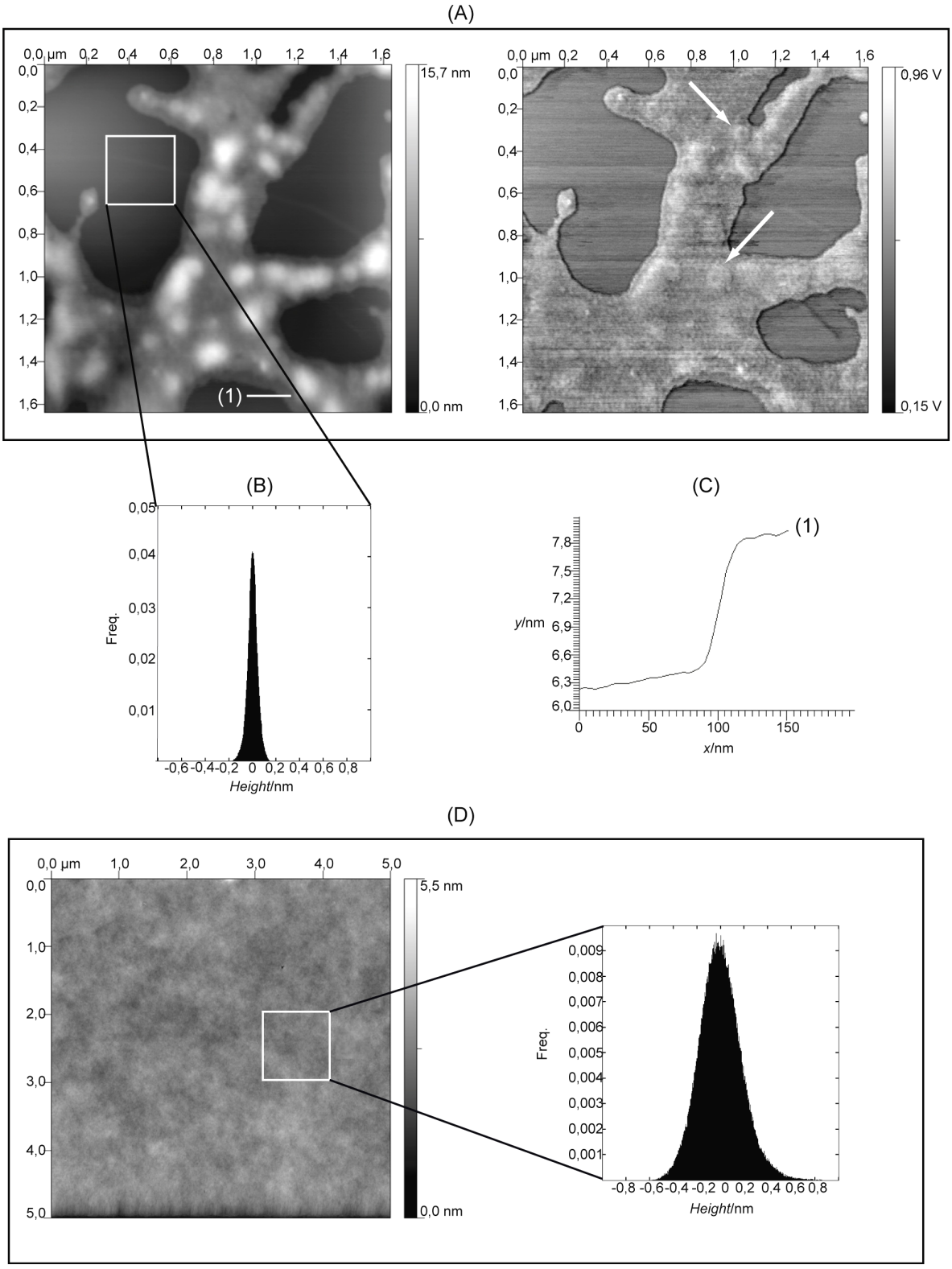

Figure 3. See description below.

Figure 3. Deposition of the copolymer vesicles on HOPG (A) and mica (D) substrates from acidic dispersion (pH=5, 0.1 wt.%). (A) Overview, topography (left) and phase (right) modes are presented. The HOPG substrate is only partially covered by copolymer material. The collapsed copolymer vesicles are visible with better contrast in the phase mode (right, white arrows). The white frame indicates the region of interest that was taken for the surface analysis. (B) Surface histogram of the uncovered part of the substrate shows a low surface roughness identical to the bare HOPG substrate. Thin rims are visible on the periphery of the covered areas. (C) Example of the cross section profile of the periphery rims. The thickness of the rim corroborates the 1.5±0.04 nm value that was measured for the polymer rims obtained after deposition of the polymer dispersion at higher pH. A large area (5x5 μm) of polymer membrane on freshly cleaved mica substrate shows no defects in the polymer layer. A white frame represents the region of interest that was taken for the surface analysis. (D, right image) The surface histogram demonstrates a roughness of the membrane similar to the one obtained after deposition of the vesicles from dispersion at pH=8.0 (see Figure 3, B in the manuscript)

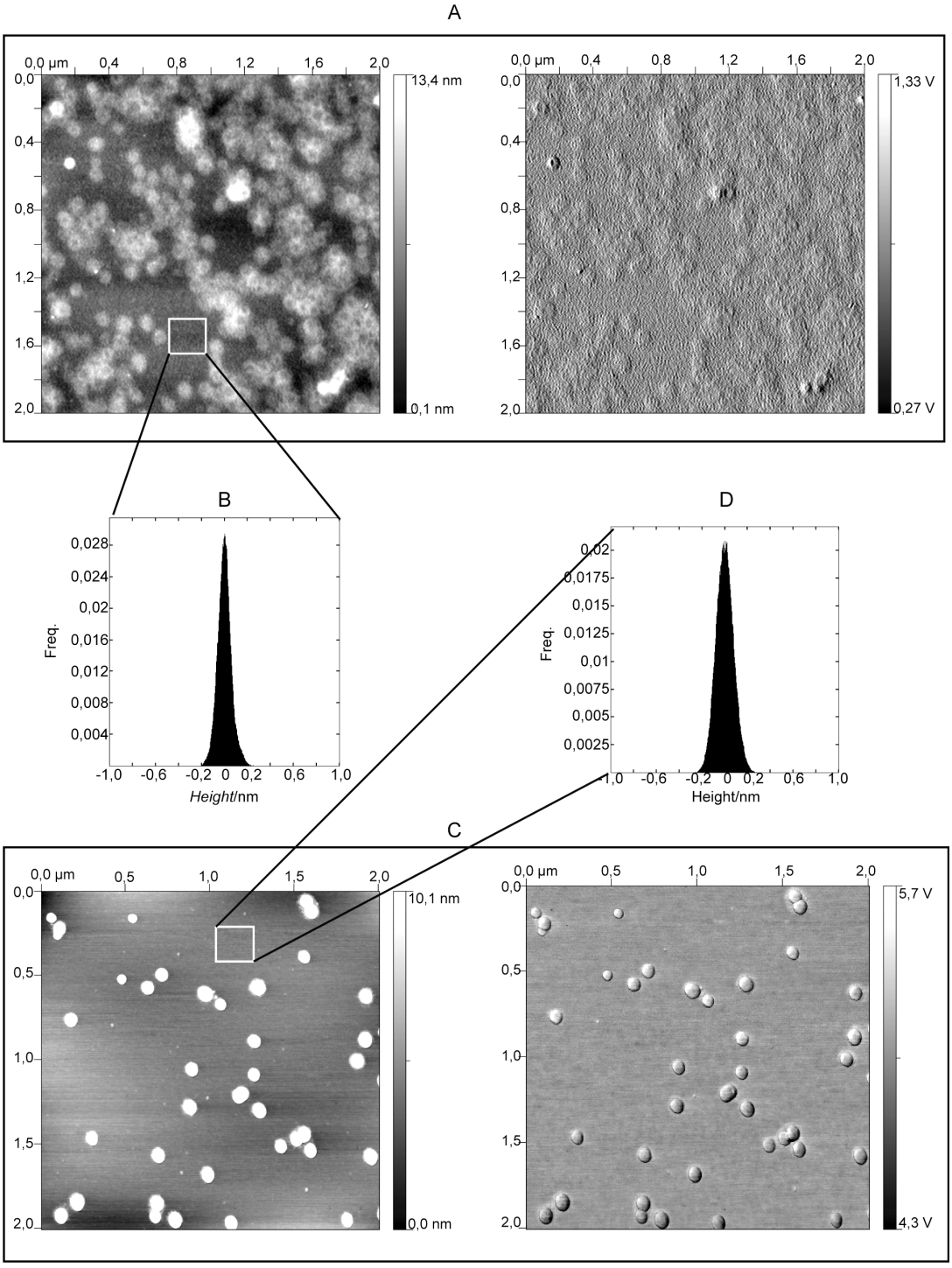

Figure 4. AFM images (topography mode-left, phase-right) of the copolymer vesicles deposited onto SiO_2 substrate from acidic pH=5 (A) and basic pH=9 (C) dispersions (0.1 wt.%). A white frame shows the region of interest that was taken for the surface analysis. (B) Surface histogram of the vesicle free area demonstrates the surface roughness identical to the bare SiO_2 substrate (see manuscript, Figure 2, D). Thus, the copolymer vesicles are adsorpted onto the SiO_2 surface and no formation of a membrane structure occurred. (C) Copolymer vesicles deposited onto SiO_2 surface from a basic dispersion, pH=9 (0.1 wt. %). (D) Surface histogram of the vesicle free area indicates underlying surface roughness identical to the bare SiO_2 substrate (see manuscript, Figure 2, D).

Scan area	Profile	Rim thickness, nm
1	1	1,6
	2	1.4
	3	1.6
	4	1.7
	5	1.3
	6	1.4
	7	1.5
	8	1.4
2	9	1.6
	10	1.5
	11	1.8
	12	1.4
3	13	1.4
	14	1.9
	15	1.4
	16	1.3
4	17	1.7
	18	1.6
	19	1.7
	20	1.4
	21	1.3
	22	1.3
Average		1.505
Standard deviation		0.177
Standard error		0.038

Table 1. Estimation of the average thickness of the copolymer monolayer on the HOPG substrate. Analysis of the cross-section profiles (n=22) was performed using base line correction and data obtained from different scan areas of the sample.

The mean thickness of the copolymer layer on the HOPG (rim thickness) of 1.5±0.04 (standard error) nm is used in the manuscript.

Scan area	Profile	Vesicular height, nm
1	1	8.9
	2	9.6
	3	10.2
	4	9.1
	5	9.3
	6	10.5
2	7	9.0
	8	8.9
	9	9.6
	10	9.4
	11	9.4
3	12	9.7
	13	9.1
	14	10.8
	15	9.0
	16	9.3
	17	9.4
4	18	9.2
	19	9.1
	20	10.3
	21	8.9
	22	9.4
	23	9.0
	24	9.1
Average		9.425
Standard deviation		0.528
Standard error		0.108

Table 2. Estimation of the average height of the block copolymer vesicles on the SiO_2 substrate. Analysis of the cross-section profiles (n=24) was performed using base line correction and data obtained from different scan areas of the sample.

The average height of the collapsed copolymer vesicle on the silicon oxide substrate of 9.4±0.1 (standard error) nm is used in the manuscript.

4. Functionalization of Gold and Silicon Surfaces by Copolymer Brushes using Surface-initiated ATRP

Ekaterina Rakhmatullina[1], Thomas Braun[2], Thomas Kaufmann[3], Hannes Spillmann[2], Violeta Malinova[1], Wolfgang Meier[1]

[1] Department of Chemistry, University of Basel, Klingelbergstrasse 80, CH-4056

[2] Department of Physics, University of Basel, Klingelbergstrasse 82, CH-4056

[3] Maurice E. Muller Institute, Biozentrum, University of Basel, Klingelbergstrasse 70, CH-4056

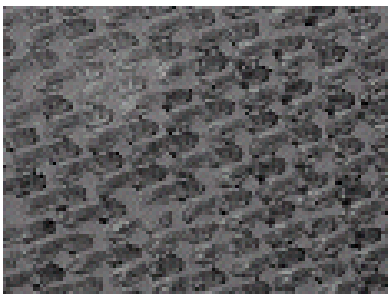

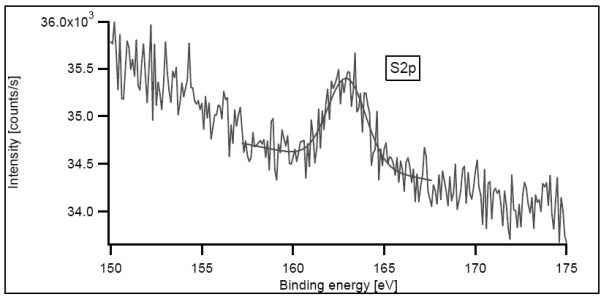

Published in: *Macromol. Chem. Phys.* **2007**, *208,* 1283-1293.

4.1. Introduction

Creation of various sensors and micro\nano devices based on polymer chemistry demands a well-defined surface functionalization as well as control over many parameters such as polymer architecture, thickness and homogeneity of layers, stability, etc. A lot of different techniques were developed for polymer deposition onto surfaces.[1, 2] Grafting approaches are the most common methods to achieve this purpose. A „grafting to“ technique was developed first and represents anchoring of previously synthesized polymers to a substrate via chemical or physical interactions. However the reactive groups are often buried in the interior of the polymer globules as a result of their random coil conformation. Hence, not all of them are accessible for reactions with the functional groups on a solid surface. Additionally, excluded volume effects of the macromolecules prevent a full coverage of the surface. Hence surface-attached polymer layers are frequently inhomogeneous or have a rather low density of brushes. Another disadvantage of the “grafting to” method is related to the orientation of the chains that cannot be controlled during the anchoring procedure leading to the formation of disordered layers. Thus, in spite of experimentally simple procedures, this approach is frequently not reproducible.

A more efficient way for surface functionalization is the “grafting from” method. The latter involves a covalent immobilization of small initiator molecules to a surface followed by subsequent polymerization. This leads to high density of initiator molecules on the surface and, thus, the polymer chains grow step by step with a defined architecture. Among various polymerization techniques, the radical polymerization,[3, 4] living cationic,[5] living anionic[6, 7] and living atom transfer radical polymerization (ATRP)[8-12] attracted much attention for surface functionalization. Particularly, the ATRP appeared to be of special significance for modification of gold and silicon substrates with polymer brushes. For instant, various monomers such as styrene,[13] methacrylates,[14, 15] acrylates[16] were polymerized by ATRP on silicon surfaces. Many authors described microcontact printing of ATRP initiator molecules on silicon and gold supports followed by polymerization in order to create structured surfaces.[17-20] In addition, surface-initiated ATRP can be accomplished easily at ambient temperature by using water as solvent.[21, 22] ATRP is also frequently used for block copolymer synthesis due to the possibility to create copolymers with a high molecular weight and low polydispersity index.

Amphiphilic block copolymers consist of hydrophilic and hydrophobic blocks. These polymers self-assemble in aqueous media to micelles,[23-25] vesicles[26-28] and lyotropic liquid

crystalline phases.[29, 30] Compared to low molecular weight amphiphiles, block copolymers frequently form more stable aggregates. Since the self-assembly of macromolecules are only minimal affected by the limited introduction of new chemical groups, they allow tailoring of their properties for a specific purpose. This is not possible with low molecular weight amphiphiles to this extend.

Recently, block copolymer membranes gained an increasing interest due to their similarity to biological membranes.[31-34] Block copolymers are known to form chemically and mechanically more stable membranes than conventional lipid bilayers.[35, 36] This makes them highly attractive as a model system in the field of biosensing. Typically for such applications solid-supported membrane structures are required. Here we present an approach to grow amphiphilic block copolymer brushes consisting of hydrophobic PBMA and hydrophilic PDMAEMA segments on gold and silicon surfaces. By using these two substrates for polymer growth, we aimed to check whether the type of solid support has an impact on reproducibility of the synthesis and dimensions of the polymer chains. Subsequent detachment of the polymer brushes made possible determination of the molecular weights and thus, preliminary comparison between polymers grown on gold and silicon substrates.

4.2. Experimental Part

4.2.1. Materials

n-Butyl methacrylate (n-BMA) (Fluka; 99%) and 2-dimethylaminoethyl methacrylate (DMAEMA) (Aldrich; 98%) were purified by passing through a column of activated basic alumina before use for removal of the inhibitor. Copper (I) bromide (Aldrich; 98%) was purified according to the method of Keller and Wycoff.[37] The ligand N-(n-Propyl)-2-pyridylmethanimine and tris(2-dimethylaminoethyl)amine (Me_6TREN) were prepared as reported elsewhere.[38, 39] Toluene and tetrahydrofuran were stirred over sodium/benzophenon mixture and freshly distilled under nitrogen environment. Analogically acetonitrile was dried over $MgSO_4$ overnight and filtered prior to use. The disulfide initiator, $(BrC(CH_3)_2 COO(CH_2)_{11} S)_2$, was synthesized according to a literature procedure.[40] 6-((2-Bromo-2-methyl)-propionyloxy)hexyltrichlorosilane (I) was prepared by hydrosilylation of 5-hexen-1-yl 2-bromo-2-methylpropionate with trichlorosilane and kept in anhydrous toluene.[41] 6-((2-Bromo-2-methyl)-propionyloxy)hexylmonochlorosilane (II) was synthesized in the same

manner but monochlorosilane was used instead of trichlorosilane. 11-Mercapto-1-undecanol (MUD) was purchased from Aldrich. All other chemicals were obtained from Fluka and used without any further purification.

4.2.2. Cleaning of Silicon Slides

For the preparation of gold substrates silicon slides were cleaned in piranha solution (H_2SO_4: H_2O_2, 3:1, vol.-%) using sonication. Slides were rinsed thoroughly with bidistilled water, sonicated in bidistilled water, washed once more with water, ethanol and dried under a stream of nitrogen. Clean slides were directly used for gold deposition.

Prior to chemical modification silicon wafers were rinsed and sonicated in ethanol and dried in oven at 120°C for 6 hours.

4.2.3. Gold Sputtering

Cleaned silicon slides were coated on one side with 5 nm chromium adhesion layer followed by 50 nm of gold (Baltec SCD 050 for Cr 120 mA, 0,05mbar; Baltec MED 020 for Au 50 mA, 0.02 mbar, all in argon atmosphere).

4.2.4. Preparation of Initiator Functionalized Substrates

Functionalization of Gold Surfaces

The initiator functionalized substrates were prepared in two different ways (Scheme 1). *(I)* Gold plates were immersed in 2 wt.-% THF solution of $(BrC(CH_3)_2\,COO(CH_2)_{11}\,S)_2$ and left overnight at room temperature to form a self-assembled monolayer (SAM) of the initiator molecules on the surface. Samples were washed with THF, ethanol and dried in nitrogen stream. *(II)* Gold surfaces were immersed in 2 wt.-% ethanol solution of MUD and left overnight to form SAM monolayers. The substrates were repeatedly washed with ethanol and dried in nitrogen stream. A reaction mixture consisted of 0.1M solution of 2-bromo-2-methylpropionyl bromide in THF and 0.01 wt.-% triethylamine was prepared in which MUD-modified surfaces were placed for 2 hours at room temperature and permanent shaking. Finally, samples were washed with THF, ethanol, dried in nitrogen stream and immediately used for polymerization.

Initiator SAMs were characterized by contact angle measurements and X-ray photoelectron spectroscopy.

Functionalization of Silicon Surfaces

Silicon wafers were placed into two-neck reaction flask which was degassed. 2 wt.-% solution of silane (I) or (II) in dry toluene was injected in the flask and the system was left in dark for 4 hours at room temperature and permanent shaking. Wafers were sonicated in toluene, ethanol and rinsed with the same solvents. All samples were dried under nitrogen stream and immediately used for further applications.

4.2.5. Growth of Polymer Brushes from Immobilized Initiator SAMs

BMA Polymerization

To a 2 M degassed monomer solution in toluene, 144 mg (1 mmol) CuBr, 22.4 mg (0.1 mmol) $CuBr_2$ and 300 mg (2 mmol) N-(n-Propyl)-2-pyridylmethanimine were added under a flow of nitrogen. The mixture was degassed using three freeze-pump-thaw cycles and stirred until a homogeneous dark brown solution was formed.

Initiator modified substrates were placed into another flask and sealed with a rubber septum. The flask was degassed and filled with the above described polymerization solution and the reaction was carried out at 40°C for 1.5 hours. After this time the reaction was quenched by injecting solution of $CuBr_2$ and N-(n-Propyl)-2-pyridylmethanimine (1:2 molar ratio, 0.02 M $CuBr_2$) in order to keep the end-functionality of the poly-BMA block. The substrates were cleaned with toluene, THF, ethanol and dried in nitrogen stream.

DMAEMA Copolymerization

The same procedure as the one described for BMA was applied for DMAEMA polymerization, but THF/acetonitrile (1:1, vol.-%) mixture was used as solvent, Me_6TREN (1 mmol) was chosen as ligand and metallic Cu (0.1 mmol) was added together with copper salts in the reaction.

4.2.6. Detachment of Copolymer Chains from the Substrate

From gold: Substrates with polymer brushes were immersed in 5% solution of iodine in chloroform and left for 15 hours at room temperature in flask wrapped by alumina foil. Then the slides were taken out and solvent was evaporated under vacuum. The residue was dissolved in THF and passed through a column with neutral alumina.

From silicon: Substrates with polymer brushes were immersed in soft etching bath (20 wt.-% HF, 40 wt.-% H_2O, 23 wt.-% K_2CO_3, 8 wt.-% KOH, 9 wt.-% Na_2SO_4) for 5 h, sonicated for 1h. The solution was neutralized to pH=7 and passed through a column with basic alumina.

4.2.7. Measurement Methods

^{1}H NMR

Spectra were recorded in $CDCl_3$ on a 400.1300 MHz Varian Unity 400NMR spectrometer with sweep width of 8278.146 Hz and a 22° pulse width of 2.96 μs.

Gel permeation chromatography (GPC)

Agilent Technologies GPC instrument with a ODS Hypersil column (5 μm) and polystyrene standards were used. The data obtained were corrected for polymethacrylate standards as described by Mori.[42] A refractive index detector was applied for sample detection. Tetrahydrofuran was used as eluent. GPC data were confirmed by additional control experiments on PBMA-PDMAEMA copolymers synthesized in solution that showed a very good correlation between molecular weights determined by GPC, ^{1}H NMR and vapor osmometry (see supporting information).

Contact angle determination

All measurements were performed as described by Kaufmann.[43] 5 μl drop of bidistilled water was used for the surface wetting. The presented results (Table 2) were taken as average values from three measurements.

Ellipsometry

Film thicknesses were determined using a spectroscopic multi angle ellipsometer (M2000U from J. A. Woollam Co., Inc) measuring at three angles of 65°, 70°, and 75°. The refractive index of the films at all angles was fitted to1.4.

X-ray photoelectron spectroscopy (XPS)

Analyses of the electronic structure of the initiator layers were performed by VG ESCALAB MKII instrument at pressure of 10^{-10} mbar. The XPS experiments were performed with a non-monochromatized Mg/Al twin anode as x-ray source. The photon energies of the Mg and Al sources (Kα lines) were 1253.6 eV and 1486.6 eV, respectively. The electrons emitted from the sample were detected under normal emission conditions in a hemispherical 150° analyzer with three channeltron electron counters.

Atomic Force Microscopy (AFM)

Contact mode AFM was performed using PycoLE System, Molecular Imaging, and gold coated silicon nitride cantilevers (k=0.12 N/m). Images were recorded at scan speed 0.8 lines/s, force set point 0.147 V. All measurements were done at room temperature.

4.3. Results and Discussion

We synthesized amphiphilic diblock copolymer brushes on gold and silicon interfaces by the "grafting from" method. This procedure included the immobilization of initiator molecules on substrates followed by ATRP of n-butyl methacrylate (BMA) and 2-dimethylaminoethyl methacrylate (DMAEMA) monomers. In situ analysis of the copolymer brushes, detachment from the solid substrates and further characterization of detached polymers were performed to get information about the obtained materials.

4.3.1. Initiator SAMs on Gold Surface

The formation of self-assembled monolayers (SAMs) of thiolated molecules on gold is well known.[44] This property of thiol compounds was used to prepare SAMs of ATRP initiator molecules that often contain a bromine atom at the other end of the thiol linker. Here we used 11-mercapto-1-undecanol (MUD) activated by the reaction with α-bromoisobutyryl bromide.

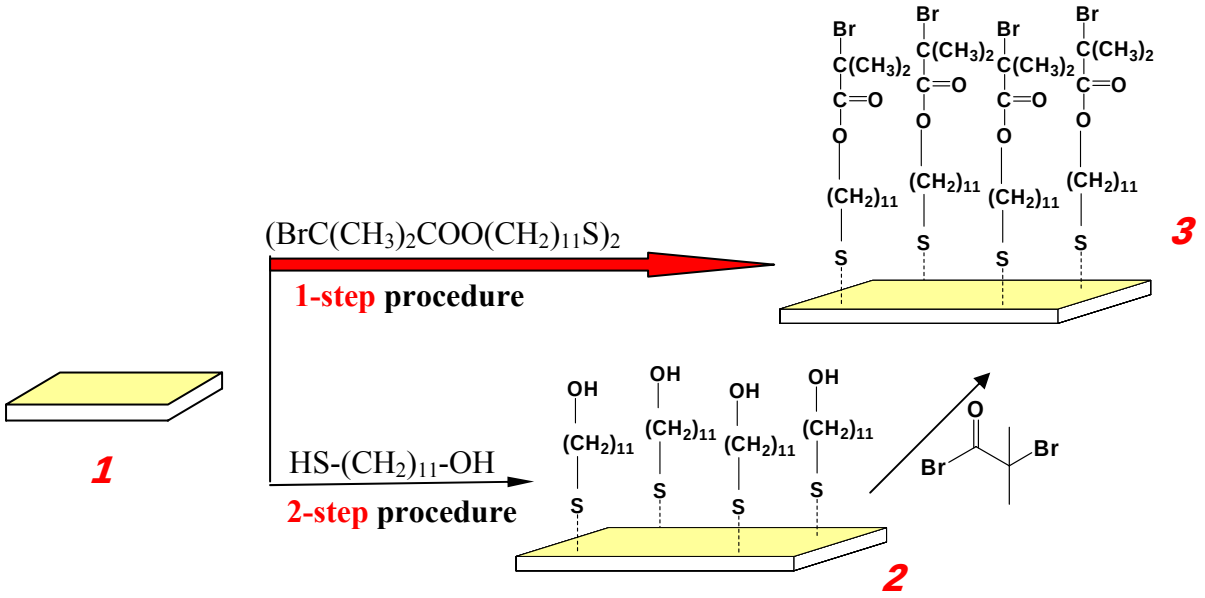

Scheme1. Anchoring of ATRP initiator on gold substrate. Two different approaches to create initiator SAM: 1-step and 2-step procedures. ***1:*** gold surface; ***2:*** MUD monolayer; ***3:*** ATRP initiator SAM.

Two ways of gold functionalization by ATRP initiators are described in literature.[45-49] They are compared in Scheme 1. In the first method, the initiator is synthesized in solution and then immobilized directly on the gold surface by SAM formation (1-step procedure). In the second method, the gold interface was functionalized with the initiator precursor (MUD) and subsequently activated in a second reaction step (2-step procedure). In order to find out the most efficient approach for initiator immobilization, we applied both methods and the resulting monolayers were characterized and compared.

The atomic composition of the initiator SAMs was determined by XPS. The results are displayed in Figure 1. In both cases, XPS spectra showed an oxygen peak (O1s) at 534 eV and a carbon signal (C1s) at 286 eV associated with the organic part of the initiator molecules. More specific signals are the sulfur atom (S2s, S2p) peaks and the small bromine signal at 73 eV (not presented) which are assigned to the Au-S bonds of the initiator SAM. The XPS data qualitatively proved the presence of initiator layers after application of both procedures.

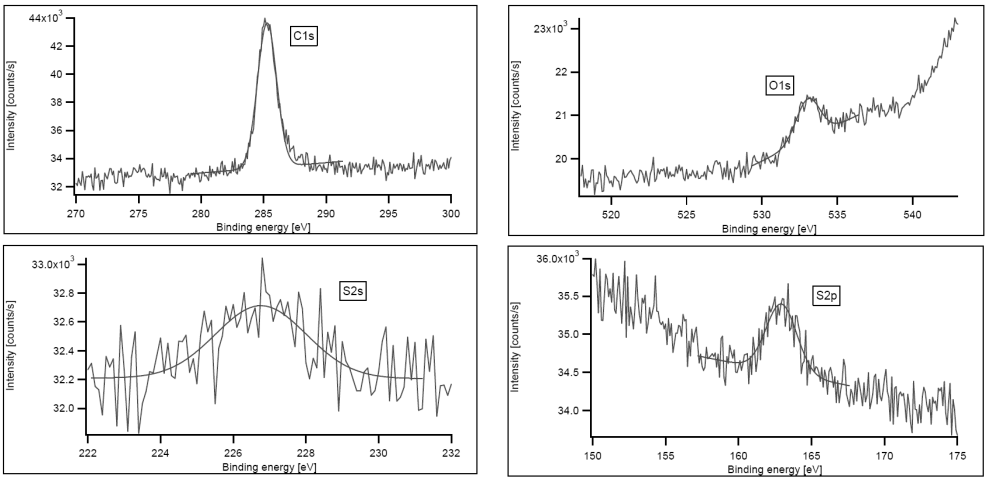

Figure1. XPS spectra of self-assembled initiator layers on gold surfaces.

By ellipsometric measurements the thickness of the initiator SAMs was found to be 1.4± 0.1 nm after application of the 1-step procedure (Table 1), while the 2-step procedure resulted in layer with thickness of 1.3±0.1 nm. The thickness of the SAMs prepared by two methods was found to be identical within experimental error and corresponded well to the theoretical length of 1.28 nm for a fully stretched initiator molecule.

Analyzed layer	Thickness, nm
Initiator SAM on gold (1-step procedure)	1.4±0.1
Initiator SAM on gold surface (2-step procedure)	1.3±0.1
Trichlorosilane **(I)** initiator on silicon (2 wt.-% solution)	128±17
Trichlorosilane **(I)** initiator on silicon (0, 02 wt.-% solution)	121±9
Monochlorosilane **(II)** SAM on silicon	1.7±0.2
PBMA brushes on gold substrate	12.3±0.8
PBMA brushes on silicon	14.1±3.1
PBMA-PDMAEMA brushes on gold	23.9±2.8
PBMA-PDMAEMA brushes on silicon	24.3±2.2

Table 1. Thicknesses of subsequent layers on gold and silicon surfaces measured by ellipsometry

The individual steps during the preparation of the initiator SAMs lead to characteristic changes in the polarity of the surfaces that are directly reflected in the wetting behavior. Hence we performed contact angle measurements to quantify the corresponding changes after each modification step (Table 2). Basically, the more hydrophilic the surface is, the larger is the contact area of a water droplet on it and, therefore, the smaller is the value of the contact angle. Hence the presence of hydroxy-terminated MUD SAM (***2***, Scheme 1) converted the hydrophobic gold into a more hydrophilic surface (Table 1). Therefore the contact angle decreased from 72.6° (gold) to 22.4° (after gold functionalization). The attachment of initiator molecules containing bromine atoms (***3***, Scheme 1) decreased the hydrophilicity of the surface and again the contact angle increased to 56.4°. For the 1-step procedure we detected a contact angle of 68.8° for the initiator SAM. Obviously the two different methods resulted in a different wettability of the surface. Since both procedures lead to the initiator SAMs with identical chemical structure, the difference in contact angles (56.4° and 68.8°) can be explained by a different density of the end groups. Most likely not all hydroxy groups reacted with α-bromoisobutyryl bromide in the two step procedure (Scheme 1) due to steric hindrance and lower reaction rate at the surface compared to solution. Such unreacted hydroxyl groups of MUD promoted higher hydrophilicity of the final layer. As consequence the two-step procedure resulted in SAMs where only a part of the surface-immobilized

molecules were active in a subsequent polymerization. Since this might lead to inhomogeneous polymer brushes at the surfaces, we used the one-step procedure for surface functionalization in all subsequent experiments.

Sample	Contact angle, °
Gold substrate	**72.6** 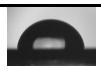
MUD SAM on gold	**22.4** 
Initiator SAM (2-step procedure) on gold	**56.4** 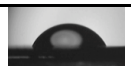
Initiator SAM (1-step procedure) on gold	**68.8** 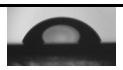
First PBMA block on gold	**65.3** 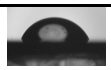
Diblock copolymer brushes on gold	**63.1** 
Silicon wafer before functionalization	**35.8** 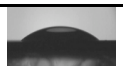
Silicon with monochlorosilane (I) SAM	**71.6** 

Table 2. Contact angles of water droplet on the functionalized gold and silicon surfaces.

4.3.2. Initiator SAMs on Silicon

The 1-step procedure was also applied to anchor the initiator molecules on the silicon wafers. The reaction of trichlorosilane (I) with silicon wafer resulted in formation of initiator layers of 128±17 nm thickness as determined by ellipsometry (Table 1). This indicates the formation of multilayers because the estimated length of a fully stretched trichlorosilane (I) molecule corresponds approximately to 1 nm. Self-assembly of trichlorosilanes into multilayers was reported before.[44, 50, 51] To avoid multilayer formation, we decreased the trichlorosilane (I) concentration gradually from 2 wt.-% to 0.02 wt.-% solution. In contrast to previously reported results,[41, 52] such low concentration of trichlorosilane did not result in significant decrease of the layer thickness, i. e. 0.02 wt.-% solution provided still a 121±9 nm thick multilayer (Table 1). Therefore we synthesized a less reactive monochlorosilan (II). The thickness of this initiator layer on silicon was found to be 1.7±0.2 nm (Table 1) which corresponds well to monolayer structure. As expected the contact angle measurements

demonstrated an increase of the angle values for the initiator monolayer (71.6°) in comparison to the rather hydrophilic silicon wafers (35.8°) (Table 2). Moreover, this contact angle was also in a good agreement with previous results on gold indicating the equal quality of the initiator functionalization in both experiments.

4.3.3. Surface-Initiated Polymerization of BMA and DMAEMA

Scheme 2 shows the synthetic pathway for the preparation of copolymer brushes on gold and silicon surfaces.

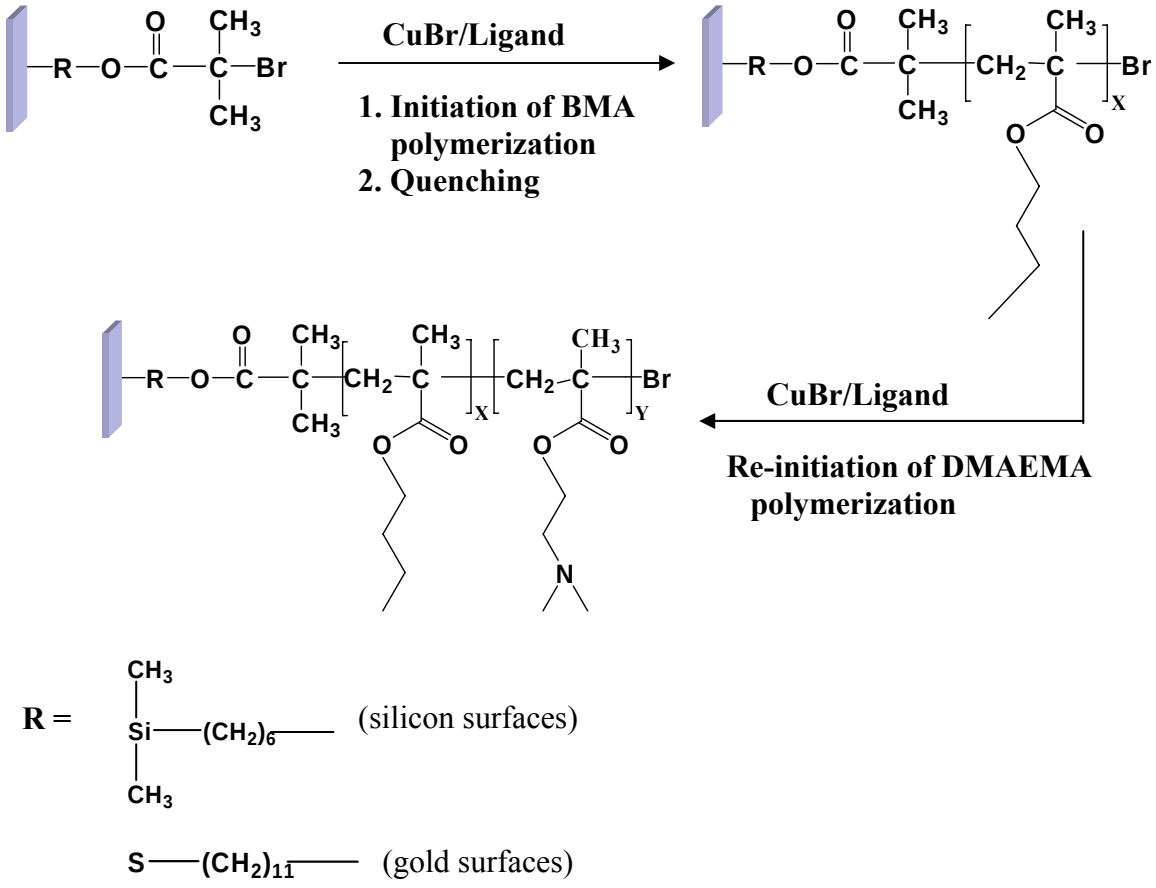

Scheme 2. Synthesis of PBMA-PDMAEMA diblock copolymer brushes via surface initiated ATRP.

The mechanism and kinetics of ATRP is well established.[53, 54] As reported before, N-(n-Propyl)-2-pyridylmethanimine as a ligand in conjunction with Cu(I)Br is effective for polymerization of alkyl methacrylates even in non-polar, non-coordinating solvents such as toluene. This ligand provides high monomer conversion and polymers with low polydispersity index.[55, 56] Therefore, we used N-(n-propyl)-2-pyridylmethanimine for ATRP of BMA. In order to preserve the chain end functionality, the polymerization of BMA was

quenched after 1.5 h reaction time. Thus, the PBMA brushes still containing active bromine atoms at the chain ends served as macroinitiators for the second step of the synthesis. Recently it was reported that the ATRP of DMAEMA proceeds more efficiently in polar media[53, 57] and in presence of multidentate aliphatic tertiary amine ligands. Hence, we chose Me_6TREN as a ligand and THF/acetonitrile solvent mixture for the polymerization of DMAEMA. Such polar solvents provide a better solubility of the copper salts which is particularly important for a surface reaction where no efficient mixing of the solution is possible. Additionally we added a small amount of metallic copper to reduce Cu (II) to Cu (I) and thus to minimize the deactivation process.

4.3.4. Characterization of Copolymer Brushes

As expected, the supporting material (gold, silicon) did not have any measurable influence on the polymer layer thickness (Table1) and the wettability (Table 2) of the PBMA and diblock copolymer layers. This demonstrates the reproducibility of the surface modification on the different supporting materials.

The contact angle of the PBMA brushes (65.3°) was slightly lower than for the initiator SAMs (68.8°) despite of identical end groups. However, apart from the end groups, also the order and packing of the polymer coils containing hydrophobic side chains play an important role for the wetting behavior of the layer. The contact angles for PBMA layers and the diblock brushes were rather similar, i. e. 65.3 and 63.1° respectively (Table 2). However the diblock copolymer brushes were always slightly more hydrophilic than PBMA layer. Most probably this is an influence of the polar amino groups of PDMAEMA which are located close to the film surface. Due to their amphiphilic nature, the surface attached block copolymers can adopt a conformation that allows the highly polar PDMAEMA segment to be oriented towards the aqueous phase, thus shielding the hydrophobic PBMA block inside the supported membrane structure.[45, 58-60]

We further characterized the polymer brushes on the silicon substrates by AFM. The polymer materials on the gold surfaces were not tested because of the rather high roughness of the sputtered gold film. The initial flat silicon surfaces before modification had roughness of ±0.15 nm (Figure 2, A). The polymer brushes caused a change of the surface morphology as well as an increase of the surface roughness up to ±6 nm (Figure 2, B). Similarly to previous reports,[1, 61] we observed a dimple morphology of polymer brushes that seems to be related to the packing of the amphiphilic chains,[1] while the roughness of the layer increased

presumably due to the polydispersity of copolymer and/or formation of micellar like aggregates between different chains.

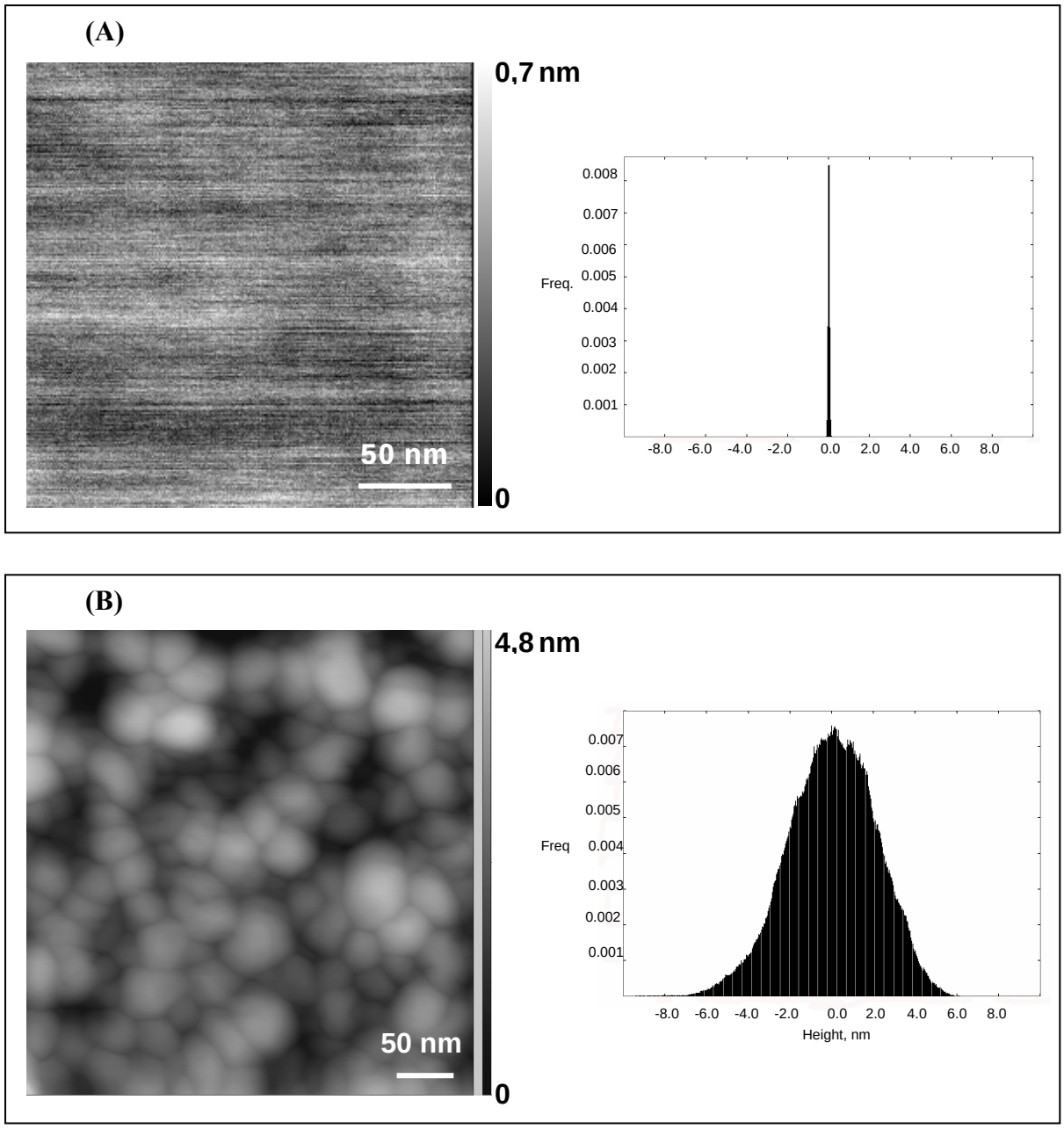

Figure 2. Contact mode AFM images of initial silicon substrate **(A)** and PBMA-PDMAEMA brushes grown on silicon **(B)**. Right pictures demonstrate surface roughness histograms before silicon functionalization **(A)** and after growth of copolymer brushes **(B)**.

Ellipsometric measurements showed a large increase of the film thickness after growth of the polymer layer (Table 1). The thickness of PBMA brushes on gold substrate was found to be 12.3±0.8 nm, i. e. 10.9 nm for the PBMA layer and 1.4 nm for the initiator SAM. Subsequent

DMAEMA copolymerization resulted in further growth of the brushes and a corresponding increase of the layer thickness to overall 23.9±2.8 nm. Hence, the presence of the hydrophilic PDMAEMA block led to an increase of the layer thickness by another 11.6 nm. Analogically, the growth of the first PBMA block from silicon surfaces resulted in a film with overall thickness 14.1±3.1 nm, i. e. after subtraction of the initiator length, the PBMA brushes had a thickness of 12.4 nm. A subsequent polymerization of the second monomer DMAEMA increased the layer thickness up to 24.3±2.2 nm (including initiator SAM). Thus, no significant difference in thickness was observed for membrane structures on gold and silicon surfaces being prepared under the same conditions. However, in situ measurements of the film thickness and topology by ellipsometry and AFM did not provide information about the molecular weight and the polydispersity of the polymers. In order to determine and compare these parameters for the macromolecules grown on gold and silicon surfaces, we detached the polymer brushes from the solid substrates and performed GPC and ^{1}H NMR studies. Oxidation of the thiol group by iodine results in cleavage of the Au-S bond and a release of polymer brushes. This procedure was described to detach polymer chains as individual molecules and dimerization via disulfide-bridge formation was not observed.[38] The detachment of the polymer material from silicon was performed in an etching bath containing 20 wt.-% HF, 40 wt.-% H_2O, 23 wt.-% K_2CO_3, 8 wt.-% KOH and 9 wt.-% Na_2SO_4. The empirically found composition of this mixture provides a soft etching of the silicon layers. It is important to note that the detachment procedure for silicon substrates might cause hydrolysis of the ester bounds. To check whether the polymer structure was affected during the detachment, silicon samples were incubated for different periods of time in the etching bath. Subsequent analysis by GPC and ^{1}H NMR revealed that the polymer structure was not changed by this detachment method.

The chemical composition of the detached PBMA and PBMA-*co*-PDMAEMA diblock polymer brushes was investigated by ^{1}H NMR. The main characteristic protons of PBMA (a- 0.87 ppm, b- 3.96 ppm) and PDMAEMA (c- 2.31 ppm, d- 4.08 ppm) are clearly seen in the spectra (Figure 3). As shown by GPC data (Table 3) all copolymer brushes had relatively narrow polydispersity indexes in the range of 1.13-1.20. Moreover, the polymer brushes grown from gold and silicon substrates under similar conditions had about the same molecular weights. The PBMA brushes from gold and silicon substrates had molecular weights of 16300 g/mol and 15650 g/mol and the molecular weights of detached diblock polymers from gold and silicon were 25550 g/mol and 24500 g/mol respectively. Obviously

the type of the substrates did not influence the growth of the brushes. This corroborates the ellipsometric results that the polymer layers have similar thickness on different substrates.

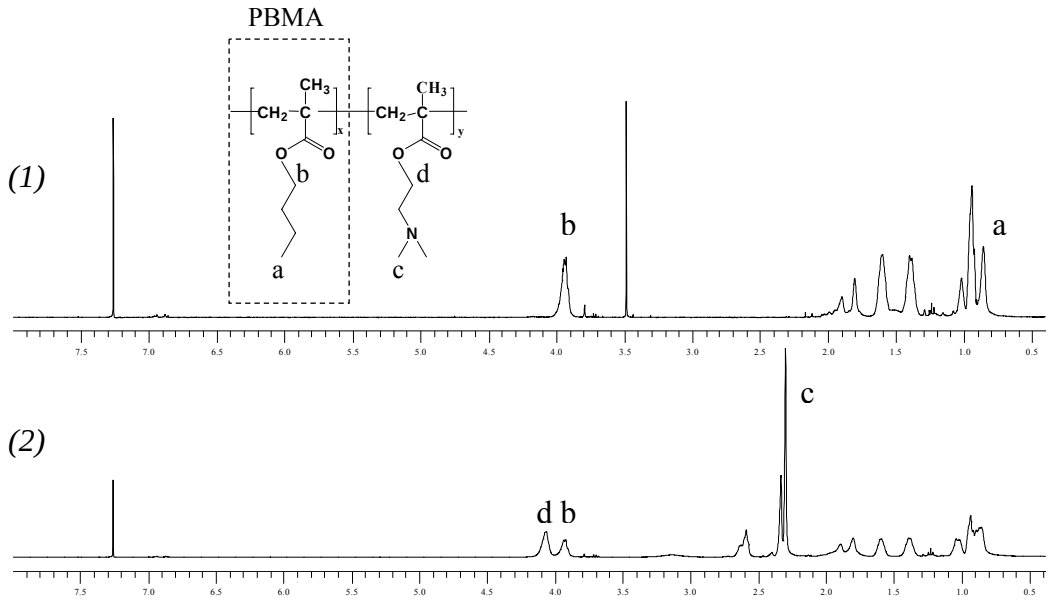

Figure 3. ^{1}H NMR spectra of detached PBMA *(1)* and diblcok copolymer brushes *(2)* in $CDCl_3$.

sample	Polymer	M_n, g/mol	PDI [a)]
1	PBMA detached form gold surface	16300	1.15
2	PBMA detached from silicon	15650	1.18
3	Diblock copolymer brushes PBMA-PDMAEMA from gold substrate	25550	1.13
4	PBMA-PDMAEMA from silicon substrate	24500	1.20

Table 3. Number average molecular weights and polydispersity indexes of copolymer brushes detached from substrates

[a)] Polydispersity index as a ratio of the mass average molecular weight to the number average molecular weight

A comparison between the layer thickness and the molar masses of the block copolymers allowed us to draw conclusions about the conformation of the attached chains. The block copolymers detached from gold surfaces consisted of 115 BMA and 58 DMAEMA units. The

polymers from silicon surfaces were determined to consist of 110 BMA and 56 DMAEMA units. If we assume that the macromolecules are maximally stretched (C-C bonds – 1.5Å, 109. 28° angle), the determined constitution of PBMA brushes must result in a 17.2 nm layer on gold and 16.5 nm layer on silicon. The composition of the PDMAEMA block should correspond to a 8.7 nm size of PDMAEMA part on gold and 8,4 nm on silicon. Hence, the expected membrane thickness for fully stretched block copolymer chains would be 25.9 nm (gold) and 24.9 nm (silicon). These theoretical values are slightly higher than the experimental results from ellipsometry that showed 22.5 nm and 22.6 nm thickness (without initiator layer) of the brushes on gold and silicon surfaces respectively. Therefore we can conclude that the brushes have nearly completely stretched conformation.

Furthermore, we compared the theoretically calculated and experimentally found sizes of PBMA and PDMAEMA blocks separately. Thus, the calculations predict 17.2 nm thick PBMA brushes on gold and 16.5 nm layer on silicon. Interestingly, only a layer thickness of 10.9 nm on gold and 12.4 nm on silicon were measured by ellipsometry. Based on this data we can conclude that the first PBMA block had not a fully stretched conformation before copolymerization of the PDMAEMA. The theoretical size of totally extended PDMAEMA part is 8.7 nm (gold) and 8.4 nm (silicon) while the ellipsometry showed addition of 11.6 nm (gold) and 10.2 nm (silicon) after copolymerization of the second block. Such contradiction of the values might be explained by a conformational change of the first PBMA block that contributed into the overall thickness increase of the brushes. We propose that the first hydrophobic block undergoes stretching after growth of the PDMAEMA on it. The comparison of experimentally found thicknesses and composition of the brushes also support this assumption. Thus, the 2:1 ratio between repeating units of PBMA and PDMAEMA blocks (115 BMA/58 DMAEMA on gold and 110 BMA/56 DMAEMA on silicon) does not fit the ellipsometric data on layer thicknesses that are approximately in ratio 1:1. This corroborates the model for a conformational change of the PBMA block during growth of brushes.

4.4. Conclusions

ATRP was successfully applied for the growth of supported block copolymer membranes from gold and silicon surfaces. We showed that the direct immobilization of initiator molecules resulted in more homogeneous layers while modification of precursor molecules

attached to a surface led to an incomplete initiator film (not 100% conversion). It was found that trichlorosilane (I) formed multilayer structures on the silicon surface even at low concentration of 0.02 wt.-%. In order to optimize the structure of the initiator SAM, monochlorosilane (II) was prepared and used for brush growth. Polymer brushes on the solid supports were well characterized by ellipsometry and contact angle measurements. A successful detachment of the macromolecules from the substrates allowed further characterization using GPC and ^{1}H NMR. The performed experiments clearly showed that the nature of the selected substrates had no significant influence on the molecular weights and PDIs of the polymer brushes. Comparing theoretical calculations and experimental data, we concluded that the first polymer block had a slightly stretched conformation while the copolymerization of the hydrophilic PDMAEMA causes a transition to a fully extended PBMA chains. Further we explored the potential of the presented functionalization approach to structure silicon surface by microcontact printing (available as supporting information).

4.5. Outlook

The growth of amphiphilic ABA and ABC triblock copolymers where the middle block B is hydrophobic and the end blocks are hydrophilic is a next step in our work. Such a polymeric membrane can provide a model of lipid bilayer. Here the first hydrophilic block provides a spacer that decouples the membrane from the surface and allows investigating the molecular transport across the polymer membrane.

4.6. Acknowledgements

The authors thank Daniel Mathys, ZMB UniBasel, Switzerland, for SEM analysis and Heiko Wolf, IBM Research laboratory, Rueschlikon, Zurich, Switzerland, for providing microcontact printing PDMS stamp. Special thanks to Rupert Konradi and the group of Prof. Markus Textor, ETH Zurich, Switzerland, for the access to ellipsometer. This work was supported by NCCR Nanoscale Science, Swiss National Science Foundation and MRTN-CT-2003-505027.

4.7. References

[1] Luzinov I., Minko S., Tsukruk V. V. *Prog. Polym. Sci.* **2004**, *29*, 635.

[2] Pyun J., Matyjaszewski K. *Chem. Mater.* **2001**, *13*, 3436.

[3] Tsubokawa N., Saton M. J. *Appl. Sci.* **1997**, *65*, 2165.

[4] Hyun J., Chilkoti A. *Macromolecules* **2001**, *34*, 5644.

[5] Jordan R., Ulman A. *J. Am. Chem. Soc.* **1998**, *120*, 243.

[6] Advincula R., Zhou Q., Park M., Wang S., Mays J., Sakellariou G., Pispas S., Hadjichristidis N. *Langmuir* **2002**, *18*, 8672.

[7] Zhou Q., Wang S., Fan X., Advincula R. *Lanqmuir* **2002**, *18*, 3324.

[8] Matrab T., Chehimi M. M., Boudou J. P., Benedic F., Wang J., Naguib N. N., Carlisle J. A. *Diamond & Related Materials* **2006**, *15*, 639.

[9] Bontempo D., Tirelli N., Feldmann K., Masci G., Crescenzi V., Hubbell J. A. *Adv. Mater.* **2002**, *14*, 1239.

[10] Huang W., Kim J.-B., Bruening M. L., Baker G. L. *Macromolecules* **2002**, *35*, 1175.

[11] Xu C., Wu T., Beers K. L. *Polym. Mater.:Sci. & Engineering* **2006**, *94*, 308.

[12] Ejaz M., Ohno K., Tsujii Y., Fukuda T. *Macromolecules* **2000**, *33*, 2870.

[13] Jeyaprakash J. D., Samuel S., Dhamodharan R., Rühe J. *Macromol. Rapid Commun.* **2002**, *23*, 277.

[14] Kobayashi M., Takahara A. *Chemistry letters* **2005**, *34*, 1582.

[15] Yu W. H., Kang E. T., Neoh K. G. *Langmuir* **2004**, *20*, 8294.

[16] Cringus-Fundeanu I., Luijten J., Van der Mei H. C., Busscher H. J., Schouten A. J. *Langmuir* **2007**, *23*, 5120.

[17] Ryoko I., Piyawan S., Vipavee P., Atsushi T., Kazunari A., Yasuhiko I. *Biomacromolecules* **2004**, *5*, 2308.

[18] Xu C., Wu T., Beers K. L. *Polym.Mater.:Sce.&Engineering* **2006**, *94*, 308.

[19] Zhou F., Huck W. T. S. *Chem.Commun.* **2005**, 5999.

[20] Osborne V. L., Jones D. M., Huck W. T. S. *Chem. Commun.* **2002**, 1838.

[21] Kim D. J., Kang S. M., Bokyung K., Wan-Joong K., Hyun-Jong P., Hyeon C., Insung C. *Macromol. Chem. Phys.* **2005**, *206*, 1941.

[22] Zhang K., Li H., Zhao S., Wang W., Wang S., Xu Y., Yu W., Wang J. *Polym. Bulletin* **2006**, *57*, 253.

[23] Antonietti M., Förster S., Hartmann J., Oestreich S. *Macromolecules* **1996**, *29*, 3800.

[24] Weaver J. V. M., Bannister I., Robinson K. L., Bories-Azeau X., Armes S. P. *Macromolecules* **2004**, *37*, 2395.

[25] Yamamoto Y., Yasugi K., Harada A., Nagasaki Y., Kataoka K. J. *Controlled. Release* **2002**, *82*, 359.

[26] Discher D. E., Eisenberg A. *Science* **2002**, *297*, 967.

[27] Antonietti M., Förster S. *Adv. Mater.* **2003**, *15*, 1323.

[28] Stoenescu R., Meier W. *Chem. Commun.* **2002**, 3016.

[29] Ivanova R., Lindman B., Alexandridis P. *Adv. Colloid Interface Sci.* **2001**, *89-90*, 351.

[30] Wang L., Chen X., Chai Y., Hao J., Sui Z., Zhuang W., Sun Z. *Chem. Commun.* **2004**, 2840.

[31] Vriezema D. M., Hoogboom J., Velonia K., Takazawa K., Christianen P. C. M., Maan J. C., Rowan A. E., Nolte R. J. M. *Angew. Chem.* **2003**, *42*, 772.

[32] Kita-Tokarczyk K., Grumelard J., Haefele T., Meier W. *Polymer* **2005**, *46*, 3540.

[33] Opster J. A., Cornelissen J. J. L. M., Van Hest J. C. M. *Pure Appl. Chem.* **2004**, *76*, 1309.

[34] Nardin C., Thoeni S., Widmer J., Winterhalter M., Meier W. *Chem. Commun.* **2000**, 1433.

[35] Bermudez H., Aranda-Espinoza H., Hammer D. A., Discher D. E. *Europhys. Lett.* **2003**, *64*, 550.

[36] Mecke A., Dittrich C., Meier W. *Soft. Matter.* **2006**, *2*, 751.

[37] Keller R. N., Wycoff H. D. *Inorg. Synth.* **1947**, *2*, 1.

[38] Haddleton D. M., Crossman M. C., Dana B. H., Duncalf D. J., Heming A. M. *Macromolecules* **1999**, *32*, 2110.

[39] Queffelec J., Gaynor S. G., Matyjaszewski K. *Macromolecules* **2000**, *33*, 8629.

[40] Shah R. R., Merreceyes D., Husemann M., Rees I., Abbott N. L., Hawker C. J., Hedrick J. L. *Macromolecules* **2000**, *33*, 597.

[41] Husseman M., Malmström E. E., McNamara M., Mate M., Mecerreyes D., Benoit D. G., Hedrick J. L., Mansky P., Huang E., Russell T. P., Hawker C. J. *Macromolecules* **1999**, *32*, 1424.

[42] Mori S. *J. Liquid Chromatogr.* **1990**, *13*, 1719.

[43] Kaufmann T. C., Engel A., Remigy H.-W. *Biophysical J.* **2006**, *90*, 310.

[44] Ulman A. *Chem. Rev.* **1996**, *96*, 1533.

[45] Huang W., Kim J-B., Baker G. L., Bruening M. L. *Nanotechnology* **2003**, *14*, 1075.

[46] Huang W., Kim J-B., Bruening M. L., Baker G. L. *Macromolecules* **2002**, *35*, 1175.

[47] Shah R. R., Merreceyes D., Husemann M., Rees I., Abbott N. L., Hawker C. J., Hedrick J. L. *Macromolecules* **2000**, *33*, 597.

[48] Kim J.-B., Bruening M. L., Baker G. L. *J. Am. Chem. Soc.* **2000**, *122*, 7616.

[49] Kim J.-B., Huang W., Miller M. D., Baker G. L., Bruening M. L. *J. Polym. Scie. A* **2003**, *41*, 386.

[50] Maoz R., Yam R., Berkovic G., Sagiv J. *Thin films*, A. Ulman Ed.; New York **1995**, p. 20.

[51] Maoz R., Sagiv J., Degenhardt D., Möhwald H., Quint P. *Supramol. Sci.* **1995**, *2*, 9.

[52] Matyjaszewski K., Miller P. J., Shukla N., Immaraporn B., Gelman A., Luokala B. B., Siclovan T. M., Kickelbick G., Vallant T., Hoffmann H., Pakula T. *Macromolecules* **1999**, *32*, 8716.

[53] Wang J.-S., Matyjaszewski K. *Macromolecules* **1995**, *28*, 7901.

[54] Coessens V., Pintauer T., Matyjaszewski K. *Prog. Polym. Sci.* **2001**, *26*, 337.

[55] Haddleton D. M., Heming A. M., Jarvis A. P., Khan A. *Macromol. Symp.* **2000**, *157*, 201.

[56] Haddleton D. M., Crossman M. C., Dana B. H., Duncalf D. J., Heming A. M. *Macromolecules* **1999**, *32*, 2110.

[57] Zhang X., Matyjaszewski K. *Macromolecules* **1999**, *32*, 1763.

[58] Kong X., Kawai T., Abe J., Iyoda T. *Macromolecules* **2001**, *34*, 1837.

[59] Zhao B., Brittain W. J. *J. Am. Chem. Soc.* **1999**, *121*, 3557.

[60] Hu D., Cheng Z., Zhu J., Zhu X. *Polymer* **2005**, *46*, 7563.

[61] Prokhorova S. A., Kopyshev A., Ramakrishnan A., Zhang H., Rühe J. *Nanotechnology* **2003**, *14*, 1098.

4.8. Supporting information

We used ATRP to synthesize diblock copolymers of the same chemical structure, i.e. PBMA-PDMAEMA having different molecular weights. These block copolymers were prepared in solution and the molecular weights were determined using three methods: GPC, vapor osmometry and ^{1}H NMR. The data obtained showed good correlation between the three methods that allowed us to establish the copolymer composition accurately (see Table below) and let us to rely on the GPC data. Therefore, we used GPC analysis for molecular weight estimation of PBMA-PDMAEMA block copolymers detached from the surfaces.

№	M_n, g/mol			PDI	Polymer composition [a)]
	GPC	^{1}H NMR	VO		
1	6810	6250	6700	1,10	$PBMA_{45}$
2	16000	16100	16520	1,15	$PBMA_{45}$ – $PDMAEMA_{60}$
3	13120	13310	13600	1,12	$PBMA_{45}$ – $PDMAEMA_{42}$
4	9360	9600	9700	1,10	$PBMA_{45}$ – $PDMAEMA_{20}$

Table. Number average molecular weights (M_n) and composition of PBMA-PDMAEMA copolymers determined using three methods: GPC, ^{1}H NMR and vapor osmometry (VO).

[a)] Contribution from initiator fragments of 193 g/mol was taken into account. Polymer composition demonstrates the average values from three methods

The structuring of polymers on the surface and creation of patterned polymeric membranes are highly interesting for applications in the area of biosensing and molecular recognition. Surface patterning allows a special design with a well defined location of the target molecules. Silicon supports are the most promising surfaces for this application because silicon chemistry provides covalent-bounded composite materials which are mechanically and chemically stable. Therefore it was interesting for us to apply the proposed synthetic approach for microcontact printing (μCP) on silicon surface. The structure and size of μCP PDMS mask is presented in Scheme 3. The mask was inked by monochlorosilane **(II)** initiator and left on the silicon surface for 5 minutes. Since the thickness of the initiator layer is around 1,7±0,2 nm, it was not visible under SEM conditions. Subsequent polymerization resulted in the formation of polymer brushes (Figure below). To make sure that the synthetic

procedure was successfully applied, we performed control experiment to show that the PDMS mask inked by ethanol does not leave any traces on the silicon surface.

Further experiments to prove the composition of brushes are in progress and will be reported elsewhere.

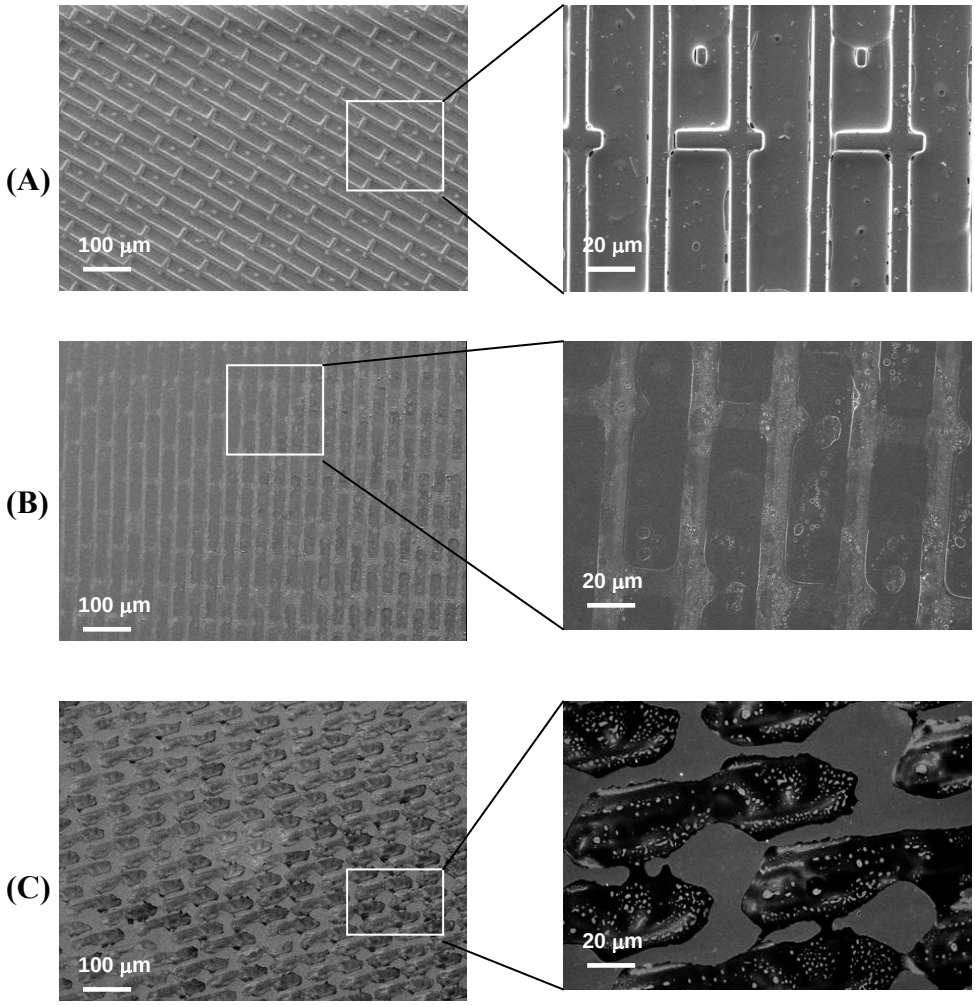

Figure. Microcontact printing on silicon surface. **(A)** structure of PDMS μCP stamp, **(B)** PBMA brushes, **(C)** diblock copolymer PBMA-PDMAEMA brushes.

5. Solid-supported amphiphilic triblock copolymer membranes grafted from gold surface

Ekaterina Rakhmatullina[1], Alexandre Mantion[1], Thomas Bürgi[2], Violeta Malinova[1], Wolfgang Meier[1]

[1] Department of Chemistry, University of Basel, Klingelbergstrasse 80, CH-4056

[2] Department of Chemistry, University of Neuchatel, Avenue de Bellevaux 51, CH-2007

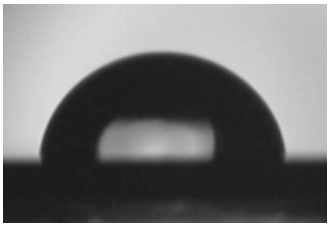

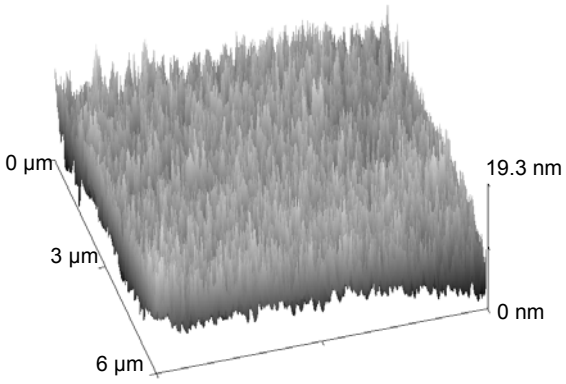

Submitted to: *Macromolecules 2008*

5.1. Introduction

Within the recent years the design of model membrane systems mimicking the properties of natural biomembranes has received a lot of scientific attention. This is due to the fact that such systems may allow for a better understanding of membrane-related processes as well as for preparation of biosensors.[1] To date, the most commonly used model system is based on the so called "tethered bilayer lipid membrane" (tBLM),[2] which consists of a lipid bilayer that is tethered via a hydrophilic polymer,[3-5] lipopolymer[6, 7] or peptide[8-10] to a solid support (Scheme 1, b). Often gold is chosen as a support material since it is suitable for surface analytical techniques and can serve as electrode to study the dielectric properties of the system. To provide the system with robustness and stability, the tethered spacers (polymers, peptides) have to be covalently linked to the substrate. Such membranes are commonly prepared from self-assembled monolayers,[11] by Langmuir-Blodgett (LB) transfer[12, 13] or by fusion of lipid vesicles onto 'activated' surfaces.[14] Besides the delicate and complex route of preparation and aspects such as the polymer-lipid bilayer interactions that have to be carefully considered, the final system is often deficient of stability.

On the other hand, amphiphilic block copolymer membranes have proven to be a very useful model of the cellular membrane permitting also an incorporation of functional proteins and enzymes.[15] Block copolymers are known to form chemically and mechanically more stable membranes than conventional lipids.[16, 17] They allow tailoring of their properties for a specific purpose by introducing desired functional groups, which is not possible with lipids to such extent. Moreover, the membrane thickness can be easily controlled through controlling the polymer molecular weight.[18] These hallmarks make amphiphilic block copolymer membranes highly attractive also as model systems for biosensing. Typically, for such applications solid-supported membrane structures are required. Recently we demonstrated that similar to conventional phospholipid vesicles[19, 20] also block copolymer vesicles with charged hydrophilic blocks can fuse on mica and glass surfaces to solid-supported, planar block copolymer membranes.[21] Previous experiments showed also that amphiphilic diblock copolymer brushes could successfully be grown from silicon and gold surfaces using a surface initiated ATRP.[22] However a closer mimicking of the characteristic morphology of a biological membrane requires a sequence of hydrophilic, hydrophobic and again hydrophilic polymer blocks (Scheme 1, a), i.e. an amphiphilic ABA' or ABC triblock copolymer.[23-25] Here we applied a "grafting from" approach[26] to synthesize amphiphilic ABA' triblock copolymer membranes by surface-initiated ATRP. This technique provides a good control

over the brush thickness through a control of the polymer molecular weights[27] and allows preparation of block copolymers by simply activating the functional chain end in the presence of different monomers.[28, 29] As a model we synthesized poly(2-hydroxyethyl methacrylate)-co-poly(n-butyl methacrylate)-co-poly(2-hydroxyethyl methacrylate) (PHEMA-co-PBMA-co-PHEMA) block copolymers with the first PHEMA block being anchored to the gold surface while the other PHEMA block is exposed to the outer interface (Scheme 1, a). The hydrophilic PHEMA blocks of the biomimetic membranes are not fully water-soluble, but take up water and considerably swell in aqueous media. It should be noted that the pendant hydroxy groups of this polymer can conveniently be functionalized,[30] which allows further tuning of their properties. Here we prepared block copolymer brushes with different block lengths and characterized them both on the gold surfaces and - after detaching them from the solid support - in solution. Notably, we monitored also the orientation of the amphiphilic copolymer brushes during their growth since this might be an important parameter regarding the insertion of different biological objects into the membrane.

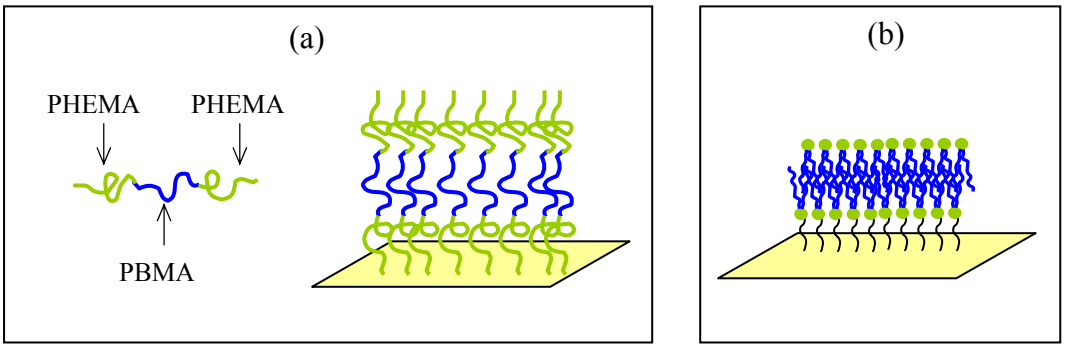

Scheme 1. Schematic representations of the solid-supported amphiphilic PHEMA-co-PBMA-co-PHEMA membrane (left) and tethered lipid bilayer (right).

5.2. Experimental Part

5.2.1. Materials

n-Butyl methacrylate (n-BMA) (Fluka; 99%) and 2-hydroxyethyl methacrylate (HEMA) (Aldrich; 98%) were purified by passing through a column of activated basic alumina before use for removal of the inhibitor. Copper (I) bromide (Aldrich; 98%) was purified according to the method of Keller and Wycoff.[28] The ligand N, N, N', N'', N'''-Pentamethyldiethylenetriamine (≥98%) (PMDETA) (Fluka) was used without further purification. The disulfide initiator $(BrC(CH_3)_2\,COO(CH_2)_{11}\,S)_2$ was synthesized according

to a literature procedure.[29] Filters Durapore-PVDF were acquired from Millipore Corporation. All other chemicals were obtained from Fluka and used without any further purification.

5.2.2. Preparation of the gold substrates

Silicon slides were cleaned in piranha solution (H_2SO_4: H_2O_2, 3:1, vol.%) using sonication. Wafers were rinsed thoroughly with bidistilled water, then sonicated in bidistilled water, washed once more with water, ethanol and dried under a stream of nitrogen. Clean silicon slides were directly used for the sputtering of 15 nm chromium adhesion layer followed by 50 nm of gold (Baltec SCD 050 for Cr 120 mA, 0.05mbar; Baltec MED 020 for Au 50 mA, 0.02 mbar, all in argon atmosphere).

5.2.3. Functionalization of gold surfaces by ATRP initiator monolayer

2 wt.-% THF solution of $(BrC(CH_3)_2\ COO(CH_2)_{11}\ S)_2$ (initiator) was passed through a Durapore-PVDF filter. In order to form self-assembled monolayers (SAM) of the initiator molecules on the gold surface, gold substrates were immersed into the prepared initiator solution overnight at room temperature. After that, the samples were washed with THF, ethanol and dried in nitrogen stream.

5.2.4. Growth of Polymer Brushes from Immobilized Initiator SAM

Synthesis of the first PHEMA block

To a degassed 2 M HEMA solution in methanol:water (1:1,vol.-%), 144 mg (1 mmol) CuBr, 22.4 mg (0.1 mmol) $CuBr_2$, 6.3 mg (0.1 mmol) Cu and 300 mg (1 mmol) PMDETA were added under a flow of nitrogen. The mixture was degassed using three freeze-pump-thaw cycles and stirred until a homogeneous blue solution was formed.

The initiator modified substrates were placed into another flask equipped with a rubber septum. The flask was degassed, filled with the above described polymerization solution and the reaction was carried out at 35°C for 35 min (experiment **1**) and 50 min (experiment **2**). After this time the reaction was quenched by injecting an ethanol/water solution of $CuBr_2$ and PMDETA (1:1 molar ratio, 0.02 M $CuBr_2$) in order to preserve the end-functionality of the PHEMA block. The substrates were consecutively cleaned with ethanol, water, ethanol and dried under a nitrogen stream.

Synthesis of the second PBMA block

The same procedure as the one described for HEMA was applied for BMA polymerization, but dimethylformamide (DMF) was used as a polymerization solvent. The reaction was

carried out for 50 minutes (experiment **1**) and 70 min (experiment **2**) and quenched by addition of a $CuBr_2$/PMDETA solution.

The substrates were cleaned with DMF, several portions of ethanol and dried under a nitrogen stream.

Synthesis of the third PHEMA block

A similar procedure as in *2.4.2.* was applied for HEMA copolymerization. Reactions were carried out for 1 h (experiment **1**) and 1.5 h (experiment **2**) and stopped without quenching.

The substrates were cleaned with DMF, several portions of ethanol and dried under a nitrogen stream.

5.2.5. Solvent treatment for AFM study

The polymer functionalized gold substrates were immersed into ethanol overnight. The samples were dried at room temperature prior to AFM investigation. To investigate the influence of selective solvents the same samples were re-immersed into hexane overnight, dried at room temperature and further analyzed by AFM. For the AFM analysis of amphiphilic copolymer brushes in water, the sample was immersed into ethanol for 2 hours, ethanol/water (1:1, vol.%) mixture for 2 hours and left in aqueous medium overnight.

5.2.6. Detachment of the copolymer brushes from the gold substrate

Gold substrates with polymer brushes were immersed for 15 hours in flask containing 5% iodine solution in THF. The flasks were wrapped by alumina foil. Then the slides were taken out and the residual THF solution was passed through a column with neutral alumina.

5.2.7. Measurement Methods

^{1}H NMR

Spectra were recorded in THF-d8 on a 400.1300 MHz Varian Unity 400NMR spectrometer with sweep width of 8278.146 Hz and a 22° pulse width of 2.96 μs.

Gel permeation chromatography (GPC)

Agilent Technologies GPC instrument with a ODS Hypersil column (5 μm) and polystyrene standards were used. The data obtained were corrected for polymethacrylate standards as described by Mori.[30] A refractive index detector was applied for sample detection. Tetrahydrofuran was used as eluent.

Contact angle determination

All measurements were performed using plate method, Tensiometer K100MK2, Krüss Gmbh. Bidistilled water was applied for the analysis. The presented results were taken as average values from three measurements.

Ellipsometry

Film thicknesses were determined using a spectroscopic multi angle ellipsometer (SENTECH SE 850-STE, Sentech Instruments Gmbh) measuring at three angles of 45°, 55°, and 65°. Measurements were carried out with dried samples.

Attenuated Total Reflectance Fourier Transform Infrared spectroscopy (ATR-FTIR)

ATR-FTIR measurements were performed using a FTIR-8400S spectrophotometer applying Golden Gate ATR setup, Shimadzu. Spectra were recorded with 128 scans repetition for the blank gold surface and the sample, with 2 cm^{-1} resolution.

Atomic Force Microscopy (AFM)

Contact mode AFM was performed using PycoLE System, Molecular Imaging, and gold coated silicon nitride cantilevers (k=0.12 N/m). Images were recorded at scan speed 1 line/s, force set point 0.147 V, in topography and friction modes with a pixel number of 512 x 512. All measurements were done at room temperature.

Polarization Modulation Infrared Reflection Absorption Spectroscopy (PM-IRRAS)

The sample was mounted in the complementary setup for PM-IRRAS measurements within the compartment of a Bruker PM 50, connected to an external beam port of a Bruker Tensor 27 Fourier Transform Infrared spectrometer. The detector was a photovoltaic MCT element cooled with liquid nitrogen. Polarization was modulated with a photoelastic modulator (Hinds, PEM 90) at a frequency of 50 kHz. Demodulation was performed with a lock-in amplifier (Stanford Research, SR830 DSP). All spectra were recorded with a resolution of 1 cm^{-1}. Bare plasma cleaned gold surface served as a reference for the PM-IRRAS spectra. Data analysis was performed using Fytik. Peaks were modeled using Gaussian curves. Reference spectra for PBMA and PHEMA were recorded using commercial non crystalline polymers.

Since the polymer brushes were grown on a polycrystalline gold surface, the angle Φ could not be determined. The angle θ was determined using the Debe method.[34] The azimuthal

factor was taken into the relative concentration factor and was further ignored.[35] We selected vibrations from the ester functionality ν(C=O) at 1732 cm^{-1} and ν(C-C-O) at 1080 cm^{-1} for the analysis.[36]

5.3. Results and discussion

The synthesis of the triblock PHEMA-*co*-PBMA-*co*-PHEMA copolymer brushes included an immobilization of initiator molecules on gold substrates followed by ATRP of HEMA and BMA monomers. Subsequent analyses of the copolymer brushes on surface and a characterization of the detached polymers are described below.

5.3.1. Initiator SAM

As we showed before,[22] anchoring of the initiator molecules $(BrC(CH_3)_2\ COO(CH_2)_{11}\ S)_2$ resulted in a densely packed homogeneous self-assembled monolayer (SAM) on the gold surface. Therefore, we used the same procedure to functionalize gold with initiator molecules. Ellipsometric measurements showed that the obtained initiator layer had a thickness of 1.6±0.2 nm (Table 1).

Since the modification of gold changes the surface polarity, which is directly reflected in the wetting behavior, we performed contact angle measurements on gold slides before and after initiator immobilization. Basically, the more hydrophilic the surface, the larger is the contact area of a water droplet on it and, therefore, the smaller is the value of the contact angle. Thus, we detected a change in the contact angle from 75,3° (gold) to 69,5° (gold with initiator layer, Table 2). Freshly prepared and analyzed initiator-modified gold substrates were directly used for the following polymerization step.

5.3.2. Synthesis of the amphiphilic triblock PHEMA-PBMA-PHEMA brushes

Scheme 2 represents the surface-initiated ATRP of HEMA and BMA applied for the preparation of the triblock copolymer brushes on gold. The mechanism and kinetics of ATRP are well established.[37,38] A methanol/water solvent mixture was chosen for the polymerization of the first PHEMA block since it allowed a fast growth of the PHEMA brushes[39-42] and provided a good solubility of the copper salts. However, we used DMF as a solvent for copolymerization of both the PBMA- and the third PHEMA-blocks. It was shown that DMF is a good and non-selective solvent for the triblock copolymers,[43] thus providing accessible polymer chain ends for the subsequent growth reactions.

In order to preserve the chain end functionality, after the corresponding reaction time, each polymerization step was quenched by addition of a $CuBr_2$/PMDETA solution in the same solvent as applied for the ATRP. Additionally, we added a small amount of metallic copper to reduce Cu (II) to Cu (I) and thus to minimize the deactivation process. Hence, the corresponding polymer brushes (PHEMA and PHEMA-co-PBMA) containing active bromine atoms at the chain ends served successfully as macroinitiators for the next synthetic step.

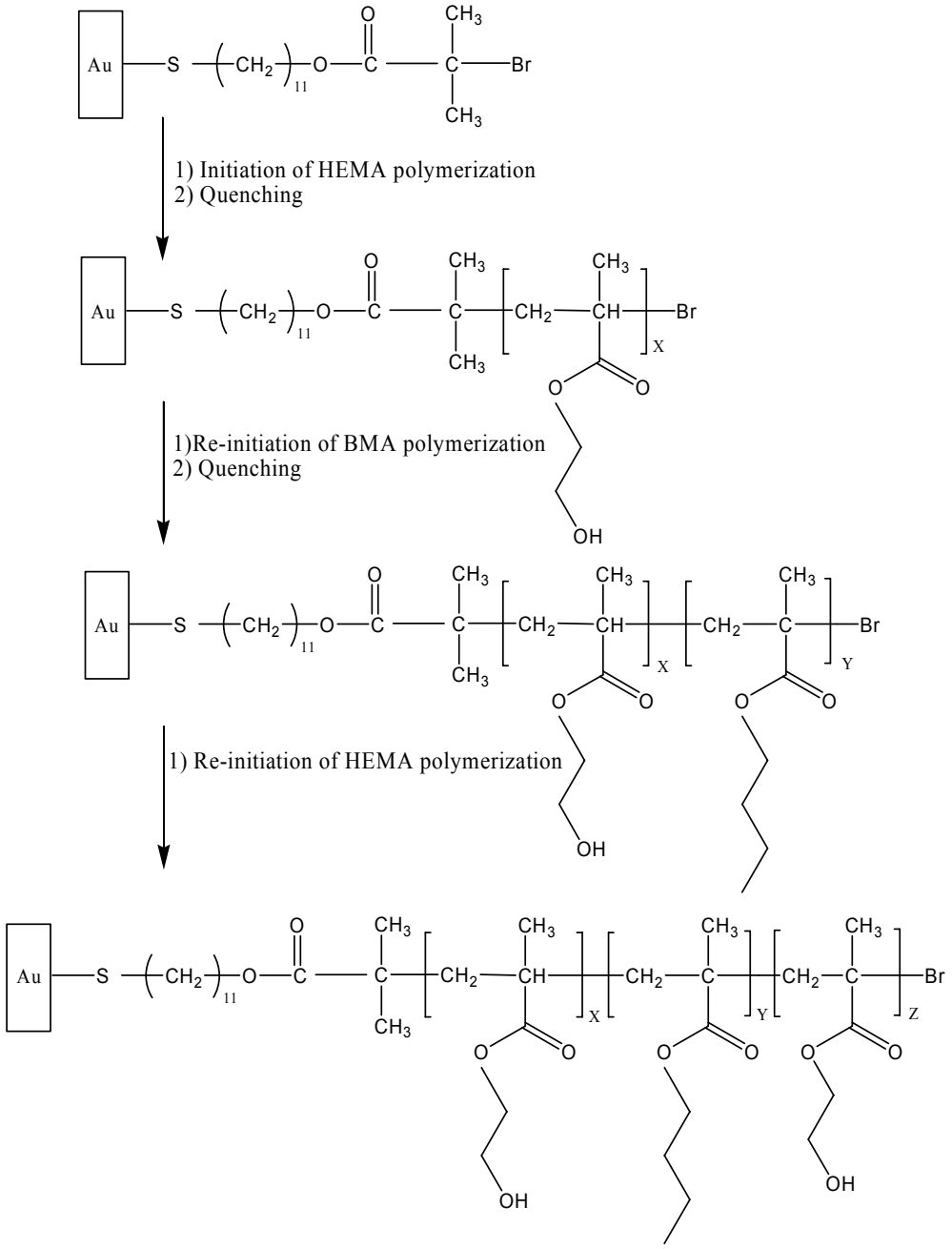

Scheme 2. Synthesis of PHEMA-co-PBMA-co-PHEMA triblock copolymer brushes via surface initiated ATRP.

5.3.3. Characterization of the copolymer brushes

Two experiments, i.e. experiments 1 and 2, were performed where we varied the applied polymerization time for the synthesis of polymer blocks (see Experimental part, 2.4.). After each modification step, a subsequent change in the surface wetting behavior was detected. Since the measured contact angle values for the polymer brushes synthesized in experiment 1 and 2 were identical within experimental error, average values of the angles are presented in Table 2. The contact angle decreased from 69.5° (initiator SAM) to 60.8° (Table 2) after the first PHEMA block was grown on the surface. Thus, in spite of the identical bromine end groups, the PHEMA layer exhibited more hydrophilic surface compared to the initiator SAM. It is known that the contact angles are very sensitive to the topmost surface composition changes, with a sensing depth of approximately 0.5-1.0 nm.[41] Therefore, the hydroxyl side groups of the PHEMA block can potentially contribute to the overall hydrophilicity of the film.

The contact angles for the subsequent diblock brushes (63.4°) did not differ significantly from those measured for PHEMA layers (60.8°) (Table 2). However, we noted that the diblock brushes in all samples were consistently slightly more hydrophobic than the PHEMA layer. Most probably, this is an influence of the hydrophobic n-butyl side groups which can be partially exposed outside of the layer.

Exp. №	Reaction time, min	Sample	Thickness, nm	M_n, g/mol	PDI *
		Initiator SAM	1.6±0.2	-	-
1	35	PHEMA	3.9±0.5	2800	1.1
	50	PHEMA-co-PBMA	6.0±0.4	7700	1.2
	60	PHEMA-co-PBMA-co-PHEMA	8.1±0.5	11800	1.3
2	50	PHEMA	7.2±0.6	6000	1.1
	70	PHEMA-co-PBMA	12.2±0.8	14300	1.2
	90	PHEMA-co-PBMA-co-PHEMA	15.1±0.8	17800	1.6

Table 1. Thickness of the polymer layers on the gold surface measured by ellipsometry. Number average molecular weights (M_n) and polydispersity indexes (PDI) of detached copolymer brushes.

* Polydispersity index as a ratio of the mass average molecular weight to the number average molecular weight

However, the contact angle value of the triblock copolymer layer was found to be 62.6°, i.e. did also not change drastically from the contact angle of the diblock PHEMA-co-PBMA brushes. Thus we assume that the different side groups in the polymer chains do not provide a considerable change in the contact angle values since order and packing of the macromolecules also play an important role for the wetting behavior of the complete polymer layer. Additionally, both PHEMA and PBMA blocks have an identical backbone which can also contribute to the rather similar contact angle values.

The experiments with different reaction times should yield block copolymers with various chain lengths and hence, a variation of the overall layer thicknesses. Indeed ellipsometric measurements showed a significant increase of the film thickness after growth of each polymer block (Table 1). Polymerization of the first PHEMA block resulted in the increase of the layer thickness from 1.6 nm for the pure initiator SAM to 3.9 nm (experiment **1**) and 7.2 nm (experiment **2**), respectively. This corresponds to a thickness of the PHEMA layers of 2.3 nm and 5.6 nm. A subsequent growth of the polymer brushes upon BMA polymerization caused a further increase of the polymer layer thickness to overall 6.0 nm (experiment **1**) and 12.2 nm (experiment **2**). After addition of the third block-PHEMA, the polymer layer thickness raised to overall 8.2 nm (experiment **1**) and 15.1 nm (experiment **2**). Hence, the last copolymerization step provided approximately 2.2 nm (experiment **1**) and 2.9 (experiment **2**) nm thick PHEMA layers. These results confirm the successful growth of the individual blocks of the polymer brushes.

Sample	**Contact angle, °**
gold	75.3
Initiator SAM	69.5
PHEMA brushes	60.8
PHEMA-co-PBMA	63.4
PHEMA-co-PBMA-co-PHEMA	62.6

Table 2. Contact angle measurements of the functionalized gold surfaces*. The presented values are an average from three measurements of each sample obtained in the experiment 1 and 2.

* Bidistilled water was used for the analysis

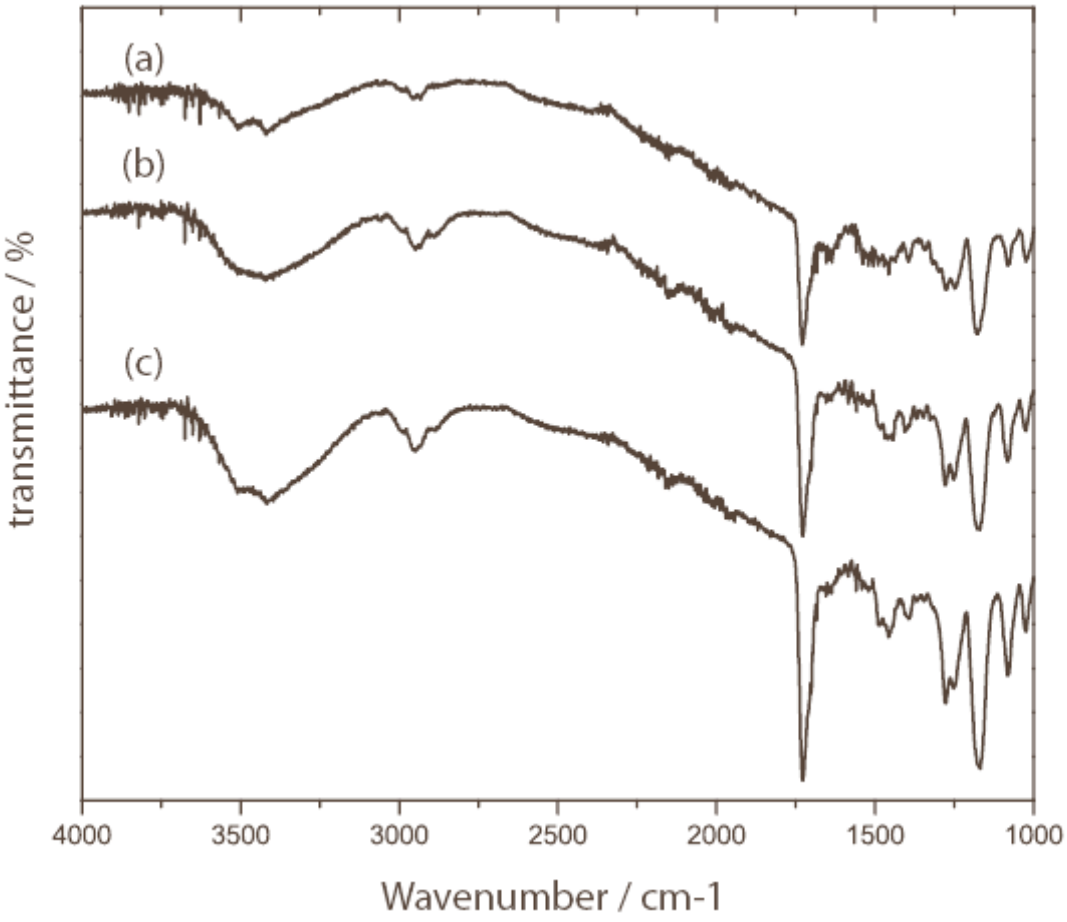

Figure 1. ATR-FTIR spectra of the first PHEMA block (a), PHEMA-co-PBMA diblock (b) and PHEMA-co-PBMA-co-PHEMA triblock (c) brushes (experiment 2) on the gold support.

We further investigated the copolymer brushes using ATR-FTIR spectroscopy to prove the growth of the individual blocks. For the samples from both experiments an increase of the peak intensity of the main characteristic functional groups was detected (Figure 1). The PHEMA spectrum (Figure 1, a) demonstrated characteristic absorption bands for $\nu(CH_2)$ and $\nu(CH_3)$ at around 2880-2990 cm^{-1} and $\delta(CH_3)$ and $\delta(CH_2)$ at around 1360 cm^{-1} and 1470 cm^{-1}, respectively. The presence of the ester group of the methacrylate copolymer chains was confirmed by the strong signal $\nu(C=O)$ at 1740 cm^{-1}. After copolymerization of the PBMA block, the ATR-FTIR spectrum (Figure 1, b) showed an increase of the intensity of all characteristic peaks. The most significant change of the peak intensity corresponded to the carbonyl signal at 1740 cm^{-1}. Additional increase in the intensity of absorption bands corresponding to CH, CH_2, CH_3 and C=O functional groups (Figure 1, c) was detected also after growth of the third PHEMA block. The broad peak at about 3500 cm^{-1} belongs to the

OH groups of the PHEMA where the two bands at 3414 and 3515 cm^{-1} can be clearly attributed to hydrogen bonds between hydroxyl groups of the PHEMA blocks.

Moreover, we performed polarization modulation reflection absorption IR spectroscopy (PM-IRRAS) measurements in order to detect the change of the polymer brush orientation towards the surface during their growth. A signal in PM-IRRAS is observed when the transitory dipole moment of a molecule is perpendicular to the surface; otherwise the signal remains invisible. PM-IRRAS was proved to be an effective method to determine the molecular orientation at surfaces, not only for small molecules,[45, 46] but also for polymers.[47, 48]

For our analysis we used the sample synthesized in experiment **2**. The angle conventions are given in Figure 2. Simply, Φ represents the angle by which the chain is rotated around the z axis, while Ψ is the angle of molecule rotation around its main axis and θ shows the tilt of the main molecular axis with respect to the normal of the surface. We took into consideration the dipolar moment associated with the ester functionality, since the signal attribution was already performed in similar systems.[49, 50] Furthermore, the vibrations from the methacrylate ester groups ν(C=O) at 1732 cm^{-1} and ν(C-C-O) at 1080 cm^{-1} (Figure 3) have orthogonal, unambiguous character and do not overlap with other groups which make their interpretation easier compared to the signals of methyl and ethyl groups.[36] Taking into account the coordinate analysis of the dipolar moment changes,[51] and deconvolution of the PM-IRRAS spectra, the angles θ were determined for different samples. The results are summarized in Table 3. Obviously, the angle θ increased with increasing number of polymer blocks in the row PHEMA → PHEMA-co-PBMA → PHEMA-co-PBMA-co-PHEMA. This means that the tilt of the polymer chains towards the gold surface increased with polymerization of each new block. It seems that the increase of the angle value depended also on the chemical nature of the corresponding polymer blocks. Thus, a thickness increase of 5 nm after addition of the second PBMA block induced 8° change of the chain orientation towards the gold surface, while further growth of the third PHEMA block (only 2.9 nm) provided an additional 10° tilting of the brushes. Most probably, interchain interactions such as hydrogen bonding between the hydroxyl groups of PHEMA play also an important role for the final orientation of the polymer brushes inside the membrane. It is also possible that a premature termination caused a local decrease of the grafting density and induced a subsequent change of the tilt angle between neighboring brushes. Note that the angles given by this method are averages that are also influenced by the polydispersity of the brushes.

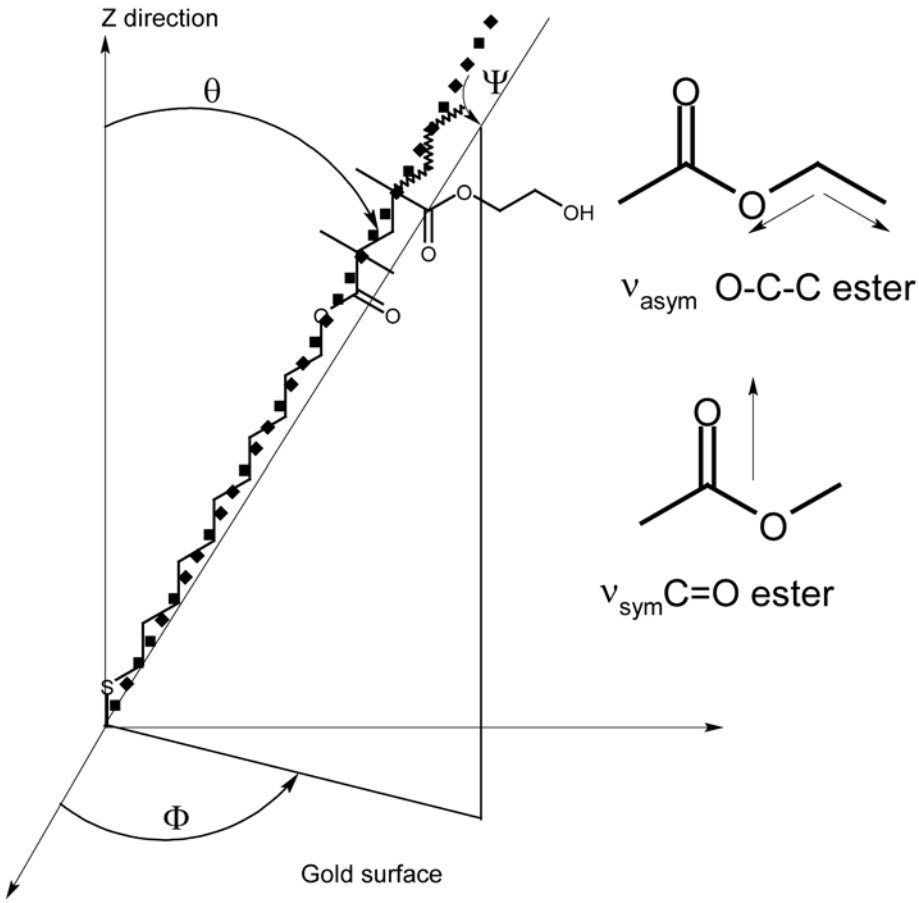

Figure 2. *Left:* Angle convention as described in the text. Set of axes refers to the surface, and not to the polymer chain main molecular axis. The molecule is oriented with respect to the surface as indicated on the scheme. The chain is rotated around the z axis (angle Φ), tilted by the angle θ (dotted line), and rotated around the molecular main axis by an angle Ψ. Angle Φ and Ψ are either averaged or included in the relative concentration factor respectively, and not further determined. *Right:* Vector representation of the ester group transient dipolar moments. Note the orthogonal character of the two chosen vibrations.

	PHEMA	PHEMA-co-PBMA	PHEMA-co-PBMA-co-PHEMA
θ	30	38	48

Table 3. Values of the angle θ for the copolymer brushes (experiment **2**).

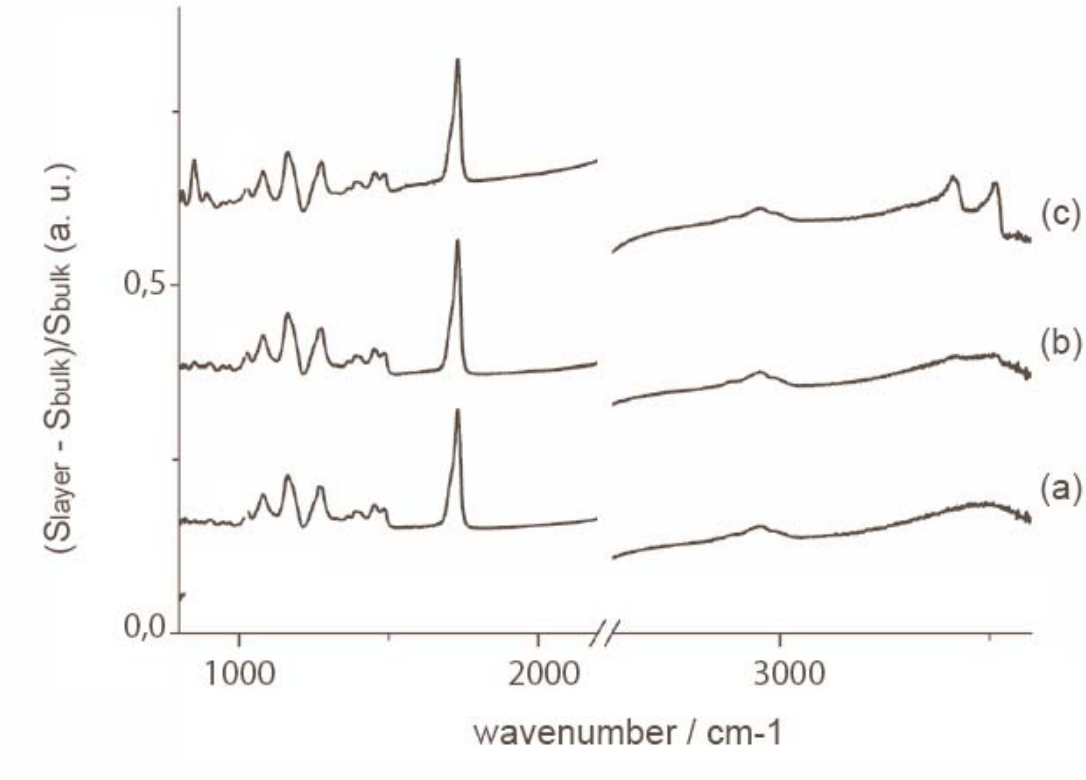

Figure 3. PM-IRRAS spectra: (a) PHEMA block, (b) PHEMA-co-PBMA diblock brushes, and (c) PHEMA-co-PBMA-co-PHEMA triblock brushes (experiment 2). S_{Layer} and S_{Bulk} represent the PM-IRRAS signal from the covered and bulk metal surface, respectively. The break represents the position in cm^{-1} where the Bessel function is not determined.

An important feature of PM-IRRAS is its ability to distinguish the orientation of functional groups with respect to the surface. This clearly explains the differences in the PM-IRRAS (Figure 3) and the ATR-FTIR (Figure 1) signals. Thus, upon the brush growth we observed an increase of the peak intensities in the ATR-FTIR spectra, while the characteristic signals had similar intensities in PM-IRRAS spectra. This discrepancy is attributed to the change in the angle θ. As the polymer chains grow, the number of functional groups increases and thus, their total absorption increases in ATR-FTIR (Figure 1). However, the tilt of the polymer chains towards the surface, i.e. angle θ, also increases. Therefore, the intensity of the final measured signal of the growing chain remains almost constant in PM-IRRAS spectra. Another important feature of the PM-IRRAS spectra is the absence of a signal for the H-bonded hydroxyl groups of the first PHEMA block, despite its clear presence in ATR-FTIR. This is presumably a result of hydrogen bonds oriented in a plane parallel (or only slightly tilted) to the gold surface. Most likely, these interactions are intermolecular (since they are coplanar and not collinear) and provide a tight binding mode and a densely

coated polymer surface, respectively. Addition of the second PBMA block led to the appearance of two very small peaks at positions identical to those measured in ATR-FTIR and identified as hydrogen bonds. The detection of these two small bands indicated a change of hydrogen bond orientation towards the gold surface upon addition of the second PBMA block. We suppose that the shift of the hydrogen bond orientation was rather minor since the adsorption peaks were very small. However, a significant increase of the bands at 3414 and 3515 cm^{-1} was detected after the last polymerization step. Thus, further growth of the third PHEMA resulted in the intensity increase of two hydrogen bond peaks indicating perhaps a formation of different hydrogen bond network compared to the first PHEMA brushes. We assume that in the case of triblock copolymer brushes steric effects of the second PBMA block prevent the formation of a dense network of hydrogen bonds in a plane parallel to the surface and shifts the interactions in a direction significantly tilted from the surface. In summary, the interactions among the polymer chains of the first and the third PHEMA blocks are different and depend on the neighboring environment within amphiphilic polymer brushes.

The surface analysis of the polymer films, however, did not provide information about the molecular weight and the polydispersity of the polymer brushes. In order to determine these parameters, after each polymerization step we detached the polymer chains from the solid substrate and performed GPC and ^{1}H NMR studies. Oxidation of the thiol groups by iodine resulted in a cleavage of the Au-S bond and a release of the polymer brushes. This procedure was already described before.[52] A dimerization via disulfide-bridge formation was not observed.[52]

The chemical compositions of the detached PHEMA, PHEMA-co-PBMA and PHEMA-co-PBMA-co-PHEMA triblock polymer chains were verified by ^{1}H NMR (Figure 4). The main characteristic protons of PHEMA (a- 4.03 ppm, b- 3.74 ppm) and PBMA (c- 3.95 ppm, d- 0.88 ppm) were clearly seen in the spectra of the diblock copolymers (Figure 4, (1)). The copolymerization of the third PHEMA block was reflected in a decrease of the ratio between the corresponding PHEMA (Figure 4, (2), a and b) and PBMA (Figure 4, (2), c) peaks.

The number average molecular weights (M_n) and the polydispersity indexes (PDI) were measured by GPC and are presented in Table 1. The first PHEMA as well as the PHEMA-co-PBMA diblock copolymer brushes from both experiments had relatively narrow polydispersities, i.e. 1.1 and 1.2 respectively. However, the triblock copolymer chains revealed broader PDIs, especially for the experiment **2** (PDI=1.6) where longer polymer chains were synthesized. This result can be explained by the fact that the probability of

termination processes increases with increasing chain length during conventional surface-initiated ATRP,[53-55] thus leading to broader polydispersities of polymers with higher molecular weights.

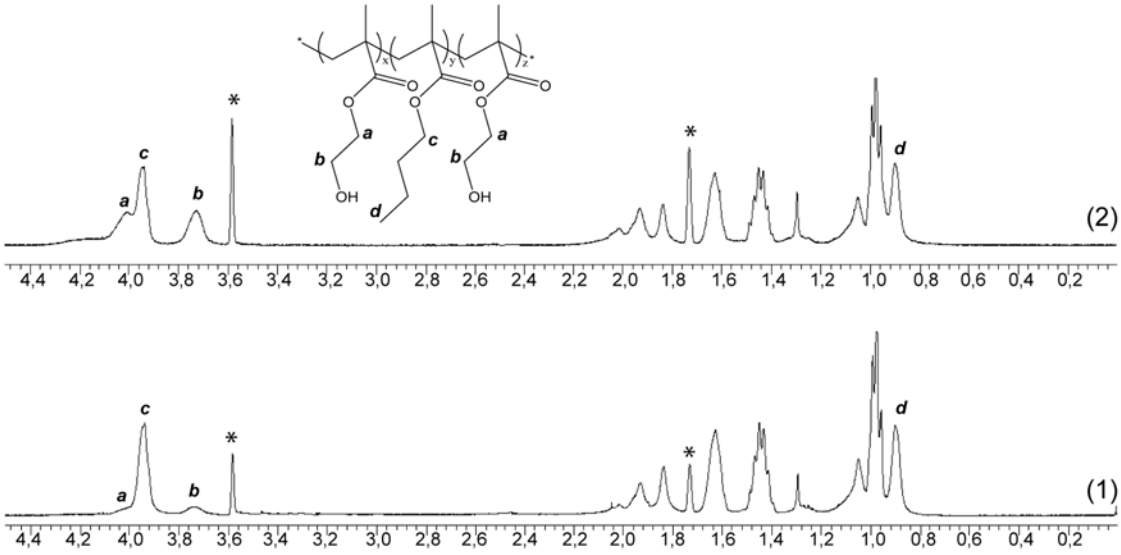

Figure 4. Typical ^{1}H NMR spectra of detached diblock PHEMA-co-PBMA brushes (1) and triblock PHEMA-co-PBMA-co-PHEMA brushes (2) in THF-d8. Peaks at δ=3,58 ppm and 1,73 ppm correspond to THF-d_8 and are marked by asterisks.

Having information about the molecular weights, we established the copolymer compositions to be $PHEMA_{21}$-co-$PBMA_{34}$-co-$PHEMA_{31}$ (experiment **1**) and $PHEMA_{46}$-co-$PBMA_{58}$-co-$PHEMA_{27}$ (experiment **2**) respectively (Table 1). Thus, the increase of the polymer chain lengths corroborates the increase of the layer thicknesses measured by ellipsometry.

5.3.4. AFM investigations

Since the triblock copolymer brushes have an amphiphilic structure we used block-selective solvents as well as a good solvent for the whole triblock copolymer to investigate the surface morphology and solvent-responsive behavior of the $PHEMA_{46}$-co-$PBMA_{58}$-co-$PHEMA_{27}$ membrane from experiment **2**. Ethanol was chosen as a good solvent for the triblock copolymer chains, while hexane and water selectively swell the PBMA and PHEMA blocks, respectively. A gold support functionalized with the triblock copolymer membrane was immersed into ethanol and left overnight. After drying at room temperature, the polymer surface was analyzed by contact mode AFM (Figure 5, A).

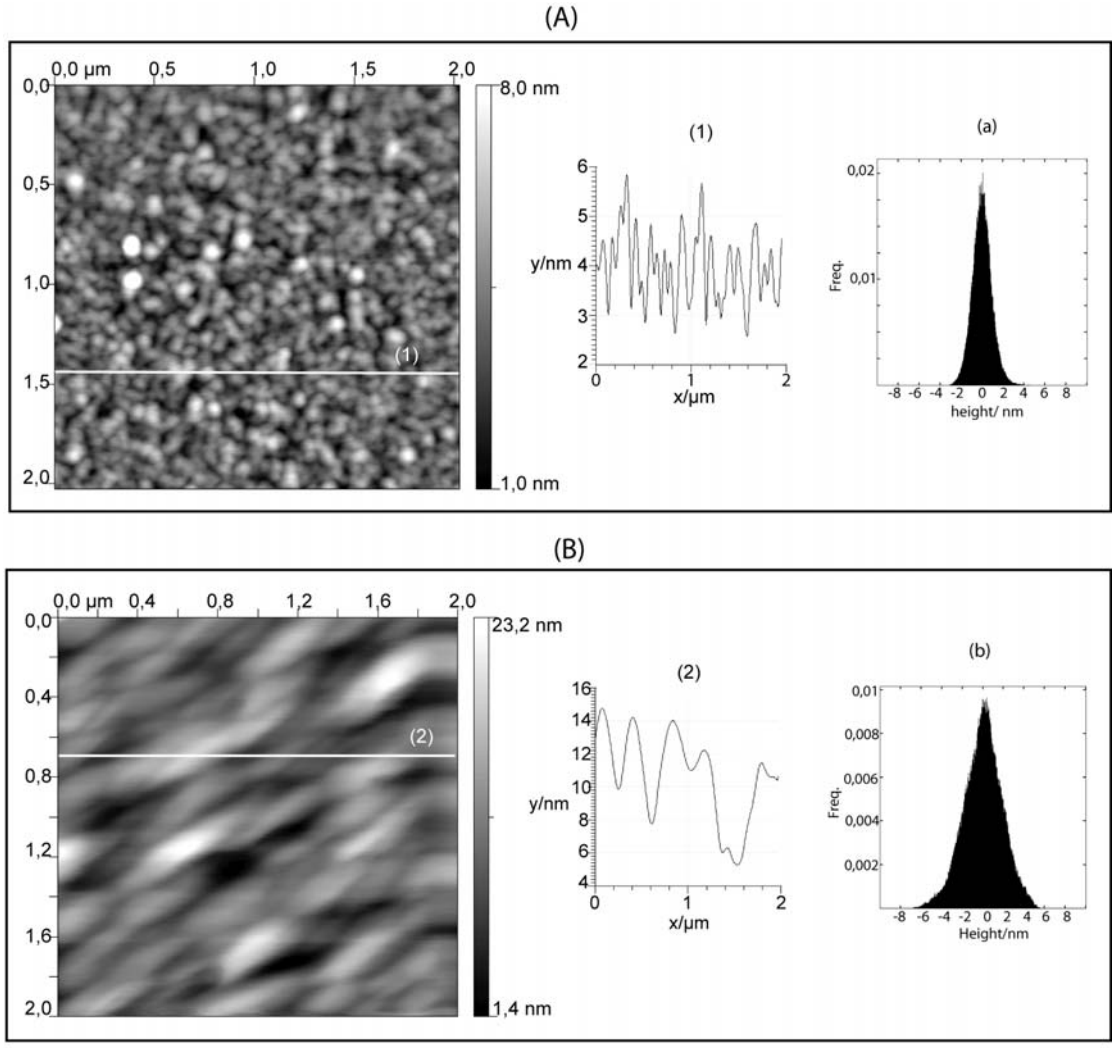

Figure 5. AFM analysis of the amphiphilic triblock copolymer brushes treated with ethanol (A) and hexane (B). The cross-section profiles of the polymer brushes stored in ethanol (1) and hexane (2) show different surface interface. The histograms of the polymer brushes treated with hexane (b) reveals an increase of the surface roughness compare to the surface roughness of the polymer brushes treated with ethanol (a).

Globular domains with an average size of around 70 nm were seen on the AFM images. The analysis of different areas of the sample showed similar topography indicating homogeneity of the polymer film. An analogous surface morphology was reported for polystyrene-co-polymethyl methacrylate brushes when treated in a good solvent for both blocks.[56, 57] The authors demonstrated that the average size of the domains and roughness of the polymer surface depended on the interchain interactions as well as on the polymer block lengths that were assumed to be proportional to ellipsometric thicknesses.[56] Although we describe an amphiphilic polymer system with different brush thicknesses than the one discussed in literature, similar effects could explain the appearance of the observed nanomorphologies. Briefly, as ethanol is a good solvent for the triblock brushes, we assume that the polymer

chains are stretched away from the gold support forming a brush-like structure. Removing ethanol from the polymer layer leads to a collapse of the polymer chains and creation of nanodomains.[58] Additionally, we also suggest that the removal of ethanol supports hydrogen bond formation between neighboring PHEMA chains that contribute the nanodomain morphology of the surface.

Overnight incubation of the amphiphilic copolymer membrane in hexane resulted in a completely different topography of the surface. Figure 5, B shows a ripple surface of the polymer film. The cross section analysis (Figure 5, B, (2)) revealed a different surface profile in contrast to the results obtained after sample treatment with ethanol (Figure 5, A, (1)). The surface histogram demonstrated an increase of the height deviation (Figure 4, B, b) compared to the histogram of the polymer film treated with ethanol (Figure 5, A, a). Thus, change in the solvent polarity caused a reorganization of the polymer brushes. Supported by similar previous observations,[58] we propose that triblock copolymers rearranged so that the more hydrophobic PBMA part was exposed towards hexane thus shielding the PHEMA from an unfavorable contact to the poor solvent. Drying of the sample caused a collapse of these shielding PBMA loops and a featureless surface was formed correspondingly.[58]

Finally, the amphiphilic copolymer brushes were subsequently immersed in ethanol, ethanol/water (1:1, vol.%) and water and left overnight in water prior to the AFM measurements. Commonly, the PHEMA blocks considerably swell in water, while the hydrophobic PBMA block tends to avoid contact to the aqueous surrounding. Figure 6, (a) shows the 3D topography image of the wet copolymer chains on gold surface. The brush-like structure of the macromolecules is in agreement with a stretching of the PHEMA chains upon swelling with water. After drying the sample acquired again a nanodomain topography of the surface (Figure 6, b), which was similar to the surface of the polymer brushes treated in ethanol (Figure 5, a). Most probably, also here drying caused a collapse of the polymer brushes and thus, formation of the nanodomains. This observation corroborates well with the data on polymer brushes reported before.[59]

Interestingly, all these phase segregation processes were reversible since a re-immersion of the sample into one of three tested solvents resulted in a reproducible morphologies described above. This proves not only the covalent attachment of the block copolymer layer but could potentially also be used to create responsive surfaces.

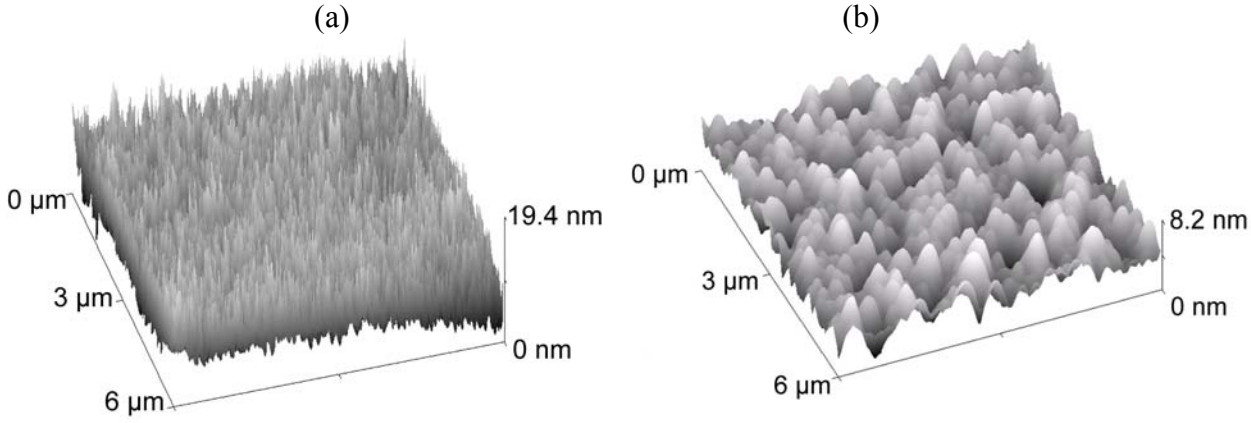

Figure 6. Contact mode AFM analysis of the amphiphilic triblock copolymer membrane in water (a) and after sample drying (b).

5.4. Conclusions

ATRP was successfully applied for grafting of amphiphilic ABA'-triblock copolymer membranes from gold supports. Our experiments indicated that the length of the individual blocks could be controlled by varying the polymerization time. In addition we confirmed the formation of PHEMA-co-PBMA-co-PHEMA brushes by a variety of different analytical techniques that did not only give information about layer thickness and surface topography but allowed also a preliminary estimation of the chain orientation inside the membrane. The amphiphilic character of the triblock copolymer brushes provided a responsive surface that showed a solvent dependent arrangement of the block copolymer chains, which was also reflected in the morphologies of the dried films.

Most interestingly the polymer brushes with a hydrophilic-hydrophobic-hydrophilic sequence can be regarded as a first example of a solid supported, biomimetic block copolymer membrane that has been prepared by a 'grafting-from' approach.

Upon insertion of membrane proteins these systems could allow for the preparation of mechanically and chemically robust and, potentially, even air-stable biosensor devices. It should be noted, that the insertion of membrane proteins and preservation of their functionality requires also a certain mobility of the polymer molecules within the membranes. Since here all the individual chains are covalently attached to the solid support they cannot undergo lateral diffusion. However, block copolymer membranes are known to be highly flexible and compressible, which, in our system, can additionally be influenced by the grafting density of the polymer chains. Therefore we expect that a solubilization of

functional building blocks might still be possible. Further experiments to investigate protein insertion and lateral diffusion of 'guest-molecules' within the membranes are in progress.

5.5. Acknowledgments

The authors thank Dr. Teresa de los Arcos and Dr. Laurent Marot for the access to ellipsometer, Dr. Thomas Braun for the help with preparation of gold substrates. This work was supported by the NCCR Nanoscale Science, the Swiss National Science Foundation and NEST Projects 029084 and 043431.

5.6. References

[1] Tanaka M., Sackmann E. *Nature* **2005**, *437*, 656.

[2] Knoll W., Frank C. W., Heibel C., Naumann R., Offenhäusser A., Rühe J., Schmidt E. K., Shen W. W., Sinner A. *Reviews in Molecular Biotechnology* **2000**, *74*, 137.

[3] Burns C. J., Field L. D., Morgan J., Petteys B. J., Prashar J., Ridley D. D., Sandanayake K. R. A. S., Vignevich V. *Aust. J. Chem.* **2001**, *54*, 431-438.

[4] Sharma M. K., Jattani H., M. Lane Gilchrist, Jr. *Bioconjugate Chem.* **2004**, *15*, 942.

[5] Munro J. C., Frank C. W. *Langmuir* **2004**, *20*, 10567.

[6] Theato P., Zentel R., Schwarz S. *Macromol. Biosci.* **2002**, *2*, 387.

[7] Hwang L. Y., Götz H., Hawker C. J., Frank C. W. *Colloids and Surfaces B: Biointerfaces* **2007**, *54*, 127-135.

[8] Naumann R., Baumgart T., Gräber P., Jonczyk A., Offenhäusser A., Knoll W. *Biosens. Bioelectron.* **2002**, *17*, 25.

[9] Peggion C., Formaggio F., Toniolo C., Becucci L., Moncelli M. R., Guidelli R. *Langmuir* **2001**, *17*, 6585.

[10] Becucci, L.; Guidelli, R.; Liu, Q.; Bushby, R. J.; Evans, S. D. *J. Phys. Chem. B* **2002**, *106* (40), 10410-10416.

[11] Munro J. C., Frank C. W. *Langmuir* **2004**, *20*, 10567.

[12] Purrucker O., Förtig A., Jordan R., Tanaka M. *Chem. Phys. Chem.* **2004**, *5*, 327.

[13] Naumann C. A., Prucker O., Lehmann T., Rühe J., Knoll W., Frank C. W. *Biomacromolecules* **2002**, *3*, 27.

[14] Theato P., Zentel R. *Langmuir* **2000**, *16*, 1801.

[15] Onaca O., Nallani M., Ihle S, Schenk A., Schwaneberg U. *Biotechnol. J.* **2006**, *1*, 795.

[16] Bermudez H., Aranda-Espinoza H., Hammer D. A. & Discher D. E. *Europhys. Lett.* **2003**, *64*, 550.

[17] Mecke A., Dittrich C., Meier W. *Soft. Matter.* **2006**, *2*, 751.

[18] Discher D. E., Ahmed F. *Annu. Rev. Biomed. Eng.* **2006**, *8*, 323.

[19] Cha T., Guo A., Zhu X.-Y. *Biophys. J.* **2006**, *90*, 1270.

[20] Jass J., Tjärnhage T., Puu G. *Biophys. J.* **2000**, *79*, 3153.

[21] Rakhmatullina E., Meier W. *Langmuir* **2008**, *24*, 6254.

[22] Rakhmatullina E., Braun T., Kaufmann T., Spillmann H., Malinova V., Meier W. *Macromol. Chem. Phys.*, **2007**, *208*, 1283.

[23] Stoenescu R., Meier W. *Chem. Commun.* **2002**, 3016.

[24] Meier W., Nardin C., Winterhalter M. *Angew. Chem. Int. Ed.* **2000**, *39 (24)*, 4599.

[25] Discher D. E., Eisenberg A. *Science* **2002**, *297*, 967.

[26] Zhao B., Brittain W. J. *Prog. Polym. Sci.* **2000**, *25*, 677.

[27] Kim J.-B., Huang W., Miller M. D., Baker G. L., Bruening M. L. *J. Polym. Sci. A: Polym. Chem.*. **2003**, *41*, 386.

[28] Hussemann M., Malmstrom E. E., McNamara M., Mate M., Mecerreyes O., Benoit D. G., Hedrick J. L., Mansky P., Huang E., Russell T. P., Hawker C. J. *Macromolecules* **1999**, *32*, 1424.

[29] Matyjaszewski K., Miller P. J., Shukla N., Immaraporn B., Gelman A., Luokala B. B., Siclovan T. M., Kickelbick G., Vallant T., Hoffmann H., Pakula T. *Macromolecules* **1999**, *32*, 8716.

[30] Huang W., Kim J.-B., Bruening M. L., Baker G. L. *Macromolecules* **2002**, *35*, 1175.

[31] Keller R. N., Wycoff H. D. *Inorg. Synth.* **1947**, *2*, 1.

[32] Shah R. R., Merreceyes D., Husemann M., Rees I., Abbott N. L., Hawker C. J., Hedrick J. L. *Macromolecules* **2000**, *33*, 597.

[33] Mori S. *J. Liquid Chromatogr.* **1990**, *13*, 1719.

[34] Debe, M. K. *J. Appl. Phys.*, **1984**, *55*, 3354-3366.

[35] Arnold R., Terfort A., Wöll C. *Langmuir*, **2001**, *17*, 4980-4989.

[36] Thompson H.W., Torkington P. *J. Chem. Soc.* **1945**, 640-645.

[37] Wang J.-S., Matyjaszewski K. *Macromolecules* **1995**, *28*, 7901.

[38] Coessens V., Pintauer T., Matyjaszewski K. *Prog. Polym. Sci.* **2001**, *26*, 337.

[39] Jones D. M., Huck W. T. S. *Adv. Mater.* **2001,** *13*, 1256.

[40] Wang X.-S., Lascelles S. F., Jackson R. A., Armes S. P. *J. Chem. Soc., Chem. Commun.* 1999, 1817.

[41] Robinson K. L., Khan M. A., de Paz Banez M. V., Wang X.-S., Armes S. P. *Macromolecules* **2001**, *34*, 3155.

[42] Robinson K. L., Khan M. A., de Paz Banez M. V., Wang X. S., Armes S. P. *Macromolecules* **2001**, 34, 3155.

[43] Huang H., Hu X., Stafford C. M. *Adhesion Society Extended Abstracts* **2007**, 352.

[44] Zhao B., Brittain W. J. *Macromolecules* **2000**, *33*, 8813.

[45] Bieri M., Bürgi T. *J. Phys. Chem. B.*, **2005**, *109*, 22476-22485.

[46] Allara D. L., Swalen J. D. *J. Phys. Chem.*, **1982**, *86*, 2700-2704.

[47] Elzein T., Brogly M., Schultz J. *Polymer*, **2003**, *44*, 3649-3660.

[48] Elzein T., Brogly M., Schultz J. *Surf. Interface Anal.*, **2003**, *35*, 231-236.

[49] Colthup N. B., Daly L. H., Wells C. H. J. *Introduction to molecular Spectroscopy* **1970**, Academic Press, New York.

[50] Thompson H.W., Torkington P. *J. Chem. Soc.*, **1945**, 640.

[51] Schrader, B. *Infrared and Raman spectroscopy, methods and applications,* Wienheim,: VCH, 1995

[52] Haddleton D. M., Crossman M. C., Dana B. H., Duncalf D. J., Heming A. M. *Macromolecules* **1999**, *32*, 2110.

[53] Ejaz M., Ohno K., Tsujii Y., Fukuda T. *Macromolecules* **2000**, *33*, 2870.

[54] Jones D. M., Huck W. T. S. *Adv. Mater.* **2001**, *13*, 1256.

[55] Kim J.-B., Huang W., Bruening M. L., Baker G. L. *Macromolecules* **2002**, *35*, 5410.

[56] Zhao B., Brittain W. J., Zhou W., Cheng S. Z. D. *Macromolecules* **2000**, *33*, 8821.

[57] Zhao B., Brittain W. J., Zhou W., Cheng S. Z. D. *J. Am. Chem. Soc.* **2000**, *122*, 2407.

[58] Luzinov I., Minko S., Tsukruk V. V. *Prog. Polym. Sci.* **2004**, *29*, 635.

[59] Farhan T., Azzaroni O., Huck W. T. S. *Soft Matter* **2005**, *1*, 66.

6. General conclusions and Outlook

My PhD research work was focused on the synthesis and investigation of amphiphilic methacrylate block copolymers. This study started with the synthesis of different polymer amphiphiles in solution followed by the characterization of their self-assembly behavior. Further, the research shifted from solution to surfaces to take another step towards the development of solid-supported amphiphilic polymer membranes. The main findings of this work are:

- Amphiphilic block copolymers with different hydrophilicity and architecture of the chains, i.e. AB and ABA, were synthesized using ATRP. We showed that in spite of the similar hydrophobic-to-hydrophilic ratio of the copolymers, the chain architecture (di- or triblock) plays an important role for the macromolecular self-organization. Interestingly AB diblock copolymers self-assemble into micelles and compound micelles while the corresponding ABA triblock copolymers formed vesicles in aqueous solutions. The small size of the polymer vesicles (around 50 nm) and their low polydispersity are promising parameters for their further application as carriers for drug delivery.
- Adsorption of polymer vesicles on substrates with different charge density allowed us to reveal the average size of the vesicular walls, which is one of the crucial parameters for the application of vesicles.
- For the first time the formation of smooth and planar solid-supported block copolymer membranes was achieved through the adsorption of polyelectrolyte vesicles onto mica surface.
- To improve the membrane stability, amphiphilic diblock copolymer brushes grafted from gold and silicon surfaces were synthesized using surface-initiated ATRP. The procedure for the immobilization of the initiator molecules was optimized for further synthetic steps. We achieved patterning of the substrates by copolymer brushes using microcontact printing.
- Applying a surface-initiated ATRP it was possible to grow for the first time biomimetic amphiphilic triblock copolymer membranes from gold substrates.

  The orientation of the polymer chains changed during the growth of the individual blocks. This was attributed to changing interchain interactions inside the membrane

using PMIRRAS. The solvent responsive reorganization of the amphiphilic brushes was demonstrated.

- Finally, we created solid-supported biomimetic amphiphilic copolymer membranes by both "grafting to" and "grafting from" approaches. This achievement is a significant contribution to the field of polymer biomimetic membranes.

The discovered properties of the polymer membranes and polymer self-assemblies as well as developed synthetic approaches for their preparation lead to the following possible outlooks:

- The small charged polymer vesicles could be of a great interest for drug encapsulation and drug delivery. The small size gives an opportunity to encapsulate small amount of drugs while the "hairy" surface structure and the tunable charge density of the shell might prevent unspecific binding into biological interfaces.
- Furthermore, it was reported that PDMAEMA has an ability to disrupt the cell membrane. It would be interesting to investigate the vesicular behavior in the cell media and the possibility of their migration inside the cell. Additionally, the positive charges on the outer surface of self-assemblies lead to stronger interactions with mammalian cell membranes, which are mostly negatively charged.
- The polymer vesicles can be also tested to stabilize the membrane proteins for purifications.
- Further studies on solid-supported polymer membranes obtained through the adsorption of charged polymer vesicles can be carried out in order to elucidate different parameters of the membrane such as chain density, tilt and the reproducibility of the structure. This information can be used to improve functionality of the membrane.
- Also the investigation of the inner structure of the polymer membranes prepared by surface-initiated polymerization can be continued to find the optimum membrane parameters (thickness, density of the polymer chains) for its functionality.
- The resulting knowledge and comparison of the structure of the polymer membranes prepared by two different approaches ("grafting to" and "grafting

After science has done its best the mystery is as great as ever,
and the imagination and the emotions have just as free a field as before.

John Burroughs

Acknowledgments

„I am among those who think that science has great beauty. A scientist in his laboratory is not only a technician, he is also a child placed before natural phenomena, which impress him like a fairy tale. We should not allow it to be believed that all scientific progresses can be reduced to mechanism…Neither do I believe that the spirit of adventure runs any risk of disappearing in our world." (Marie Curie)

I thank my supervisor, Prof. Wolfgang Meier, for that spirit of adventure and freedom of "playing" that he provided. I am thankful to him for all his patience, trust and support that I constantly felt during my work in the group. All these together helped to find my way in the research and to perform my best ever.

I thank Dr. Thomas Braun for his great contribution and help during my PhD study. Some experiments, discussions and conclusions were done together in the atmosphere of complete faith and appreciation. Much collaboration was established due to his participation. He is the one I have learned a lot from and exactly that truly scientist whose belief in science always amazed me. It was him who taught me to be self-confident and stubborn.

I thank the best friend of mine, Elena Davydova for the time we spent together, for her unlimited optimism and support, for our adventures and discoveries in this country.

****

This work would not have been completed without people who helped me with measurements and techniques. Many thanks are addressed to my collaborators:

Dr. Thomas Kaufmann (Biozentrum, University of Basel)

Dr. Hannes Spillmann (Department of Physics, University of Basel)

Dr. Mohamed Chami (Biozentrum, University of Basel)

Dr. Shirley Müller (Pharmazentrum, University of Basel)

Dr. Teresa de Los Arcos (Department of Physics, University of Basel)

Dr. Laurent Marot (Department of Physics, University of Basel)

Dr. Rupert Tobias Konradi (Department of Materials, ETHZ Zurich)

Dr. Heiko Wolf (IBM Research laboratory, Zurich)

Dr. Alexandre Mantion (Department of Chemistry, University of Basel)

Prof. Thomas Bürgi (Surface spectroscopy and Nanoscience laboratory, University of Neuchatel)

I thank my co-referee, Prof. Marcus Textor for his interest to my research work.

I also gratitude Daniel Mathys and Marcel Düggelin, Microscopy Center at the University of Basel.

I thank Dr. Violeta Malinova and Dr. Corinne Vebert who helped to correct manuscripts and thesis. Special thanks are to Mariusz Grzelakowski, Julia Razumovich and Lucy Kind for the nice time shared together and friendly atmosphere in our office. I thank each member of our group for the daily help in solving different problems and questions.

I thank Natalija Backmann, Natalia Nugaeva, Murali Ghatkesar, Tatiana Kutz for being together and that invaluable countenance and approval I met.

I thank my family whose support were indispensable and made me stronger.

The Swiss National Foundation and the National Center of Competence in Research Nanoscale Science are acknowledged for financial support

Curriculum Vitae

Personal data

Name	Ekaterina Rakhmatullina
Address	Mittlere Strasse 33
	CH-4056 Basel
	E.Rakhmatullina@unibas.ch
Phone	+41 78 8652855
Nationality	Russian
Age	29
Marital status	single

Professional experience

04/2004-06/2008	PhD research, group of Prof. Wolfgang Meier Polymer synthesis and characterization; analysis of the polymer self-assemblies in aqueous solutions; Creation of the polymer biomimetic membranes on gold and silicon surfaces, investigation of thin polymer films, surface functionalization, surface chemistry
08/2001 – 04/ 2004	Research assistant, Institute of Macromolecular Compounds, Russian Academy of Sciences, St. Petersburg Institute of Experimental Medicine, Russian Academy of Medicine Research project was dedicated to the development of polymer-glass composite materials in cooperation with BIA Separations d. o. o.
01/2003 – 03/2003	Project collaboration, BIA Separations d. o. o., Ljubljana, Slovenia Microstructure optimization of the polymer matrix for further analytical application

Education

04/2004-06/2008	PhD thesis, Department of Chemistry, University of Basel

10/2001-04/2004	Research project, Institute of the Experimental Medicine, Russian Academy of Medicine, St. Petersburg; and Institute of Macromolecular Compounds, Russian Academy of Sciences, St. Petersburg
09/1996 - 06/2001	Studies in the Department of Chemistry, St. Petersburg State University, Specialization: organic and polymer chemistry MS in chemistry
09/1994 - 06/1996	High school diploma. Academic gymnasium of St. Petersburg State University, Russia; specialization in chemistry

Experimental skills

SYNTHESIS AND CHARACTERIZATION	Chemistry – synthetic organic and polymer chemistry, analytical chemistry, surface functionalization (gold, silicon, glass).
	Methods - NMR, IR, UV, MS, GPC, osmometry, ellipsometry; microscopy: AFM, TEM, SEM; light scattering techniques, XPS, contact angle measurement
	Biology – microbiology practice (E. coli), immunoassay, extraction and purification of proteins
LANQUAGES	English (fluent) German (A8/A2 level) Russian (native)
PC user	MS Windows 2000/XP/Vista, MS Office, Origin, Excel, Adobe software (Photoshop, Illustrator), ChemDraw, Mestrec, AFM image processing, Structure databases/ search

Personal profile

	Active and easy-going person who enjoys communication and traveling.
Hobbies:	artistic photography, psychology, sport (hiking, badminton, swimming), traveling, communication and internet resources

References

Prof. Dr. Wolfgang P. Meier
Department of Chemistry, University of Basel
Klingelbergstrasse 80, CH-4056 Basel
Tel.: +41(0)61 2673802
E-mail: wolfgang.meier@unibas.ch

Dr. Thomas Braun
Department of Physics, University of Basel
Klingelbergstrasse 82, CH-4056 Basel
Tel.: +41(0)79 7337269
E-mail: thomas.braun@unibas.ch

Dr. Andreas Taubert
Assistant Professor of Supramolecular Chemistry
University of Potsdam
D-14476 Golm
Tel.: 0049 (0)331 977 5773
Email: ataubert@uni-potsdam.de

Dr. Ales Podgornik
BIA Separations d. o. o.
Teslova 30
1000 Ljubljana
Tel.: +386 477 66 96
E-mail: ales.podgornik@guest.arnes.si

Basel, 12.06.2008

Publications

- Rakhmatullina E., Mantion A., Bürgli T., Malinova V., Meier W., *Macromolecules* **2008**, submitted
- Ghatkesar M., Rakhmatullina E., Lang H-P., Gerber C., Hegner M., Braun T., *Sensors and Actuators A*. **2008**, accepted for publication
- Rakhmatullina E. and Meier W., *Langmuir* **2008**, *24*, 6254.
- Rakhmatullina E., Braun T., Chami M., Malinova V., Meier W., *Langmuir* **2007**, *23*, 12371.
- Rakhmatullina E., Braun T., Kaufmann T., Spillmann H., Malinova V., Meier W., *Macromol. Chem. Phys.* **2007**, *208*, 1283.
- Khimich G. N., Rakhmatullina E. N., Slabospitskaya M. Y., Tennikova T. B., *Russian J. Appl. Chem.* **2005**, *78(4)*, 617.
- Rakhmatullina E. N., Gupalova T. V., Palagnuik V. G., Totolian A. A., *Russian J. Biotechnology* **2005**, 90.
- Aref'ev D. V., Domnina N. S., Komarova E. A., Aref'eve G. V., Rakhmatullina E. N., Bilibin A. Y., *Russian J. Appl. Chem.* **1999**, *72 (4)*, 697.

Presentations

Oral presentations

- *Amphiphilic block copolymers: from solution to the surface*
  E. Rakhmatullina, W. Meier
  The global challenges and nanotechnology
  Venice, Italy 2008

- *Temperature sensitive copolymer nanocontainers*
  E. Rakhmatullina, T. Braun, W. Meier
  EMPA PhD symposium
  Dübendorf, Switzerland 2007

- *Small temperature sensitive vesicles from an amphiphilic block copolymer*
  E. Rakhmatullina, T. Braun, W. Meier
  Frontiers Annual Meeting
  Leuven, Belgium 2007

- *Grafting of amphiphilic brushes from gold and silicon substrates*
  E. Rakhmatullina, T. Braun, T. Kaufmann, H. Spillmann, W. Meier
  Exploring New Frontiers in Bio/Nano
  Zermatt, Switzerland 2007

Poster presentations

- *Methacrylate-based amphiphilic copolymer vesicles: synthesis and characterization*
  E. Rakhmatullina, T. Braun, W. Meier
  The global challenges and nanotechnology
  Venice, Italy 2008

- *Grafting of amphiphilic copolymer brushes from gold and silicon substrates*
  E. Rakhmatullina, T. Braun, T. Kaufmann, H. Spillmann, W. Meier
  NCCR meeting 2008, Basel, Switzerland

- *Synthesis and self-assembly of amphiphilic methacrylate triblock copolymers*
  E. Rakhmatullina, T. Braun, W. Meier
  Frontiers Research Meeting 2007, Toulouse, France

- *Growth of amphiphilic copolymer membranes from gold substrates*
  E. Rakhmatullina, T. Braun, T. Kaufmann, H. Spillmann, W. Meier
  NanoBio Europe congress 2007, Münster, Germany

- *Functionalization of the silicon surfaces by amphiphilic diblock copolymer brushes*
  E. Rakhmatullina, W. Meier
  Frontiers Annual Meeting 2006, Sicily, Italy

- *Growth and characterization of the amphiphilic copolymer brushes on silicon and gold surfaces*
  E. Rakhmatullina, W. Meier
  Swiss Chemical Society - Fall Meeting 2006, Zurich, Switzerland

- *Application of surface-initiated ATRP for the synthesis of amphiphilic diblock copolymer brushes from silicon surfaces*
  E. Rakhmatullina, W. Meier
  International Conference on Nanoscience and Technology (ICN+T) 2006, Basel, Switzerland

- *Synthesis and self-assembly of amphiphilic methacrylate diblock copolymers*
  E. Rakhmatullina, S.M. Flores, W. Meier
  Frontiers Research Meeting 2006, Sicily, Italy

- *Synthesis of amphiphilic polymer brushes from inorganic substrates using surface-initiated atom transfer radical polymerization*
  E. Rakhmatullina, W. Meier
  Europolymer Conference of the European Polymer Federation (EUPOC) 2005, Gargnano, Lake Garda, Italy

- *Synthesis and Aqueous Solution behavior of Amphiphilic diblock copolymers based on n-Buthyl Methacrylate and 2-Dimethylaminoethyl Methacrylate*
  E. Rakhmatullina, W. Meier
  7th young scientists' conference on chemistry – *Frühjahrssymposium 2005*, Berlin, Germany

- *Macroporous monolithic layers for screening procedures based on affinity interaction*
  E. Rakhmatullina, G. Khimich, T. Gupalova, A. Podgornik, A. Strancar, T. Tennikova
  15th International Symposium on Pharmaceutical and biomedical analysis (PBA) 2004, Florence, Italy

- *Macroporous composite materials for screening diagnostic technique*
  E. Rakhmatullina, G. Khimich, T. Gupalova, T. Tennikova, *27th Symposium on High Performance Liquid Phase Separations and Related Techniques 2003*, Nice, France

- *Macroporous composite materials for screening diagnostic technique*
  E. Rakhmatullina, G. Khimich, T. Gupalova, A. Podgornik, A. Strancar, T. Tennikova
  3rd International Symposium on Separations in BioSciences (SBS) 2003, Moscow, Russia

Other activities

- Frontiers Strategic Research Area (SRA 5)
  Meeting on Biosensors, 2-3 May 2007 Basel, Switzerland

- COST P12 meeting
  Structuring of polymers, 8-9 October 2006 Mittelwihr, France